Pavol Jozef Šafárik University in Košice
Faculty of Science

Exactly Solvable Models in Statistical Physics

Jozef Strečka

Košice 2022

Exactly Solvable Models in Statistical Physics

Academic textbook

Author:
doc. Jozef Strečka

Pavol Jozef Šafárik University in Košice, Slovakia

Reviewers:

prof. Oleg Derzhko
Institute for Condensed Matter Physics, L'viv, Ukraine

prof. Johannes Richter
Otto-von-Guericke Universität, Magdeburg, Germany

prof. Marcelo Leite Lyra
Universidade Federal de Alagoas, Maceió, Brazil

Available at: www.unibook.upjs.sk
Publication date: 28.09.2022

ISBN 978-80-574-0124-7 (e-publication)

Contents

Preface to the first edition

The present textbook deals with exactly solved models and their diverse applications in several branches of physics such as mathematical physics, statistical physics, condensed matter physics and so on. Exactly soluble models are currently considered as an inspiring research field in its own right, which regrettably requires a considerable knowledge of sophisticated mathematics. Accordingly, my primary ambition was to provide an introductory course for undergraduate students that would cover the simplest exactly solved models, whose rigorous solutions are available even after modest calculation. The present textbook should be therefore regarded as an auxiliary graduate-level textbook, which should serve as the student's guide on this beautiful but surely intricate subject.

Even although I attempted to write largely self-contained textbook for undergraduate students, it is worthy of notice that the course on *Exactly Solvable Models in Statistical Physics* demands essential knowledge from the quantum mechanics, statistical physics, phase transitions and critical phenomena, which are its indispensable prerequisites. The most crucial fundamentals of these theories are briefly recalled in introductory remarks just for remembering and not for substituting those comprehensive courses. The rest of this textbook is entirely devoted to exactly solved lattice-statistical models with the main emphasis laid on their possible applications in the condensed matter physics. It is the author's hope that the presented exact solutions are detailed enough in order to be easily followed by undergraduate students even without a support of tedious proofs, cumbersome theorems, longer argumentations, or obvious facts. This rather necessary compromise has of course a certain inadvisable impact on 'exactness' of the presented solutions.

Finally, it is worthwhile to remark that the present textbook makes just a slight introduction into the simplest exactly solvable models and thus, the interested reader is referred for the follow-up study to several excellent books on exactly solved models quoted in the bibliography listed at the end of this textbook. Note that the listed books were the major knowledge sources used by creating this textbook and they might be regarded as more advanced literature on this exciting research field.

Košice, June 2007 Jozef Strečka

Preface to the second edition

Over the past fifteen years, the course on 'Exactly Solvable Models in Statistical Physics' has become an indispensable ground of the study programme 'Theoretical Physics' at Faculty of Science of Pavol Jozef Šafárik University in Košice. At first, the course based on the first edition of this textbook was intended for undergraduate students only, however, I have later prepared follow-up course taught at a postgraduate level on demand of several ambitious students who wished to continue in studying this exciting research field. It is already more than decade when our students enrolled in the study programme 'Theoretical Physics' graduate from 'Introduction to Exactly Solvable Models in Statistical Physics' at a master level and 'Exactly Solvable Models in Statistical Physics' at a postgraduate level. Of course, it was necessary somehow to rearrange topics for the courses of undergraduate and postgraduate students. More specifically, a few more challenging topics concerned with exact solutions of 2D Ising model (chapter 3) were moved to a more advanced course intended for the postgraduate students, while an introductory course intended for the undergraduate students was contrarily supplemented with a few new topics requiring the second edition of this textbook. The second edition of this textbook thus contains a completely new chapter 4 devoted to the exact solution of the Ising model on the Bethe lattice using the method of exact recursion relations, while the chapter 5 was supplemented by exact results for ground state of a few frustrated Heisenberg spin models using the variational method. It is my hope that the next edition of this textbook will come soon and it will involve all topics specifically taught within the postgraduate course as well.

Košice, August 2022 Jozef Strečka

Acknowledgments

The first edition of this textbook was financially supported by the European Social Fund (ESF) project under the contract 2005/NP1-051 11230100466 and by the Slovak Research and Development Agency, which enabled to create for me at Faculty of Science of Pavol Jozef Šafárik University in Košice the postdoctoral position during the period 2007–2009 under the contract No. LPP-0107-06.

The second edition of this textbook has largely benefited from the financial support of the Slovak Research and Development Agency, which has supported my research on exactly solvable lattice-statistical models under the contract Nos. APVV-16-0186 during the period 2017–2021 and APVV-20-0150 during the period 2021–2025.

The special thanks goes to three reviewers of the second edition of this textbook Oleg Derzhko, Johannes Richter and Marcelo Lyra for their long-standing collaboration, inspiring discussions, valuable comments and suggestions.

1 Introductory remarks

Statistical physics is one of the fundamental theories of physics dealing with equilibrium properties of a large number of particles by the use of well established concept based either on classical or quantum mechanics. In this regard, the term statistical mechanics is often used as a synonym to statistical physics that covers probabilistic (statistical) approach to classical or quantum mechanics concerning with many-particle systems. The most important benefit resulting from this theory consists in that it relates the microscopic properties of individual particles (atoms, molecules, or ions) to the macroscopic (bulk) properties of matter. Even though the relationship between some macroscopic properties and the essential properties of particles is occasionally elementary (for instance the mass of material is simply a sum over particle masses), many material properties cannot be simply elucidated from the microscopic point of view. In particular, statistical physics enables to explain characteristic features of real materials at the microscopic level just by imposing forces between constituent particles. Therefore, one necessarily needs merely some plausible assumption about internal forces between the constituent particles to make theoretical predictions for a given material. This assumption, built on some realistic microscopic idea of how individual particles interact among themselves, constitutes a framework for some simple idealization known as model.

Of course, each *model* serves only as an approximate description of physical reality with the main goal to describe the macroscopic properties quantitatively. It is usually very difficult to define a realistic model, which is on the one hand mathematically tractable, but on the other hand provides a comprehensive description of all macroscopic features. However, the most vigorous difficulties are encountered by attempting to formulate and to solve the relevant model mathematically. There are nevertheless few valuable exceptions. The most common example surely represents an ideal gas (no matter whether consisting of classical particles or fermions and bosons) in which the constituent particles do not interact among themselves until they undergo perfectly elastic collisions. Once the interparticle interactions are established, suppose for instance the real gas instead of the ideal gas, realistic models are highly celebrated if they are still exactly soluble. Unfortunately, such

models are usually beyond the scope of standard courses on statistical physics because rather sophisticated mathematics must be involved to obtain a rigorous solution. The main goal of the present textbook is to make a slight introduction into the beauty of the simplest exactly solvable models, which can be solved analytically by the use of simple mathematical tools familiar even for undergraduate students.

1.1 Foundations of ensemble theory

For the benefit of the reader, we first briefly recall some foundations of statistical physics to which the reader is often referred to in the next sections. Specific constraints laid on environment of a macroscopic system (macrosystem) allows us to use the different types of ensembles. In the present textbook, all calculations will be done either within the canonical or grand-canonical ensemble. Within the *canonical ensemble*, which admits only an interchange of energy between the macrosystem and its environment (the number of particles is kept constant), the probability p_i of finding the macrosystem at a certain microscopic state (microstate) with the energy E_i is given by the Boltzmann's factor

$$p_i = \frac{1}{\mathcal{Z}} \exp(-\beta E_i), \tag{1.1}$$

where $\beta = 1/(k_{\mathrm{B}}T)$, k_{B} is Boltzmann's constant, T is the absolute temperature and $\mathcal{Z}$ denotes the normalizing factor, which ensures that the macrosystem is certainly found in one of its possible microstates. In the consequence of that, the sum over probabilities ascribed to a whole set of microstates is equal to unity ($\sum_i p_i = 1$) and this condition unambiguously determines the normalizing factor

$$\mathcal{Z} = \sum_i \exp(-\beta E_i), \tag{1.2}$$

which is usually referred to as the *partition function*, statistical sum or sum-over-states. The physical meaning of the partition function rests in enumerating the number of microstates accessible to the macrosystem at a given temperature. The partition function thus represents the most important quantity inasmuch as it allows to find the expected (averaged) value of any microscopic property of the macrosystem, which is related to

some macroscopic (observable) physical quantity.[1] For instance, the averaged value of all microscopic energies can be interpreted as the microscopic definition of the internal energy

$$\mathcal{U} = \sum_i E_i p_i = \frac{1}{\mathcal{Z}} \sum_i E_i \exp(-\beta E_i) = -\frac{\partial \ln \mathcal{Z}}{\partial \beta}. \tag{1.3}$$

The latter equation proves, for instance, that the internal energy can be simply obtained by performing the derivative of the partition function with respect to the inverse temperature β. It is quite straightforward to derive similar relations connecting the partition function with other thermodynamic quantities as well. For brevity, the final microscopic expressions are listed below for the Helmholtz free energy $\mathcal{F}$ and entropy $\mathcal{S}$

$$\mathcal{F} = -k_{\mathrm{B}} T \ln \mathcal{Z} \qquad \text{and} \qquad \mathcal{S} = k_{\mathrm{B}} \ln \mathcal{Z} - \frac{1}{T} \frac{\partial \ln \mathcal{Z}}{\partial \beta}. \tag{1.4}$$

In the quantum version of the canonical ensemble, the probability of finding the macrosystem in one of its available microstates relates to the density matrix operator

$$\hat{\rho} = \frac{1}{\mathcal{Z}} \exp(-\beta \hat{\mathcal{H}}), \tag{1.5}$$

in which $\hat{\mathcal{H}}$ denotes the Hamilton operator (Hamiltonian) and $\mathcal{Z}$ is the quantum-mechanical analogue of the classical canonical partition function

$$\mathcal{Z} = \mathrm{Tr} \exp(-\beta \hat{\mathcal{H}}). \tag{1.6}$$

Obviously, the partition function can be now calculated as a trace over the whole Hilbert space constituted by arbitrary but complete basis of microstates. The density matrix operator allows us to calculate the expected (averaged) value of in principle arbitrary observable physical quantity using the relation

$$\langle \hat{A} \rangle = \mathrm{Tr}(\hat{A}\hat{\rho}) = \frac{1}{\mathcal{Z}} \mathrm{Tr}[\hat{A} \exp(-\beta \hat{\mathcal{H}})]. \tag{1.7}$$

It is worthy of notice that the calculation of the partition function (1.6) provides even within the quantum-mechanical treatment the most convenient way how to access the

[1] Expected (averaged) value means that this quantity is calculated for all available microstates of a macrosystem and then is weighted according to the corresponding Boltzmann's factors.

most important thermodynamic quantities, since the relations (1.3), (1.4) and others that connect the partition function with other thermodynamic variables still remain valid.

If the macrosystem might exchange particles with its environment, it is very advisable to pass from the canonical ensemble to the *grand canonical ensemble*. In order to ensure conservation of the total number of particles, it is necessary to introduce chemical potentials μ_j related to each kind of the constituent particles ($j = 1, \ldots, n$; one for each kind of particles) and to replace the canonical partition function with the *grand canonical partition function*

$$\Xi = \sum_i \exp\left[\beta\left(\sum_{j=1}^{n} \mu_j N_{ij} - E_i\right)\right], \tag{1.8}$$

in which N_{ij} denotes the total number of particles of jth kind in the ith microstate with the overall energy E_i and the first summation is carried out over all possible microstates. The averaged number of particles of the jth kind can be calculated from the grand canonical partition function

$$\langle N_j \rangle = k_{\mathrm{B}} T \frac{\partial \ln \Xi}{\partial \mu_j} \tag{1.9}$$

together with other basic thermodynamic potentials such as the grand potential Ω, internal energy $\mathcal{U}$, Helmholtz free energy $\mathcal{F}$, or entropy $\mathcal{S}$

$$\Omega = -k_{\mathrm{B}} T \ln \Xi, \qquad \mathcal{U} = -\frac{\partial \ln \Xi}{\partial \beta} + k_{\mathrm{B}} T \sum_j \mu_j \frac{\partial \ln \Xi}{\partial \mu_j}, \tag{1.10}$$

$$\mathcal{F} = -k_{\mathrm{B}} T \ln \Xi + k_{\mathrm{B}} T \sum_j \mu_j \frac{\partial \ln \Xi}{\partial \mu_j}, \qquad \mathcal{S} = k_{\mathrm{B}} \ln \Xi - \frac{1}{T} \frac{\partial \ln \Xi}{\partial \beta}. \tag{1.11}$$

1.2 Phase transitions and critical phenomena

Phase transitions designate an abrupt change in physical properties, which is enforced by a small change of some thermodynamic variable such as the temperature. This phase change occurs at some special points called as *critical points*, where two or more phases coexist together or become indistinguishable. As a result, the macrosystem exhibits at a critical point either discontinuity or non-analyticity in one or more thermodynamic quantities. Strictly speaking, the phase transition may (but need not) appear just in the limit

of infinite system, which is often referred to as *thermodynamic limit*. It should be mentioned that both the aforedescribed ensembles, canonical as well as grand canonical, differ merely in the way how they allow macrosystem to fluctuate between available microstates. These fluctuations become negligible in the thermodynamic limit and thus, the different ensembles yield equivalent thermodynamic functions. In other words, the bulk properties of the studied macrosystem do not depend on a particular choice of the ensemble to be used for its description. Under these circumstances, the best ensemble for calculation is that one, which allows the most straightforward derivation of the partition function.

One of the most significant achievement of the equilibrium statistical physics is closely associated with the understanding of phase transitions and critical phenomena in a wide variety of physical systems. Important revision in the understanding of phase transitions has been achieved when Lars Onsager succeeded in obtaining the exact solution for the two-dimensional (2D) Ising model [1], which became the most notable paradigm of exactly solved model. The beauty of Onsager's solution lies in an exact evidence of a striking phase transition, which is accompanied with a singular behaviour of several thermodynamic quantities in the vicinity of critical point. Besides, Onsager's famous solution afforded exciting progress in the understanding of phase transitions, since it has furnished a rigorous proof that a phase transition may result solely from short-range forces between nearest neighbours. Even though this exact solution has been initially regarded just as a mathematical curiosity without any physical relevance to the real-world behaviour, this opinion rapidly diminished in evidence of other exactly solved models. In this regard, one of the most essential questions appearing in the field of exactly soluble models relates to an exact nature of discontinuities and singularities accompanying each phase transition.

There are several ways how to classify phase transitions. For instance, phase transitions can be classified according to the degree of non-analyticity appearing at a critical point. According to *Ehrenfest's classification scheme*, phase transitions are distinguished by the lowest derivative of the free energy that becomes discontinuous at a critical point. So, first-order phase transitions exhibit a discontinuity in the first derivative of the free energy, while second-order phase transitions possess a discontinuity in the second derivative and so on. It should be stressed that this simple scheme disables classification of

phase transitions at which some of the free energy derivative(s) diverges. Therefore, the *modern (Landau) classification scheme* distinguishes two different kinds of phase transitions. At discontinuous (first-order) phase transitions, the macrosystem either absorbs or releases latent heat needed for completion of a phase change due to the finite entropy change. The most characteristic feature of the discontinuous phase transition consists in a coexistence of different phases at a critical point. On the contrary, the phases become indistinguishable at a critical point of continuous (second-order) phase transitions and hence, latent heat is not required for completion of a phase change.

1.3 Scaling and universality hypotheses

Striking and often hardly understandable aspects of critical phenomena demanded some simplification, which has been achieved through scaling and universality hypotheses. Namely, it turns out that many precise details of interactions established between constituent particles are irrelevant, at least at a critical point, in determining the bulk properties of the macrosystem. As a matter of fact, the *scaling hypothesis* presumes that each macrosystem exhibits self-similar properties near a critical point, which means, that its macroscopic properties are invariant under the transformation of scale. On the other hand, the *universality hypothesis* predicts that very different macrosystems may exhibit remarkably similar behaviour close to their respective critical points. It is worthy to mention that both the hypotheses have been developed from the same underlying foundation; constituent particles far apart in a given macrosystem are strongly correlated with each other below a critical point even if there is no direct interaction between them. Precisely at a critical point, the peculiarly strong correlation develops at an infinite distance even if only short-range forces, such as nearest-neighbour pairwise interactions, are present in the macrosystem. Intuitively, one would rather expect an exponential decay of the inter-particle correlation with a distance r between particles according to the exponential character of the Boltzmann's factor. In the consequence of that, the final expression for the correlation function Γ should follow the exponential law

$$\Gamma(r, T) = \exp[-r/\xi(T)], \tag{1.12}$$

where ξ denotes the so-called correlation length that represents a characteristic length scale above which inter-particle correlations become negligible. By contrast, the correlation function usually follows at a critical point a rather strange power-law decay

$$\Gamma(r) = r^{2-d-\eta}, \tag{1.13}$$

which is unambiguously characterized by means of the critical exponent η and the spatial dimensionality d of the considered model system. Critical exponents, such as the critical exponent η for the correlation function but also that ones for other thermodynamic quantities, seem to depend just on the most fundamental features of the macrosystem such as its spatial dimensionality and symmetry. Accordingly, the macrosystems belonging to the same *universality class* should merely have the same

- the spatial dimensionality d;
- the number of components n (symmetry) of the order parameter[2].

The concept of universality then predicts that different macrosystems, which might be diverse in their nature but belong to the same universality class, should behave very similarly close to their respective critical points. In this respect, each universality class can be characterized by the unique set of universal critical exponents valid for each its member. For further convenience, let us define critical exponents for basic thermodynamic quantities, which characterize the response of a magnetic system with respect to a change of the temperature T and the external magnetic field H

$$\text{Specific Heat} \qquad C = t^{-\alpha} \quad (t \to 0^+), \qquad C = (-t)^{-\alpha'} \quad (t \to 0^-); \tag{1.14}$$

$$\text{Magnetization} \qquad M = H^{1/\delta} \quad (t = 0), \qquad M = (-t)^{\beta} \quad (t \to 0^-); \tag{1.15}$$

$$\text{Susceptibility} \qquad \chi = t^{-\gamma} \quad (t \to 0^+), \qquad \chi = (-t)^{-\gamma'} \quad (t \to 0^-); \tag{1.16}$$

$$\text{Correlation Length} \qquad \xi = t^{-\nu} \quad (t \to 0^+), \qquad \xi = (-t)^{-\nu'} \quad (t \to 0^-); \tag{1.17}$$

in which $t \equiv (T - T_\mathrm{c})/T_\mathrm{c}$ is used to measure a relative variation of the temperature from the critical value T_c. It is worthy to notice that the aforementioned critical exponents

[2]The order parameter is the quantity, which measures the amount of ordering below a critical point.

should obey following scaling relations

$$\alpha' + 2\beta + \gamma' = 2, \qquad \text{G. S. Rushbrook} \tag{1.18}$$

$$\alpha' + \beta(\delta + 1) = 2, \qquad \text{R. B. Griffiths} \tag{1.19}$$

$$\gamma' = \nu'(2 - \eta), \qquad \text{M. E. Fisher} \tag{1.20}$$

$$d\nu' = 2 - \alpha', \qquad \text{Essam-Fisher Hyperscaling} \tag{1.21}$$

$$\alpha = \alpha', \quad \gamma = \gamma', \quad \nu = \nu', \tag{1.22}$$

which should hold as a result of the validity of the scaling hypothesis. It is not a purpose of the present course to justify all these scaling relations, however, all known exactly solved models validate them without exception, yet. The total set of scaling relations is sometimes known as a two-exponent scaling, since if two independent exponents are given, then all the other exponents can be obtained from the scaling relations (1.18)-(1.22). For illustration, exact values for critical exponents of several exactly solved models are listed in the Table 1.

Table 1: Some microscopic models, their spatial dimensionality and critical exponents.

	d	$\alpha = \alpha'$	β	$\gamma = \gamma'$	δ	$\nu = \nu'$	η
Ising	1	1	0	1	∞	1	1
Ising	2	0	$\frac{1}{8}$	$\frac{7}{4}$	15	1	$\frac{1}{4}$
Baxter-Wu	2	$\frac{2}{3}$	$\frac{1}{12}$	$\frac{7}{6}$	15	$\frac{2}{3}$	$\frac{1}{4}$
Mean-field	∞	0	$\frac{1}{2}$	1	3	$\frac{1}{2}$	0

2 1D Ising model

There is a class of exactly solvable models, which are of particular interest because of their utility and versatility in representing real-world systems. Among these, the simple-minded Ising model is perhaps the most versatile model that is mathematically tractable. Accordingly, we will start our study on exactly solvable models just with the Ising model.

Let us find the simplest model, which would provide an approximate description of insulating magnetic materials. Each insulating magnetic material consists of entities (atoms, molecules, ions), which need not be carriers of the magnetic moment and entities, which are necessarily carriers of the magnetic moment. Suppose that an array of the latter entities, i.e. those which have the non-zero magnetic moment, constitutes the magnetic lattice of this material. For simplicity, we will restrict our attention just to crystalline magnetic materials even though this assumption is not indispensable. Under this assumption, however, the magnetic lattice also shows a perfect crystal order and further simplifications immediately suggest themselves. If the carriers of magnetic moment are small dipole magnets, for which field of force decays as a third power of their distance, it would be adequate to account for nearest-neighbour interactions only. Considering that the magnetic moment arises from the spin, which is quantized and of pure quantum-mechanical origin, it is quite reasonable to suppose that little magnets can point either in one conspicuous direction, or, on the contrary, in opposite direction. Thus, one finally arrives at definition of the Ising model: spins (little dipole magnets) located at vertices of the magnetic lattice are able to point 'up' or 'down' and the total magnetic energy is thoroughly determined by overall spin configuration on the magnetic lattice. Hence, one Ising spin variable $\sigma_i = \pm 1$ ($i = 1, 2, \ldots, N$) should be ascribed to each site of the magnetic lattice (N denotes the total number of sites) and this spin variable unambiguously determines a projection of the magnetic moment at ith lattice site. Altogether, it could be concluded that all macroscopic properties will be entirely given by the overall configurational energy of the Ising spins on the magnetic lattice.

2.1 Open Ising chain: combinatorial approach

Let us start by writing the Hamiltonian of the open Ising chain

$$\mathcal{H} = -\sum_{i=1}^{N-1} J_i \sigma_i \sigma_{i+1}, \tag{2.1}$$

where $\sigma_i = \pm 1$ is the Ising spin variable located at ith lattice site, J_i denotes the exchange interaction between ith and $(i+1)$st nearest neighbours and N labels the total number of sites in the spin chain. As a rule, the crucial step represents calculation of the partition function $\mathcal{Z}$, which is given by

$$\mathcal{Z} = \sum_{\sigma_1=\pm 1} \sum_{\sigma_2=\pm 1} \dots \sum_{\sigma_N=\pm 1} \exp(-\beta \mathcal{H}). \tag{2.2}$$

Substituting the Hamiltonian (2.1) to a canonical definition of the partition function (2.2) leads after straightforward modify to the following relation

$$\begin{aligned} \mathcal{Z} &= \sum_{\sigma_1=\pm 1} \sum_{\sigma_2=\pm 1} \dots \sum_{\sigma_N=\pm 1} \exp\Big[\beta \sum_{i=1}^{N-1} J_i \sigma_i \sigma_{i+1}\Big] \\ &= \sum_{\sigma_1=\pm 1} \sum_{\sigma_2=\pm 1} \dots \sum_{\sigma_N=\pm 1} \exp(\beta J_1 \sigma_1 \sigma_2) \exp(\beta J_2 \sigma_2 \sigma_3) \dots \exp(\beta J_{N-1} \sigma_{N-1} \sigma_N). \end{aligned} \tag{2.3}$$

It is quite obvious that the spin σ_N enters exclusively into the last expression of the product listed in the latter Eq. (2.3) and hence, the partial summation over spin states of the spin σ_N can be performed independently of other summations. In this respect, it is advisable to use this property and to arrange Eq. (2.3) into the following form

$$\begin{aligned} \mathcal{Z} &= \sum_{\sigma_1=\pm 1} \sum_{\sigma_2=\pm 1} \dots \sum_{\sigma_{N-1}=\pm 1} \exp(\beta J_1 \sigma_1 \sigma_2) \exp(\beta J_2 \sigma_2 \sigma_3) \dots \sum_{\sigma_N=\pm 1} \exp(\beta J_{N-1} \sigma_{N-1} \sigma_N) \\ &= \sum_{\sigma_1=\pm 1} \sum_{\sigma_2=\pm 1} \dots \sum_{\sigma_{N-1}=\pm 1} \exp(\beta J_1 \sigma_1 \sigma_2) \exp(\beta J_2 \sigma_2 \sigma_3) \dots 2\cosh(\beta J_{N-1} \sigma_{N-1}). \end{aligned} \tag{2.4}$$

If doing so, the spin variable σ_{N-1} now enters in the last term of the expression (2.4) into the argument of even function and in the consequence of that, this argument becomes independent thereof. With all this in mind, the resulting expression for the partition function (2.4) can be further simplified to

$$\begin{aligned} \mathcal{Z} = 2\cosh(\beta J_{N-1}) \sum_{\sigma_1=\pm 1} \sum_{\sigma_2=\pm 1} \dots \sum_{\sigma_{N-1}=\pm 1} \exp(\beta J_1 \sigma_1 \sigma_2) \;\; \exp(\beta J_2 \sigma_2 \sigma_3) \dots \\ \exp(\beta J_{N-2} \sigma_{N-2} \sigma_{N-1}). \end{aligned} \tag{2.5}$$

It can be readily understood that Eq. (2.5) represents, notwithstanding of the multiplicative factor $2\cosh(\beta J_{N-1})$ in front of the summations, the partition function of the open Ising chain with in total $(N-1)$ spins. Moreover, this procedure can be recurrently repeated with the spin σ_{N-1} and also others. By performing this sequence of recurrent summations, one arrives at a final expression for the partition function

$$\begin{aligned}\mathcal{Z} &= 2\cosh(\beta J_{N-1})2\cosh(\beta J_{N-2})\ldots\sum_{\sigma_1=\pm1}2\cosh(\beta J_1\sigma_1)\\ &= 2\prod_{i=1}^{N-1}2\cosh(\beta J_i) = 2^N\prod_{i=1}^{N-1}\cosh(\beta J_i).\end{aligned} \tag{2.6}$$

The equation (2.6) represents a central result of our calculation from which all characteristic features of the open Ising chain can be particularly examined with the help of basic thermodynamical-statistical relations. For illustrative purposes, the thermodynamics of the closed Ising chain will be studied more systematically in the following part.

Exercises

1. Evaluate $\sum_{\sigma_1=\pm1}\sum_{\sigma_2=\pm1}\ldots\sum_{\sigma_N=\pm1}2$.
2. Evaluate $\sum_{\sigma_1=\pm1}\sum_{\sigma_2=\pm1}\ldots\sum_{\sigma_N=\pm1}2\sin(\alpha\sigma_1)$.
3. Evaluate $\sum_{\sigma_1=\pm1}\sum_{\sigma_2=\pm1}\ldots\sum_{\sigma_N=\pm1}2\cos(\alpha\sigma_2)$.
4. Evaluate $\sum_{\sigma_1=\pm1}\sum_{\sigma_2=\pm1}\ldots\sum_{\sigma_N=\pm1}\prod_{i=1}^{N}\Big[2\cosh(\alpha\sigma_i)\Big]$.
5. Verify for open Ising chain that $\langle\sigma_1\sigma_2\rangle = \frac{\partial\ln\mathcal{Z}}{\partial\beta J_1}$.
6. Verify for open Ising chain that $\langle\sigma_i\sigma_{i+1}\rangle = \frac{\partial\ln\mathcal{Z}}{\partial\beta J_i}$.
7. Verify for open Ising chain that $\langle\sigma_i\sigma_{i+r}\rangle = \frac{\partial^r\ln\mathcal{Z}}{\partial\beta J_{i+r-1}\ldots\partial\beta J_{i+1}\partial\beta J_i}$.
8. Calculate pairwise spin correlations $\langle\sigma_1\sigma_2\rangle$, $\langle\sigma_i\sigma_{i+1}\rangle$ and $\langle\sigma_i\sigma_{i+r}\rangle$ for open Ising chain.
9. By expanding $\exp(\alpha\sigma_i)$ into a series $\exp(\alpha\sigma_i) = \sum_{i=0}^{\infty}a_i\sigma^i$ verify a validity of the exact van der Waerden identity: $\exp(\alpha\sigma_i) = \cosh(\alpha) + \sigma_i\sinh(\alpha)$.
10. Prove Eq. (2.6) by substituting the modified van der Waerden identity for $\exp(\beta J_i\sigma_i\sigma_{i+1}) = \cosh(\beta J_i) + \sigma_i\sigma_{i+1}\sinh(\beta J_i)$ into Eq. (2.3)!

2.2 Closed Ising chain: transfer-matrix method

Now, let us start with a fairly simple Hamiltonian for the Ising model on a closed chain, which includes, in addition to the pairwise spin-spin interaction J, also the single-spin interaction H. While the former term should serve for describing the pairwise exchange interaction between the nearest-neighbour spins, the latter term should account for the magnetostatic Zeeman energy of a single spin (magnetic moment) placed in an external magnetic field H. The Hamiltonian of closed Ising chain of N spins is then given by

$$\mathcal{H} = -J \sum_{i=1}^{N} \sigma_i \sigma_{i+1} - H \sum_{i=1}^{N} \sigma_i, \tag{2.7}$$

where the same strengths of nearest-neighbour coupling are assumed for simplicity and the periodic boundary condition is imposed by the constraint $\sigma_{N+1} \equiv \sigma_1$. This is equivalent to joining the two ends of the Ising chain as to form a closed circle. It is worthwhile to remark that the periodic boundary condition ensures a translational invariance of the closed Ising chain what largely simplifies further treatment. On the other hand, the inclusion of the single-spin interaction term H into the Hamiltonian (2.7) precludes the application of the simple combinatorial approach, which has been rather efficiently used in the preceding part to attain the exact solution for the open Ising chain in an absence of the external magnetic field. The most straightforward way to obtain the exact solution for the Ising chain in a presence of the external field is offered by the *transfer-matrix method* originally introduced to statistical physics by H. A. Kramers and G. H. Wannier [2]. This rather powerful technique is of particular importance for at least two reasons. First, this method formulates the problem of finding the exact solution in a relatively easily tractable matrix form and secondly, this useful device is rather general and can be adapted to other interacting many-particle systems, as well.

For further convenience, it is very advisable to rewrite the total Hamiltonian (2.7) into the most symmetric form

$$\mathcal{H} = \sum_{i=1}^{N} \left[-J\sigma_i\sigma_{i+1} - H(\sigma_i + \sigma_{i+1})/2 \right]. \tag{2.8}$$

By the use of the symmetrized Hamiltonian (2.8), the partition function can easily be

factorized into a product of several terms each involving just two adjacent spins

$$\mathcal{Z} = \sum_{\sigma_1=\pm1} \sum_{\sigma_2=\pm1} \dots \sum_{\sigma_N=\pm1} \prod_{i=1}^{N} \exp[\beta J \sigma_i \sigma_{i+1} + \beta H(\sigma_i + \sigma_{i+1})/2]. \tag{2.9}$$

Next, let us formally substitute each factor in the product (2.9) by the function $T(\sigma_i, \sigma_{i+1})$ depending just on the two nearest-neighbouring spins σ_i and σ_{i+1} in order to obtain

$$\mathcal{Z} = \sum_{\sigma_1=\pm1} \sum_{\sigma_2=\pm1} \dots \sum_{\sigma_N=\pm1} T(\sigma_1, \sigma_2) T(\sigma_2, \sigma_3) \dots T(\sigma_i, \sigma_{i+1}) \dots T(\sigma_N, \sigma_1), \tag{2.10}$$

where

$$T(\sigma_i, \sigma_{i+1}) = \exp[\beta J \sigma_i \sigma_{i+1} + \beta H(\sigma_i + \sigma_{i+1})/2]. \tag{2.11}$$

It should be mentioned that the function (2.11) is not the only possible choice for $T(\sigma_i, \sigma_{i+1})$, it can be multiplied for instance by any factor $\exp[a(\sigma_i - \sigma_{i+1})]$ (a is arbitrary constant) without loosing a validity of the overall product (2.9). However, this choice is the only one that preserves a complete symmetry with respect to $\sigma_i \leftrightarrow \sigma_{i+1}$ interchange

$$T(\sigma_i, \sigma_{i+1}) = T(\sigma_{i+1}, \sigma_i). \tag{2.12}$$

At this stage, it is useful to make a small calculation that reveals an essence of the expression (2.11). Recalling that the spin σ_2, for example, enters in Eq. (2.10) just to the two side-by-side standing expressions $T(\sigma_1, \sigma_2)$ and $T(\sigma_2, \sigma_3)$, the summation over spin states of the spin σ_2 can be performed regardless of other expressions to emerge within this product. Thus, one easily finds that

$$\begin{aligned} \sum_{\sigma_2=\pm1} T(\sigma_1, \sigma_2) T(\sigma_2, \sigma_3) &= \sum_{\sigma_2=\pm1} \exp[\beta J \sigma_2(\sigma_1 + \sigma_3) + \beta H(\sigma_1 + 2\sigma_2 + \sigma_3)/2] \\ &= \exp[\beta H(\sigma_1 + \sigma_3)/2] \Big\{ \exp[\beta J(\sigma_1 + \sigma_3) + \beta H] + \exp[-\beta J(\sigma_1 + \sigma_3) - \beta H] \Big\}. \end{aligned} \tag{2.13}$$

Now, we will show that the same result is obtained by assuming that the expression $T(\sigma_i, \sigma_{i+1})$ is the two-by-two matrix with appropriately chosen matrix elements

$$T(\sigma_i, \sigma_{i+1}) = \begin{pmatrix} T(+,+) & T(+,-) \\ T(-,+) & T(-,-) \end{pmatrix} = \begin{pmatrix} \exp(\beta J + \beta H) & \exp(-\beta J) \\ \exp(-\beta J) & \exp(\beta J - \beta H) \end{pmatrix}, \tag{2.14}$$

which are related to four possible spin configurations available to the two adjacent spins σ_i and σ_{i+1}. The matrix element $T(+,-)$ marks for instance the Boltzmann's factor to be obtained from Eq. (2.11) by considering the particular spin configuration $\sigma_i = +1$ and $\sigma_{i+1} = -1$. Accordingly, each row in the matrix $T(\sigma_i, \sigma_{i+1})$ accounts for spin states of the former spin σ_i (in other words, by changing a row one changes a spin state of the former spin σ_i), while each column stands for spin states of the latter spin σ_{i+1} (by changing a column one changes a spin state of the latter spin σ_{i+1}). Note furthermore that the spin variable σ_2 enters in the first expression $T(\sigma_1, \sigma_2)$ as the latter spin, while in the second expression $T(\sigma_2, \sigma_3)$ it acts as the former spin. Consequently, the summation over spin states of the spin σ_2 changes the first expression $T(\sigma_1, \sigma_2)$ to the one-by-two (row) matrix and the second expression $T(\sigma_2, \sigma_3)$ to the two-by-one (column) matrix. It can be easily verified that the summation over spin configurations of the spin σ_2 is then equivalent to a matrix multiplication between the row matrix $T(\sigma_1, \sigma_2)$ and the column matrix $T(\sigma_2, \sigma_3)$

$$\begin{aligned}\sum_{\sigma_2=\pm1} T(\sigma_1,\sigma_2)T(\sigma_2,\sigma_3) = \\ \Big(\ \exp\Big[\beta J\sigma_1 + \tfrac{\beta H}{2}(\sigma_1+1)\Big] \quad \exp\Big[-\beta J\sigma_1 + \tfrac{\beta H}{2}(\sigma_1-1)\Big]\ \Big) \\ \begin{pmatrix} \exp\Big[\beta J\sigma_3 + \frac{\beta H}{2}(\sigma_3+1)\Big] \\ \exp\Big[-\beta J\sigma_3 + \frac{\beta H}{2}(\sigma_3-1)\Big] \end{pmatrix} \\ = \exp\Big[\frac{\beta H}{2}(\sigma_1+\sigma_3)\Big]\Big\{\exp[\beta J(\sigma_1+\sigma_3)+\beta H] + \exp[-\beta J(\sigma_1+\sigma_3)-\beta H]\Big\}.\end{aligned} \tag{2.15}$$

As one can see, the final expression (2.15) obtained from the matrix product is indeed consistent with the result (2.13) acquired by a straightforward summation. Besides, this final expression might be considered as some two-by-two matrix T^2, the elements of which depend on the spins σ_1 and σ_3 through Eq. (2.15)

$$\sum_{\sigma_2=\pm1} T(\sigma_1,\sigma_2)T(\sigma_2,\sigma_3) = T^2(\sigma_1,\sigma_3). \tag{2.16}$$

Accordingly, the summations over spin states of the spins $\sigma_2, \sigma_3, \ldots, \sigma_N$ can be regarded as successive matrix multiplications yielding

$$\mathcal{Z} = \sum_{\sigma_1=\pm1}\sum_{\sigma_2=\pm1}\ldots\sum_{\sigma_N=\pm1} T(\sigma_1,\sigma_2)T(\sigma_2,\sigma_3)\ldots T(\sigma_i,\sigma_{i+1})\ldots T(\sigma_N,\sigma_1)$$

$$= \sum_{\sigma_1=\pm1} \sum_{\sigma_3=\pm1} \cdots \sum_{\sigma_N=\pm1} T^2(\sigma_1,\sigma_3)\ldots T(\sigma_i,\sigma_{i+1})\ldots T(\sigma_N,\sigma_1)$$
$$= \sum_{\sigma_1=\pm1} T^N(\sigma_1,\sigma_1) = T^N(+,+) + T^N(-,-) = \mathrm{Tr}\, T^N. \tag{2.17}$$

At each step of this procedure, the matrix multiplication by T corresponds to the summation over the spin configurations of one more spin site. That is why the matrix T is called as the transfer matrix, namely, it transfers the dependence on the one spin to its neighbouring spin. In addition, it can be also easily understood from Eq. (2.17) that the last summation, which is carried out over the spin states of the spin σ_1, is equivalent to taking a trace of the matrix T^N, i.e. to performing a summation over elements of the matrix T^N on its main diagonal. The problem of finding the exact solution for the closed Ising chain thus reduces to the calculation of a trace of so far unknown matrix T^N.

For calculating a trace of the matrix T^N, it is very convenient to use an invariance of the trace with respect to a cyclic permutation of the product. For instance, the product of three square matrices A, B and C has the same trace upon following cyclic permutations $\mathrm{Tr}(ABC)$=$\mathrm{Tr}(BCA)$=$\mathrm{Tr}(CAB)$.[3] In this respect, the unitary matrix U and its inverse U^{-1} ($U^{-1}U = UU^{-1} = 1$), which convert the transfer matrix T into a diagonal form

$$U^{-1}TU = \Lambda = \begin{pmatrix} \lambda_+ & 0 \\ 0 & \lambda_- \end{pmatrix} \tag{2.18}$$

can be inserted into the latter relation (2.17) to give

$$\mathcal{Z} = \mathrm{Tr}\, T^N = \mathrm{Tr}(TT\ldots T) = \mathrm{Tr}(UU^{-1}TUU^{-1}TU\ldots U^{-1}T)$$
$$= \mathrm{Tr}(U^{-1}TUU^{-1}TU\ldots U^{-1}TU) = \mathrm{Tr}(\Lambda\Lambda\ldots\Lambda) = \mathrm{Tr}\,\Lambda^N. \tag{2.19}$$

The above result is nothing but a similarity invariance, which means that T^N and Λ^N matrices have the same trace (the trace does not depend on a particular choice of basis). Because the matrix Λ^N is actually Nth power of the diagonal matrix, thence it follows that its diagonal elements are simply Nth power of diagonal elements of the matrix Λ

$$\Lambda^N = \begin{pmatrix} \lambda_+^N & 0 \\ 0 & \lambda_-^N \end{pmatrix}. \tag{2.20}$$

[3] By invoking the definition of a matrix multiplication, it is quite elementary to prove $\mathrm{Tr}(AB) = \sum_i (AB)_{ii} = \sum_i \sum_j A_{ij}B_{ji} = \sum_j \sum_i B_{ji}A_{ij} = \sum_j (BA)_{jj} = \mathrm{Tr}(BA)$. The cyclic property of the trace of the product of three matrices A, B and C can be proved in a similar way.

To calculate the desired trace $\mathrm{Tr}\, T^N = \mathrm{Tr}\, \Lambda^N = \lambda_+^N + \lambda_-^N$, it is therefore sufficient to find elements of the diagonal matrix Λ. This eigenvalue problem can be attacked with the help of unitary transformation $TU = U\Lambda$, which can be written in the matrix representation

$$\begin{pmatrix} T(+,+) & T(+,-) \\ T(-,+) & T(-,-) \end{pmatrix} \begin{pmatrix} a_+ & a_- \\ b_+ & b_- \end{pmatrix} = \begin{pmatrix} a_+ & a_- \\ b_+ & b_- \end{pmatrix} \begin{pmatrix} \lambda_+ & 0 \\ 0 & \lambda_- \end{pmatrix} \tag{2.21}$$

and is equivalent to solving the so-called characteristic (secular) equation

$$TV_\pm = \lambda_\pm V_\pm \Longleftrightarrow \begin{pmatrix} T(+,+) & T(+,-) \\ T(-,+) & T(-,-) \end{pmatrix} \begin{pmatrix} a_\pm \\ b_\pm \end{pmatrix} = \lambda_\pm \begin{pmatrix} a_\pm \\ b_\pm \end{pmatrix}. \tag{2.22}$$

Here, $V_\pm$ denote eigenvectors of the transfer matrix T and $\lambda_\pm$ are their corresponding eigenvalues. Both secular equations are in fact a homogeneous system of linear equations, which has a non-trivial solution if and only if its determinant is equal to zero

$$\mathrm{Det}|T - \lambda_i I| = 0, \quad (i \in \{\pm\}) \tag{2.23}$$

where I is used for labeling the unit matrix of appropriate size. In this way, the eigenvalues of the transfer matrix T can be calculated without knowing explicit form of the corresponding eigenvectors $V_\pm$. As a matter of fact, both the eigenvalues can readily be calculated by solving the determinant

$$\begin{vmatrix} \exp(\beta J + \beta H) - \lambda_i & \exp(-\beta J) \\ \exp(-\beta J) & \exp(\beta J - \beta H) - \lambda_i \end{vmatrix} = 0, \tag{2.24}$$

which gives after straightforward calculation

$$\lambda_\pm = \exp(\beta J) \left[\cosh(\beta H) \pm \sqrt{\sinh^2(\beta H) + \exp(-4\beta J)} \right]. \tag{2.25}$$

The final expression for the partition function of the closed Ising chain in a presence of the external magnetic field is subsequently given by

$$\mathcal{Z} = \mathrm{Tr}\, T^N = \mathrm{Tr}\, \Lambda^N = \lambda_+^N + \lambda_-^N. \tag{2.26}$$

The equation (2.26) represents a central result of our calculation, since the whole thermodynamics of the closed Ising chain is being accessible from the partition function. In addition, it can be easily proved by setting $H = 0$ into Eq. (2.26) that the partition

functions (2.6) and (2.26) of the open and closed Ising chains become completely identical in the thermodynamic limit $N \to \infty$. This is consistent with our expectations, since the boundary effects become negligible in the limit of infinity large system. In the thermodynamic limit, the final expression for Helmholtz free energy normalized per one spin[4] is also considerably simplified by realizing that the ratio $\frac{\lambda_-}{\lambda_+}$ is always less than unity

$$\begin{aligned}\mathcal{F} &= -k_{\mathrm{B}}T\frac{1}{N}\lim_{N\to\infty}\ln\mathcal{Z} = -k_{\mathrm{B}}T\frac{1}{N}\lim_{N\to\infty}\ln(\lambda_+^N+\lambda_-^N)\\ &= -k_{\mathrm{B}}T\frac{1}{N}\lim_{N\to\infty}\ln\left\{\lambda_+^N\left[1+\left(\frac{\lambda_-}{\lambda_+}\right)^N\right]\right\} = -k_{\mathrm{B}}T\ln\lambda_+. \end{aligned} \tag{2.27}$$

According to Eq. (2.27), the Helmholtz free energy but also all other important thermodynamic quantities depend solely on the largest eigenvalue λ_+ of the transfer matrix. It is noteworthy that this is even true for any other interacting many-particle system, which can be treated within the transfer-matrix method. Thus, the problem of finding the exact solution within the transfer-matrix approach is essentially the problem of finding the largest eigenvalue of the relevant transfer matrix.

Now, let us take a closer look at thermodynamics of the closed Ising chain[5]. It can be readily understood from Eq. (2.27) that the Helmholtz free energy is a smooth analytic function of the temperature for all non-zero temperatures and thence, the exact solution admits no phase transition. The absence of phase transition in 1D Ising model means that this model cannot sustain a spontaneous magnetization at any finite temperature. To clarify this issue in detail, let us derive the exact expression for the magnetization as a function of the temperature and magnetic field. One possible route how to obtain the total magnetization is to differentiate the Helmholtz free energy with respect to the external magnetic field

$$M = \left\langle\sum_{i=1}^{N}\sigma_i\right\rangle = \frac{1}{\mathcal{Z}}\sum_{\{\sigma_i\}}\left[\left(\sum_{i=1}^{N}\sigma_i\right)\exp(-\beta\mathcal{H})\right] = -\frac{\partial\mathcal{F}}{\partial(\beta H)}. \tag{2.28}$$

In above, the summation $\sum_{\{\sigma_i\}}$ runs over all possible spin configurations. Because the closed Ising chain is translationally invariant, the expected (averaged) values of each single-site

[4]Helmholtz free energy as one of thermodynamical potentials is an extensive quantity.

[5]Open Ising chain has the same thermodynamic properties due to negligible boundary effects.

magnetization must be equal one to each other

$$m = \langle\sigma_1\rangle = \langle\sigma_2\rangle = \ldots = \langle\sigma_N\rangle. \tag{2.29}$$

With regard to this, the magnetization per one site can be obtained after straightforward differentiation and a little bit more involved algebraic procedures from

$$m = -\frac{1}{N}\frac{\partial\mathcal{F}}{\partial(\beta H)} = \frac{\sinh(\beta H)}{\sqrt{\sinh^2(\beta H) + \exp(-4\beta J)}}. \tag{2.30}$$

It is easy to prove that the magnetization is equal to zero ($m = 0$) whenever zero magnetic field ($H = 0$) is set to Eq. (2.30) and whence it follows that there is no spontaneous magnetization at any finite (non-zero) temperature. In accord with this statement, the Ising chains (no matter whether closed or open) do not exhibit a phase transition towards the spontaneously long-range ordered phase with $m \neq 0$ at any finite temperature. There is nevertheless still possibility that the absolute zero temperature ($T = 0$ K) by itself is a critical point at which the spontaneous long-range ordering might appear. Under the assumption of the ferromagnetic interaction ($J > 0$), it can be readily verified that the spontaneous magnetization takes its saturation values in the zero temperature limit

$$\lim_{\beta H \to 0} \lim_{T \to 0^+} m(T, H) = \pm 1. \tag{2.31}$$

and the conjecture about a critical point at zero temperature is indeed verified.

To provide a deeper insight into this rather intricate critical behaviour, it is necessary to study the pair correlation function between two spins and its dependence on a lattice spacing between them. For this purpose, we will need an explicit expression for both the eigenvectors $V_\pm$ creating the matrices of unitary transformation. According to Eq. (2.22), the coefficients that determine both eigenvectors $V_\pm$ must obey following conditions

$$a_\pm = b_\pm \frac{T(+,-)}{\lambda_\pm - T(+,+)} \quad \text{and} \quad a_\pm = b_\pm \frac{\lambda_\pm - T(-,-)}{T(-,+)}, \tag{2.32}$$

which can be symmetrized upon their multiplication to

$$a_\pm^2 = b_\pm^2 \frac{\lambda_\pm - T(-,-)}{\lambda_\pm - T(+,+)}. \tag{2.33}$$

The relationship between these coefficients can be rewritten in a more useful form by substituting the eigenvalues (2.25) and the elements of transfer matrix (2.14) into Eq. (2.33)

$$a_{\pm}^2 = b_{\pm}^2 \frac{\sinh(\beta H) \pm \sqrt{\sinh^2(\beta H) + \exp(-4\beta J)}}{-\sinh(\beta H) \pm \sqrt{\sinh^2(\beta H) + \exp(-4\beta J)}}. \tag{2.34}$$

For further convenience, let us introduce a new variable that is connected with the temperature T, the exchange constant J and the magnetic field H by means of the relation $\mathrm{cotg}2\phi = \exp(2\beta J)\sinh(\beta H)$, which will significantly simplify further steps in the calculation. Within the new notation, the coefficients $a_{\pm}$ and $b_{\pm}$ satisfy the relation

$$a_{\pm}^2 = -b_{\pm}^2 \frac{\cos 2\phi \pm 1}{\cos 2\phi \mp 1}, \tag{2.35}$$

which together with the normalization condition $a_{\pm}^2 + b_{\pm}^2 = 1$ unambiguously determines both the eigenvectors $V_{\pm}$. After straightforward calculation, it is possible to derive explicit expressions for the coefficients $a_{\pm}$ and $b_{\pm}$

$$a_+ = \cos\phi, \quad b_+ = \sin\phi, \qquad \text{and} \qquad a_- = -\sin\phi, \quad b_- = \cos\phi. \tag{2.36}$$

With the help of the coefficients (2.36), the explicit expression of the unitary matrix U and its inverse matrix U^{-1} can be found following the standard algebraic procedures

$$U = \begin{pmatrix} \cos\phi & -\sin\phi \\ \sin\phi & \cos\phi \end{pmatrix} \qquad \text{and} \qquad U^{-1} = \begin{pmatrix} \cos\phi & \sin\phi \\ -\sin\phi & \cos\phi \end{pmatrix}. \tag{2.37}$$

Now, the pairwise correlation $\langle \sigma_i \sigma_j \rangle$ between the two spins that reside some general ith and jth position within the closed chain can be immediately calculated. The statistical definition of the canonical ensemble average (1.7) allows us to calculate the correlation $\langle \sigma_i \sigma_j \rangle$ in terms of transfer matrices

$$\begin{aligned} \langle \sigma_i \sigma_j \rangle = \frac{1}{\mathcal{Z}} \sum_{\{\sigma_i\}} \sigma_i \sigma_j \exp(-\beta H) = \frac{1}{\mathcal{Z}} \sum_{\{\sigma_i\}} \Big[& T(\sigma_1, \sigma_2) T(\sigma_2, \sigma_3) \dots \\ & T(\sigma_{i-1}, \sigma_i) \sigma_i T(\sigma_i, \sigma_{i+1}) \dots T(\sigma_{j-1}, \sigma_j) \sigma_j T(\sigma_j, \sigma_{j+1}) \dots T(\sigma_N, \sigma_1) \Big], \end{aligned} \tag{2.38}$$

where $j > i$ is assumed without loss of the generality. If summation over spin configurations is followed by inserting the unitary and its inverse matrix to each term of the matrix product, the two-spin correlation (2.38) can be rearranged to a more appropriate form

$$\langle \sigma_i \sigma_j \rangle = \frac{1}{\mathcal{Z}} \mathrm{Tr} \left[S T^{j-i} S T^{N+i-j} \right] = \frac{1}{\mathcal{Z}} \mathrm{Tr} \left[U^{-1} S U \Lambda^{j-i} U^{-1} S U \Lambda^{N+i-j} \right] \tag{2.39}$$

using the cyclic permutation of matrices behind the relevant trace and the diagonal matrix S with elements $S(\sigma_i, \sigma_j) = \sigma_i \delta_{ij}$ (δ_{ij} is Kronecker symbol), which should account for possible spin states of σ_i and σ_j spins. An elementary calculation gives from Eq. (2.37)

$$U^{-1}SU = \begin{pmatrix} \cos 2\phi & -\sin 2\phi \\ -\sin 2\phi & -\cos 2\phi \end{pmatrix}, \tag{2.40}$$

which together with the explicit expression (2.18) of the matrix Λ yields after straightforward but little bit tedious modification the following result for the two-spin correlation

$$\langle \sigma_i \sigma_{i+r} \rangle = \frac{\lambda_+^N \cos^2 2\phi + \lambda_+^{N-r} \lambda_-^r \sin^2 2\phi + \lambda_+^r \lambda_-^{N-r} \sin^2 2\phi + \lambda_-^N \cos^2 2\phi}{\lambda_+^N + \lambda_-^N}, \tag{2.41}$$

where $r = i - j$ is used to measure a distance in between the ith and jth spins. In the thermodynamic limit, the pairwise correlation (2.41) can be largely simplified to

$$\langle \sigma_i \sigma_{i+r} \rangle = \cos^2 2\phi + \left(\frac{\lambda_-}{\lambda_+} \right)^r \sin^2 2\phi. \tag{2.42}$$

It should be mentioned that the expression (2.42) represents the most general result for the two-spin correlation, which depends on a distance r between spins, the ratio between the smaller and the larger eigenvalue of the transfer matrix and the two expressions directly connected with the relation $\mathrm{cotg} 2\phi = \exp(2\beta J) \sinh(\beta H)$ via terms

$$\cos 2\phi = \frac{\sinh(\beta H)}{\sqrt{\sinh^2(\beta H) + \exp(-4\beta J)}}, \quad \sin 2\phi = \frac{\exp(-2\beta J)}{\sqrt{\sinh^2(\beta H) + \exp(-4\beta J)}}. \tag{2.43}$$

In an absence of the external field ($H = 0$), the expression (2.42) for the two-spin correlation further reduces, because of the validity of $\cos 2\phi = 0$ and $\sin 2\phi = 1$, to

$$\langle \sigma_i \sigma_{i+r} \rangle = \left(\frac{\lambda_-}{\lambda_+} \right)^r = [\tanh(\beta J)]^r. \tag{2.44}$$

It can be easily understood from Eq. (2.44) that the two-spin correlation is determined by rth power of the ratio between the smaller and larger eigenvalue of the transfer matrix. With regard to this, the correlation between two spins exhibits a peculiar *power-low decay* with the distance r in between them. In other words, the correlation between distant spins is simply rth power of the correlation between the nearest-neighbour spins. It should be realized that the expression $\tanh(\beta J)$ is at any finite temperature always less than unity

and thus, the two-spin correlation gradually tends to zero with increasing the lattice spacing r. Actually, in the limiting case $r \to \infty$ it is easy to prove

$$\lim_{r\to\infty} \langle \sigma_i \sigma_{i+r} \rangle = 0 \qquad \text{for any} \quad T \neq 0. \tag{2.45}$$

The expression (2.45) proves in fact an absence of the long-range order at any finite temperature and hence, the Ising chain might exhibit a spontaneous ordering just at the absolute zero temperature. In the limit of zero temperature one actually finds

$$\lim_{r\to\infty} \lim_{T\to 0} \langle \sigma_i \sigma_{i+r} \rangle = 1, \tag{2.46}$$

that provides another evidence of the spontaneous ordering at zero temperature. The zero temperature can be thus considered as a very special critical point at which an onset of spontaneous ordering appears. It is therefore of particular interest to look at the critical exponents in the vicinity of this special critical point.

For this purpose, let us first evaluate the two-spin correlation function

$$\Gamma_{ij}(r) = \langle \sigma_i \sigma_j \rangle - \langle \sigma_i \rangle \langle \sigma_j \rangle = \langle \sigma_i \sigma_{i+r} \rangle = [\tanh(\beta J)]^r, \tag{2.47}$$

which can serve as a measure of fluctuations[6] to be present in the considered spin system. Because the critical temperature is in this particular case equal to zero ($T_\mathrm{c} = 0$ K), it is much more advisable to use as a deviation of the temperature from its critical value the quantity $t = \exp(-2\beta J)$ instead of the relative difference $t = (T - T_\mathrm{c})/T_\mathrm{c}$. It is worthwhile to remark that the former quantity is monotonically increasing function of the temperature with the lower bound $t = 0$ corresponding to the lowest possible temperature $T = 0$ K (which is in fact the critical temperature) and the upper bound $t = 1$ corresponding to the highest possible temperature $T \to \infty$. Therefore, the quantity $t = \exp(-2\beta J)$ can be also regarded as a new temperature variable and thus, the pair correlation function can be rewritten in terms of this new temperature variable to

$$\Gamma_{ij}(r) = \left(\frac{1-t}{1+t} \right)^r. \tag{2.48}$$

[6] An alternative definition of two-spin correlation function $\Gamma_{ij}(r) = \langle (\sigma_i - \langle \sigma_i \rangle)(\sigma_j - \langle \sigma_j \rangle) \rangle$ straightforwardly shows its intrinsic physical meaning that lies in average value of the product of two spin fluctuations, i.e. the product comprised of two differences between actual and averaged spin values.

The comparison between Eq. (2.47) [or Eq. (2.48)] and the definition (1.12), which expresses the correlation function Γ_{ij} as a function of the correlation length ξ, consecutively yields the following relationship for the correlation length

$$\xi = -\frac{1}{\ln \tanh(\beta J)} = \frac{1}{\ln\left(\frac{1+t}{1-t}\right)}, \tag{2.49}$$

which indicates that the correlation length diverges as one approaches the zero temperature. It is noteworthy that the divergence of correlation length is generally regarded as the most important vestige that reveals the critical point. Furthermore, let us expand the denominator of Eq. (2.49) in the vicinity of critical temperature ($t = 0$) into a series and let us retain just the leading-order term of the series

$$\ln\left(\frac{1+t}{1-t}\right) = 2t. \tag{2.50}$$

By substituting the expansion (2.50) to Eq. (2.49) one obtains

$$\xi = (2t)^{-1}, \tag{2.51}$$

which allows us to identify the critical exponent of the correlation length when comparing the resultant expression (2.51) with the definition (1.17) of this critical index. Whence it follows that the critical exponent of correlation length is equal to unity ($\nu = 1$) in the Ising chain. Similarly, the relation (2.48) can be utilized to determine the critical exponent η for the correlation function. According to Eq. (2.48), the correlation function becomes constant precisely at the critical point ($t_{\mathrm{c}} = 0$) and so, it is completely independent of the lattice spacing r between the spins. In this respect, the relation (1.13) predicts for the critical exponent of correlation function another simple relation $\eta = 1$. Even although critical exponents pertinent to other thermodynamic quantities (such as the magnetization, susceptibility or specific heat) could be obtained in a similar way, it is much more convenient to use the idea of the two-exponent scaling to determine their explicit values. The total set of scaling relations (1.18)-(1.22) then demands the following values of critical exponents

$$\eta = 1, \quad \nu = \nu' = 1, \quad \alpha = \alpha' = 1, \quad \gamma = \gamma' = 1, \quad \beta = 0, \quad \delta = \infty. \tag{2.52}$$

For simplicity, we will merely provide an independent check of the last two critical exponents β and δ describing the behaviour of the magnetization near the critical temperature.

For later convenience, Eq. (2.30) will be firstly rewritten in terms of the reduced temperature $t = \exp(-2\beta J)$ and the reduced magnetic field $h = \beta H$ to

$$m = \frac{\sinh(h)}{\sqrt{\sinh^2(h) + t^2}}. \tag{2.53}$$

Furthermore, the expression (2.53) should be simplified under the assumption of the small magnetic field ($|h| \ll 1$) to

$$m = \frac{h}{\sqrt{h^2 + t^2}}. \tag{2.54}$$

It is quite obvious from Eq. (2.54) that the magnetization tends in the limiting case to

$$\lim_{h\to 0}\lim_{t\to 0^+} m(t,h) = \pm 1, \tag{2.55}$$

which gives in compliance with Eq. (1.15) both the critical exponents of the magnetization. As a matter of fact, it directly follows from Eqs. (1.15) and (2.55) that the critical exponent β determining disappearance of the spontaneous magnetization upon heating must be equal to zero ($\beta = 0$), while the critical exponent δ that determines how steeply the magnetization increases in response to the rising magnetic field precisely at the critical temperature is given by $\delta = \infty$ ($\beta\delta = 1$).

Exercises

1. By imposing the periodic boundary condition $S_{N+1} \equiv S_1$, the 1D Blume-Emery-Griffiths (BEG) model [3] is described through the following spin Hamiltonian

$$\mathcal{H} = -J\sum_{i=1}^{N} S_i S_{i+1} - D\sum_{i=1}^{N} S_i^2 - Q\sum_{i=1}^{N} S_i^2 S_{i+1}^2,$$

where $S_i = \pm 1, 0$ and the parameters D and Q denote the uniaxial single-ion anisotropy and biquadratic interaction, respectively. Write the transfer matrix for BEG model, diagonalize it and find its largest eigenvalue. Express the partition function and the Helmholtz free energy in terms of the largest eigenvalue.

2. Calculate the reduced magnetization of the closed Ising chain using
$m = \langle\sigma_i\rangle = \frac{1}{\mathcal{Z}}\sum_{\{\sigma_i\}} \sigma_i \exp(-\beta\mathcal{H})$ and verify the validity of Eq. (2.30).

3. Calculate the isothermal susceptibility for the closed Ising chain using $\chi_T = \left(\frac{\partial m}{\partial H}\right)_T$.

4. Calculate the internal energy $\mathcal{U}$ for the closed Ising chain using Eq. (1.3).
5. Calculate the entropy $\mathcal{S}$ for the closed Ising chain using Eq. (1.4).
6. Calculate the specific heat for the closed Ising chain using $\mathcal{C}_H = T\left(\frac{\partial \mathcal{S}}{\partial T}\right)_H$.

2.3 Spin-Peierls phase transition

By adopting the formalism of the transfer-matrix method, it is also of particular interest to search for the structural spin-Peierls transition, which relates to a magnetoelastic phase transition driven by the spin-lattice coupling (dimerization). The spin-Peierls transition is actually a simple structural phase transition of the type *distorted* vs. *undistorted* chain resulting from the spin-lattice interaction. The simplest 1D Ising model, in which the spin-lattice coupling is restricted just to a single-phonon mode of the lattice amenable to harmonic vibrations, has been proposed by Mijatovič, Miloševič and Urumov [4]. In what follows, we shall closely follow the accurate treatment developed by these authors.

Consider the closed Ising chain consisting of N magnetic particles (the periodic boundary condition is imposed by the constraint $(N+1) \equiv 1$), whereas each of the magnetic particles has the same mass M as well as the same spin $\sigma = \frac{1}{2}$. Taking into consideration both the magnetic and the elastic energy of the closed Ising chain, the total Hamiltonian can be written as a sum of both these contributions

$$\mathcal{H} = \mathcal{H}_{\text{spin}} + \mathcal{H}_{\text{lattice}}, \tag{2.56}$$

where the former part

$$\mathcal{H}_{\text{spin}} = -\sum_{l=1}^{N} J_{l,l+1}\sigma_l\sigma_{l+1}, \tag{2.57}$$

accounts for the magnetic energy bearing a relation to the exchange interaction between the nearest-neighbour Ising spins, while the latter part

$$\mathcal{H}_{\text{lattice}} = \frac{1}{2M}\sum_{l=1}^{N} p_l^2 + \frac{1}{2}M\omega^2\sum_{l=1}^{N}(u_{l+1} - u_l)^2, \tag{2.58}$$

corresponds to the elastic energy of longitudinal lattice vibrations described within the usual harmonic approximation; p_l marks the momentum of the lth particle, u_l denotes its deviation from the equilibrium position x_l^0 and ω is a characteristic angular frequency

of the lattice vibration. It is quite apparent from Eq. (2.57) that the coupling constant $J_{l,l+1}$ of the nearest-neighbour Ising interaction depends on a relative distance between the nearest-neighbouring particles and in the consequence of that, it can be expanded into a series in terms of the particle displacement. Assuming only small lattice distortions (harmonic approximation) and retaining just first two terms from this expansion relates the exchange constant $J_{l,l+1}$ to a relative distance between the lth and $(l+1)$st particles

$$J_{l,l+1} \equiv J_{u_{l+1}-u_l} = J_0 + J_1(u_{l+1} - u_l). \tag{2.59}$$

Next, it is convenient to utilize the Fourier representation of the displacement operator

$$u_l = \sum_q \frac{1}{\sqrt{NM}} \exp(iqx_l^0) Q_q \tag{2.60}$$

and to rewrite the total Hamiltonian (2.56) by introducing the usual creation b_q^+ and annihilation b_q operators to

$$\begin{aligned}\mathcal{H} = &-J_0 \sum_{l=1}^{N} \sigma_l \sigma_{l+1} - \frac{J_1}{4} \sum_{l=1}^{N} \sum_q [1 - \exp(iqa)] \exp(iqx_l^0)[b_q + b_{-q}^+] \sigma_l \sigma_{l+1} \\ &+ \sum_q \omega(q) b_q^+ b_q. \end{aligned} \tag{2.61}$$

Here, $\omega(q) = \Omega_0 \sqrt{\sin(qa/2)}$ and a denotes the undistorted lattice spacing. For simplicity, we shall further suppose just the single-phonon mode with the angular frequency $\omega_0 = \omega(\pi/a)$. Under this assumption, the total Hamiltonian (2.61) can be further simplified by substituting the lattice distortion parameter Δ for the averaged creation and annihilation operators ($\Delta = \langle b_q^+ \rangle = \langle b_q \rangle$)

$$\mathcal{H} = N\omega_0 \Delta^2 - \sum_{l=1}^{N} [J_0 + (-1)^l J_1 \Delta] \sigma_l \sigma_{l+1}. \tag{2.62}$$

The above effective spin Hamiltonian describes the uncoupled Ising chain interacting with a single macroscopically occupied phonon mode with the frequency ω_0.

It can be readily understood from Eq. (2.62) that the spin-phonon coupling can under certain conditions lead to the bond alternation, which is further reflected in the alternating part of the nearest-neighbour exchange interaction. As a matter of fact, the exchange constant J_0 describing the interaction between the nearest-neighbour Ising spins of the

undistorted chain changes upon the lattice distortion to a sequence of the alternating exchange interactions $J_- = J_0 - J_1\Delta$ and $J_+ = J_0 + J_1\Delta$. It should be mentioned, however, that this occurs just when the gain of magnetic energy resulting from the dimerization (i.e. the alternation of the exchange constants) exceeds an increase of the elastic energy associated with the lattice distortion, otherwise there is no distortion and $\Delta = 0$. Owing to this fact, the parameter of lattice distortion Δ must be obtained in a self-consistent manner by minimizing the overall Helmholtz free energy in order to ascertain whether the regularly spaced closed Ising chain becomes unstable with respect to a static dimerization. To attack the problem of finding of the Helmholtz free energy, let us substitute the total Hamiltonian (2.62) to a statistical definition of the partition function (1.2)

$$\mathcal{Z} = \exp(-\beta N\omega_0\Delta^2) \sum_{\sigma_1=\pm1} \sum_{\sigma_2=\pm1} \dots \sum_{\sigma_N=\pm1} \prod_{l=1}^{N} \exp\left\{\beta\left[J_0 + (-1)^l J_1\Delta\right]\sigma_l\sigma_{l+1}\right\}. \quad (2.63)$$

The above equation can be also rewritten by defining transfer matrices

$$T_\pm(\sigma_l, \sigma_{l+1}) = \exp(\beta J_\pm \sigma_l\sigma_{l+1}), \quad \text{with} \quad J_\pm = J_0 \pm J_1\Delta \quad (2.64)$$

into the following form

$$\mathcal{Z} = \exp(-\beta N\omega_0\Delta^2) \sum_{\sigma_1=\pm1} \sum_{\sigma_2=\pm1} \dots \sum_{\sigma_N=\pm1} \prod_{l=1}^{N/2} T_-(\sigma_{2l-1}, \sigma_{2l}) T_+(\sigma_{2l}, \sigma_{2l+1}). \quad (2.65)$$

At this stage, let us firstly perform the summation over all possible spin configurations of the Ising spins σ_{2l} residing even lattice positions. Apparently, this kind of summation is equivalent to multiplying each couple of the side-by-side standing transfer matrices $T_-(\sigma_{2l-1}, \sigma_{2l})$ and $T_+(\sigma_{2l}, \sigma_{2l+1})$ and thereupon, this matrix product leads to a new transfer matrix $T_-T_+(\sigma_{2l-1}, \sigma_{2l+1})$ depending solely on the Ising spins from odd lattice sites. The subsequent summation performed over spin configurations of the Ising spins from the odd lattice positions (except the first one) can be thereby regarded as a successive matrix multiplications between the new transfer matrices $T_-T_+(\sigma_{2l-1}, \sigma_{2l+1})$ and the last summation of taking trace of the result of this matrix product. In this respect, the partition function of the model under investigation can be calculated from

$$\mathcal{Z} = \exp(-\beta N\omega_0\Delta^2)\mathrm{Tr}(T_-T_+)^{\frac{N}{2}}. \quad (2.66)$$

Due to an invariance of the trace, it is sufficient to calculate the relevant trace of the new transfer matrix $T_{-}T_{+}(\sigma_{2l-1},\sigma_{2l+1})$ in its diagonal form. For this purpose, let us explicitly evaluate the matrix elements of the new transfer matrix $T_{-}T_{+}(\sigma_{2l-1},\sigma_{2l+1})$

$$T_{-}T_{+} = \begin{pmatrix} 2\cosh(2\beta J_0) & 2\cosh(2\beta J_1\Delta) \\ 2\cosh(2\beta J_1\Delta) & 2\cosh(2\beta J_0) \end{pmatrix}. \tag{2.67}$$

Eigenvalues of the above matrix can be straightforwardly obtained following the same approach as described in the preceding part, actually, one readily finds after some algebra

$$\lambda_{\pm} = 2\cosh(2\beta J_0) \pm 2\cosh(2\beta J_1\Delta). \tag{2.68}$$

Using the eigenvalues (2.68), the partition function becomes

$$\mathcal{Z} = \exp(-\beta N\omega_0\Delta^2)(\lambda_{+}^{\frac{N}{2}} + \lambda_{-}^{\frac{N}{2}}). \tag{2.69}$$

and according to this, the Helmholtz free energy reduced per one Ising spin immediately follows from the exact result (2.69) and the definition (1.4). In the thermodynamic limit the Helmholtz free energy per spin is given by

$$\mathcal{F} = \omega_0\Delta^2 - \frac{k_{\rm B}T}{2}\ln\Big[2\cosh(2\beta J_0) + 2\cosh(2\beta J_1\Delta)\Big]. \tag{2.70}$$

It is quite evident from Eq. (2.70) that the Helmholtz free energy is even function with respect to the equilibrium coupling constant J_0, the magnetoelastic coupling constant J_1, as well as, the distortion parameter Δ. A few typical dependencies of the Helmholtz free energy (2.70) on the distortion parameter Δ are for better illustration plotted in Fig. 1. Both parameter sets used in Fig. 1 are consistent with existence of three local minima of the Helmholtz free energy at low enough temperatures: one local minimum refers to the undistorted chain with $\Delta = 0$ and the other two relate to the distorted chain with $|\Delta| \neq 0$. It directly follows from Fig. 1 that the magnetoelastic spin-1/2 Ising chain given by the Hamiltonian (2.62) may undergo at sufficiently low temperatures a spin-Peierls dimerization, because the global minimum of the Helmholtz free energy corresponds to nonzero value of the distortion parameter $|\Delta| \neq 0$. There are however two different mechanisms how the spin-Peierls dimerization may vanish. According to the first mechanism, the local minimum of the Helmholtz free energy corresponding to the

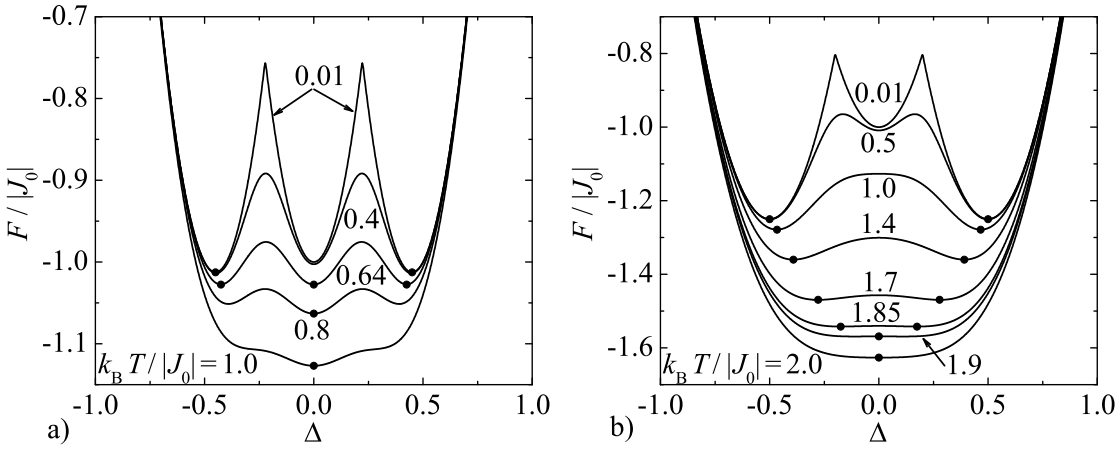

Figure 1: The Helmholtz free energy of the magnetoelastic spin-1/2 Ising chain given by the Hamiltonian (2.62) as a function of the distortion parameter Δ for a few different values of the reduced temperature $k_{\rm B}T/|J_0|$, the fixed value of the angular frequency $\omega_0/|J_0| = 5.0$ and two selected values of the magnetoelastic coupling constant: a) $J_1/|J_0| = 4.5$, b) $J_1/|J_0| = 5.0$. Black circles determine global minima of the Helmholtz free energy (2.70).

undistorted chain $\Delta = 0$ decreases upon increasing of temperature until it reaches the same value as the other two global minima at $|\Delta| \neq 0$ [see Fig. 1a)]. This mechanism thus implies that the spin-Peierls dimerization of the magnetoelastic spin-1/2 Ising chain may disappear at a temperature-driven discontinuous (first-order) phase transition. According to the second mechanism, the local minimum of the Helmholtz free energy corresponding to the undistorted chain $\Delta = 0$ at first vanishes upon rising temperature, while two global minima of the Helmholtz free energy at $|\Delta| \neq 0$ gradually get nearer to each other until they completely merge together at $\Delta = 0$. This another mechanism indicates that the spin-Peierls dimerization of the magnetoelastic spin-1/2 Ising chain may alternatively vanish at a temperature-driven continuous (second-order) phase transition.

Now, let us proceed to a more detailed analysis of the critical phenomena that might possibly occur in the investigated model system. It is worthwhile to recall that the closed Ising chain cannot sustain the spontaneous magnetic ordering at any non-zero temperature and thus, the possible phase transition could merely occur due to a static distortion arising from the spin-lattice coupling. With regard to this, the parameter Δ describing the lattice distortion should be considered as a possible order parameter determining whether the lattice distortion actually emerges or not. As we have already mentioned earlier,

the precise value of the parameter Δ must be obtained from a self-consistent equation minimizing the Helmholtz free energy (2.70) in order to ensure energetic stability of the system. Hence, we adopt the parameter Δ as the order parameter and find the extremal (minimum) value of the Helmholtz free energy by differentiating it with respect to the distortion parameter

$$\frac{\partial \mathcal{F}}{\partial \Delta} = 0 \Longleftrightarrow \omega_0 \Delta = \frac{J_1}{2} \frac{\sinh(2\beta J_1 \Delta)}{\cosh(2\beta J_1 \Delta) + \cosh(2\beta J_0)}. \tag{2.71}$$

By introducing a new set of scaled variables Δ', J_0' and T'

$$\Delta' = \frac{\omega_0}{J_1}\Delta, \quad J_0' = \frac{\omega_0}{J_1}\frac{J_0}{J_1}, \quad \text{and} \quad T' = \frac{\omega_0}{J_1}\frac{k_{\mathrm{B}}T}{J_1}, \tag{2.72}$$

it is useful to rewrite Eq. (2.71) to a more convenient form

$$\Delta' = \frac{1}{2} \frac{\sinh(2\Delta'/T')}{\cosh(2\Delta'/T') + \cosh(2J_0'/T')}. \tag{2.73}$$

In the zero temperature limit, it can be readily verified from Eq. (2.73) that there is no distortion whenever $|J_1| < \sqrt{2\omega_0|J_0|}$, since the distortion parameter becomes zero $\Delta' = 0$ (or equivalently $\Delta = 0$) in this range of parameters. On the other hand, the distortion parameter becomes non-zero $\Delta' = \frac{1}{2}$ [or $\Delta = J_1/(2\omega_0)$] as long as $|J_1| > \sqrt{2\omega_0|J_0|}$. This ground-state analysis shows that the regularly spaced Ising chain becomes unstable with respect to the static dimerization (spin-Peierls instability) just when an increase of the exchange constant induced by the lattice distortion, which is represented by the interaction parameter J_1, is greater than a square root of the product of the equilibrium exchange constant J_0, the angular frequency ω_0 and the factor 2.

Let us turn our attention to a detailed analysis of the critical phenomena at non-zero temperatures. It is quite reasonable to expect that the distortion parameter decreases upon the temperature rise in the parameter space, where the spin-Peierls instability emerges in the ground state. In the consequence of that, the dimerization should completely vanish above a certain (critical) temperature and it is therefore of particular interest to investigate this kind of critical behaviour. For simplicity, the Landau theory of phase transitions will be applied here to locate critical points of continuous (second-order) transitions and owing to this fact, the Helmholtz free energy (2.70) must be initially expanded in terms of the lattice distortion parameter

$$\mathcal{F} = A + B\Delta^2 + C\Delta^4 + D\Delta^6 + \ldots, \tag{2.74}$$

where

$$A \equiv \mathcal{F}(\Delta = 0) = -\frac{k_\mathrm{B}T}{2}\ln 2 - \frac{k_\mathrm{B}T}{2}\ln[1+\cosh(2\beta J_0)], \tag{2.75}$$

$$B \equiv \left(\frac{\partial^2 \mathcal{F}}{\partial \Delta^2}\right)_{\Delta=0} = 2\omega_0 - \frac{2\beta J_1^2}{1+\cosh(2\beta J_0)} \tag{2.76}$$

$$C \equiv \left(\frac{\partial^4 \mathcal{F}}{\partial \Delta^4}\right)_{\Delta=0} = -8\beta^3 J_1^4 \frac{\cosh^2(2\beta J_0) - \cosh(2\beta J_0) - 2}{[1+\cosh(2\beta J_0)]^3}. \tag{2.77}$$

In the spirit of the Landau theory of phase transitions, the critical points of second-order phase transitions can be located from the equality $B = 0$ whenever the stability condition $C > 0$ is fulfilled. On the other hand, the locus of a tricritical point is given by the requirements $B = 0$, $C = 0$ and the stability condition $D > 0$. According to this, the critical condition determining the critical temperature of continuous structural phase transitions can be transcribed in terms of the reduced variables to

$$B(T_\mathrm{c}) = 0 \Longleftrightarrow T_\mathrm{c}' = \left[1+\cosh(2J_0'/T_\mathrm{c}')\right]^{-1}, \tag{2.78}$$

which gives after some algebraic manipulations the following critical condition

$$J_0' = \frac{T_\mathrm{c}'}{2}\ln\left(\frac{1 - T_\mathrm{c}' \pm \sqrt{1-2T_\mathrm{c}'}}{T_\mathrm{c}'}\right). \tag{2.79}$$

It can be easily proved that the sign ambiguity of Eq. (2.79) does not affect the critical temperature by itself, but it solely determines a sign of the interaction parameter J_0'. Indeed, few lines calculation yields an equivalence between Eq. (2.79) and

$$|J_0'| = \frac{T_\mathrm{c}'}{2}\ln\left(\frac{1 - T_\mathrm{c}' + \sqrt{1-2T_\mathrm{c}'}}{T_\mathrm{c}'}\right). \tag{2.80}$$

In addition, the tricritical point is given by the conditions

$$B(T_\mathrm{t}) = 0 \Longleftrightarrow T_\mathrm{t}' = \left[1+\cosh(2J_0'/T_\mathrm{t}')\right]^{-1}, \tag{2.81}$$

$$C(T_\mathrm{t}) = 0 \Longleftrightarrow \cosh^2(2J_0'/T_\mathrm{t}') - \cosh(2J_0'/T_\mathrm{t}') = 2. \tag{2.82}$$

It can be readily shown that the latter condition is equivalent to

$$\frac{T_\mathrm{t}'}{|J_0'|} = \frac{k_\mathrm{B}T_\mathrm{t}}{|J_0|} = \frac{2}{\ln(2+\sqrt{3})}, \tag{2.83}$$

which in conjunction with the former condition determines the locus of tricritical point

$$T_\mathrm{t}' = \frac{k_\mathrm{B}T_\mathrm{t}}{J_1}\frac{\omega_0}{J_1} = \frac{1}{3} \quad \text{and} \quad |J_0'| = \frac{|J_0|}{J_1}\frac{\omega_0}{J_1} = \frac{1}{6}\ln(2+\sqrt{3}). \tag{2.84}$$

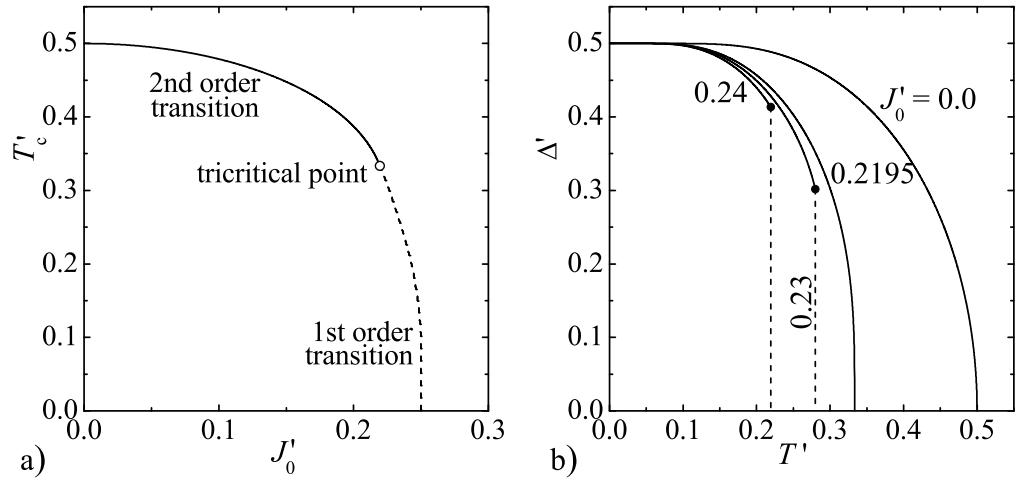

Figure 2: a) Phase diagram of the spin-1/2 Ising chain exhibiting the structural spin-Peierls phase transition; b) Temperature variations of the distortion parameter Δ' (order parameter) for several particular cases, which include the continuous as well as discontinuous phase transitions.

The complete phase diagram is shown in the J_0'-T' plane in Fig. 2a. In this figure, the lines of continuous (discontinuous) structural phase transitions between the distorted and undistorted spin chain are depicted as solid (broken) curves, while the circled point locates the tricritical point given by the coordinates (2.84). As a consequence of this, the regularly spaced chain becomes unstable with respect to a static lattice dimerization (distortion) inside the region bounded by both the displayed transition lines, while it does not exhibit an instability with respect to lattice distortions out of this region. Notice that the afore-described exact phase diagram is fully consistent also with the temperature dependence of the distortion parameter Δ', which represents the order parameter determining an extent of the lattice distortion in the model under investigation. As it can be clearly seen from Fig. 2b, the model system actually exhibits the continuous (discontinuous) phase transitions below (above) the tricritical point.

2.4 Open Ising chain with second-neighbour coupling

Only pairwise interactions between nearest-neighbour spins are usually taken into account within the standard Ising model insomuch that the exchange interaction decays very rapidly with a distance in between the spins. However, it should be also mentioned that the spin-spin interactions between more distant spins can under certain conditions

significantly affect the overall magnetic behaviour especially when the exchange pathway between nearest-neighbour spins becomes rather inefficient. In this part, we shall therefore focus on another interesting exactly solvable 1D Ising model, which allows to account for the interaction between more distant spins. Suppose for instance the open Ising chain in an absence of the external magnetic field given by the Hamiltonian

$$\mathcal{H} = -J_1 \sum_{i=1}^{N-1} \sigma_i \sigma_{i+1} - J_2 \sum_{i=1}^{N-2} \sigma_i \sigma_{i+2}, \tag{2.85}$$

in which the parameter J_1 labels a pairwise interaction between the nearest-neighbouring spins, whereas the parameter J_2 stands for a pairwise interaction between the next-nearest-neighbouring spins. Substitution of the Hamiltonian (2.85) into the canonical definition of the partition function (1.2) straightforwardly leads to the following relationship

$$Q_N = \sum_{\sigma_1=\pm 1} \sum_{\sigma_2=\pm 1} \dots \sum_{\sigma_N=\pm 1} \exp\Big(\beta J_1 \sum_{i=1}^{N-1} \sigma_i \sigma_{i+1} + \beta J_2 \sum_{i=1}^{N-2} \sigma_i \sigma_{i+2}\Big). \tag{2.86}$$

By adopting the Dobson's trick [5], which consists in performing the transformation of a set of the two-state Ising variables $\{\sigma_i\}$ with possible values ± 1 to a new set of two-state Ising variables $\{t_i\}$ with the same values ± 1

$$t_0 = \sigma_1 \quad \text{and} \quad t_i = \sigma_i \sigma_{i+1} \quad (i = 1, 2, \dots, N-1), \tag{2.87}$$

it is possible to transform the open Ising chain with the nearest- and next-nearest-neighbour interactions to the open Ising chain with the nearest-neighbour interaction only, but in a presence of some effective magnetic field. It is noteworthy that the transformation (2.87) can be uniquely inverted because of the trivial identity $\sigma_i^2 \equiv 1$ so that

$$\sigma_i = \sigma_i \sigma_{i-1} \sigma_{i-1} \sigma_{i-2} \dots \sigma_2 \sigma_1 \sigma_1 = t_{i-1} t_{i-2} \dots t_1 t_0 = \prod_{j=0}^{i-1} t_j. \tag{2.88}$$

Owing to this fact, to each possible spin configuration from a set of the Ising spin variables $\{\sigma_i\}$ there corresponds one and just one configuration from a set of new Ising spin variables $\{t_i\}$ and vice versa. In other words, there exists the one-to-one correspondence between configurations given by the old and new Ising spin variables, respectively. Note that this one-to-one correspondence ensures an equivalence between the models expressed via the

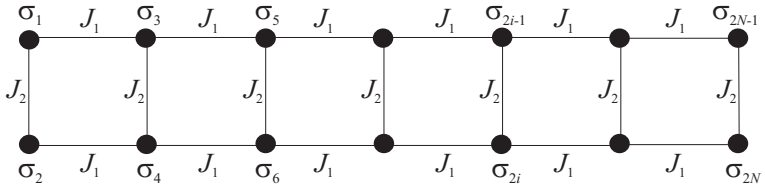

Figure 3: The schematic representation of the spin-1/2 Ising model on the two-leg ladder.

old and new Ising spin variables. Hence, the partition function (2.86) can be rewritten in terms of the new Ising spin variables $\{t_i\}$ to

$$\begin{aligned} Q_N &= \sum_{t_0=\pm1}\sum_{t_1=\pm1}\sum_{t_2=\pm1}\cdots\sum_{t_N=\pm1}\exp\Big(\beta J_1\sum_{i=1}^{N-1}t_i+\beta J_2\sum_{i=1}^{N-2}t_it_{i+1}\Big) \\ &= 2\sum_{t_1=\pm1}\sum_{t_2=\pm1}\cdots\sum_{t_N=\pm1}\exp\Big(\beta J_1\sum_{i=1}^{N-1}t_i+\beta J_2\sum_{i=1}^{N-2}t_it_{i+1}\Big), \end{aligned} \tag{2.89}$$

where we have used the property $\sigma_i\sigma_{i+2}=\sigma_i\sigma_{i+1}^2\sigma_{i+2}=t_it_{i+1}$ and the factor 2 arises from the summation over spin states of the spin t_0 not included in the other terms. Apart from the factor 2 in front of the summations, the latter relation (2.89) represents the partition function of the open Ising chain with in total $(N-1)$ spins, the effective nearest-neighbour coupling $J_{\text{eff}}=J_2$ and the effective magnetic field $H_{\text{eff}}=J_1$. In this respect, the partition function of the open Ising chain with the nearest- and next-nearest-neighbour couplings J_1 and J_2, respectively, can be calculated from the partition function of the open Ising chain with the nearest-neighbour coupling J_{eff} and the effective magnetic field H_{eff}

$$Q_N = 2\mathcal{Z}_{N-1}(\beta, J_{\text{eff}}\equiv J_2, H_{\text{eff}}\equiv J_1). \tag{2.90}$$

Since the boundary effects become unimportant in the thermodynamic limit, the partition function of the open Ising chain with the next-nearest-neighbour interaction can be transcribed also from the well-known result (2.26) for the partition function of the closed Ising chain. This allows simple calculation of the Helmholtz free energy

$$\mathcal{F} = -k_{\text{B}}T\ln\lambda_+ = -J_2 - k_{\text{B}}T\ln\left[\cosh(\beta J_1)+\sqrt{\sinh^2(\beta J_1)+\exp(-4\beta J_2)}\right] \tag{2.91}$$

and also all other important thermodynamical-statistical quantities that follow straightforwardly from here onward.

Exercises

1. By imposing the periodic boundary conditions $\sigma_{2N+1} \equiv \sigma_1$ and $\sigma_{2N+2} \equiv \sigma_2$, the spin-1/2 Ising model on the two-leg ladder (two coupled spin chains shown in Fig. 3) can be defined through the following spin Hamiltonian

$$\mathcal{H} = -J_1 \sum_{i=1}^{2N} \sigma_i \sigma_{i+2} - J_2 \sum_{i=1}^{N} \sigma_{2i-1} \sigma_{2i},$$

where J_1 and J_2 are intra- and inter-chain coupling constants, respectively. Write the transfer matrix for this ladder model, diagonalize it and find its largest eigenvalue. Express the partition function and Helmholtz free energy in terms the largest eigenvalue. Verify that all results reduce to the ones of the simple spin-1/2 Ising chain in the $J_2 \to 0$ limit.

2. Explore the temperature dependence of the specific heat for the spin-1/2 Ising chain exhibiting the spin-Peierls phase transition. How this dependence changes at the tricritical point?

3. Generalize the exact solution for the spin-1/2 Ising chain exhibiting the spin-Peierls phase transition to the case with the non-zero magnetic field. How the character of structural phase transitions changes under the inclusion of the external magnetic field?

3. Examine whether the spin-1 Ising chain exhibits the similar structural (spin-Peierls) transition as its spin-1/2 analogue. Does the spin-1 Ising model exhibit a tricritical point?

3 2D Ising model

2D Ising model is perhaps the simplest microscopic model, which has been solved exactly and it simultaneously exhibits non-trivial phase transitions and critical phenomena. It should be noted, nevertheless, that it took almost two decades of intensive efforts since Ernst Ising (1925) derived exact results for 1D version of his model [6] until the complete closed-form exact solution has been found for its 2D analogue as well [1]. It is worthwhile to remark that a wrong Ising's conclusion about the absence of phase transitions in any (even higher-dimensional) Ising model was firstly questioned by R. Peierls (1936) [7], who argued that 2D Ising model must necessarily exhibit a phase transition towards the spontaneously ordered phase at sufficiently low but non-zero temperature[7]. H. A. Kramers and G. H. Wannier (1941) were the first who exactly confirmed Peierls' conjecture by making the fundamental discovery of a duality in the low- and high-temperature expansion of the partition function [2]. As a matter of fact, the self-dual property of Ising square lattice enables to locate the critical temperature of its order-disorder phase transition in a relative straightforward manner. The subsequent Onsager's (1944) exact solution was an additional breakthrough in the statistical physics by virtue of that 2D Ising model became the most famous paradigm of exactly solved model that exhibits a non-trivial phase transition at non-zero temperature. As it has been already mentioned in the introductory part, the statistical physics took a giant step forward when Onsager's exact solution proved an existence of the phase transition resulting merely from the short-range forces represented by the nearest-neighbour spin-spin interaction only. In this section, we will provide several rigorous results for 2D Ising model available even after modest calculation.

3.1 Dual lattice and dual transformation

Once again, let us begin with a fairy simple microscopic Hamiltonian describing Ising model on arbitrary 2D lattice in an absence of the term incorporating the effect of external

[7] Peierls' original proof contained a series error, which was fully corrected by R. B. Griffiths [8] in 1964.

magnetic field

$$\mathcal{H} = -J \sum_{(i,j)}^{N_{\mathrm{B}}} \sigma_i \sigma_j. \tag{3.1}$$

Above, $\sigma_i = \pm 1$ represents Ising spin variable located at ith lattice site and the summation is carried out over all nearest-neighbour spin pairs on a lattice. Assuming that N is a total number of lattice sites and z is being its coordination number (number of nearest neighbours), then, there is in total $N_{\mathrm{B}} = Nz/2$ pairs of nearest-neighbour spins when boundary effects are neglected (i.e. in thermodynamic limit). Each line (bond), which connects two adjacent spins on a lattice, can be thus regarded as a schematic representation of the exchange interaction J between the nearest-neighbour spins. As usual, the central issue of our approach is to calculate the configurational partition function

$$\mathcal{Z} = \sum_{\{\sigma_i\}} \exp(-\beta \mathcal{H}), \tag{3.2}$$

where the suffix $\{\sigma_i\}$ denotes a summation over all possible spin configurations on a given lattice (there is in total 2^N distinct spin configurations and N tends to infinity in the thermodynamic limit). First, let us rewrite Hamiltonian (3.1) to the form

$$\mathcal{H} = -N_{\mathrm{B}} J + J \sum_{(i,j)}^{N_{\mathrm{B}}} (1 - \sigma_i \sigma_j). \tag{3.3}$$

Since the canonical ensemble average of Hamiltonian readily represents the internal energy ($\mathcal{U} = \langle \mathcal{H} \rangle$), it is easy to find the following physical interpretation of the Hamiltonian (3.3). Each couple of unlike oriented adjacent spins contributes to the sum that appears on the right-hand-side of Eq. (3.3) by the energy gain $2J$, while each couple of aligned adjacent spins does not contribute to this sum at all. With respect to this, the internal energy of a wholly ordered spin system (all spins are either 'up' or 'down') acquires its minimum value $\mathcal{U} = -N_{\mathrm{B}} J$ under the assumption $J > 0$. By substituting the Hamiltonian (3.3) into Eq. (3.2), one gets following expression for the partition function

$$\mathcal{Z} = \exp(\beta J N_{\mathrm{B}}) \sum_{\{\sigma_i\}} \exp(-n 2\beta J), \tag{3.4}$$

where n stands for the total number of unaligned adjacent spin pairs within each spin configuration. Obviously, the summation on the right-hand-side of Eq. (3.4) may in principle

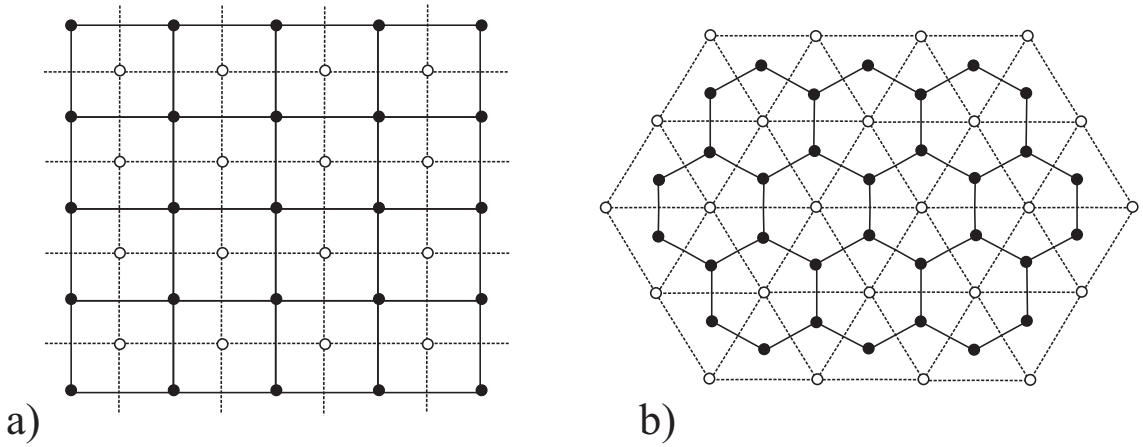

Figure 4: Two pairs of dual lattices: a) self-dual square lattices; b) hexagonal and triangular dual lattices. Solid lines and solid circles label edges and vertices of original lattices, while broken lines and empty circles stand for edges and vertices of their dual lattices, respectively.

contain just different powers of the expression $\exp(-2\beta J)$. In the limit of zero temperature ($T \to 0$), the expression $\exp(-2\beta J)$ tends to zero and thence, the power expansion into a series $\sum_n \exp(-n2\beta J)$ gives very valuable estimate of the partition function in the limit of sufficiently low temperatures (so-called *low-temperature series expansion*).

It is possible to find a simple geometric interpretation of each term emerging in the aforementioned power series by introducing the idea of a *dual lattice*. For this reason, let us introduce a basic terminology of the *graph theory*, where each site of a lattice is called as a *vertex*, while each bond (line) connecting the nearest-neighbour sites (vertices) is called as an *edge*. Further, an interior of each elementary polygon delimited by edges is a *face* and an ensemble of vertices and edges is called a *full lattice graph*. Vertices of a dual lattice are simply obtained by situating them in the middle of each face of the original lattice. The vertices situated at adjacent faces, which share a common edge on the original lattice, then represent the nearest-neighbour vertices of the dual lattice. Edges of the dual lattice are obtained by connecting each couple of adjacent vertices of the dual lattice. For illustrative purposes, Fig. 4 shows two original lattices – square and hexagonal – and their corresponding dual lattices. The bonds of original lattices are displayed as solid lines, while the bonds of their dual lattices are depicted as broken lines. As one can see, the square lattice is a self-dual, i.e. the dual lattice to a square lattice is again a square lattice. Contrary to this, the triangular lattice is a dual lattice to the

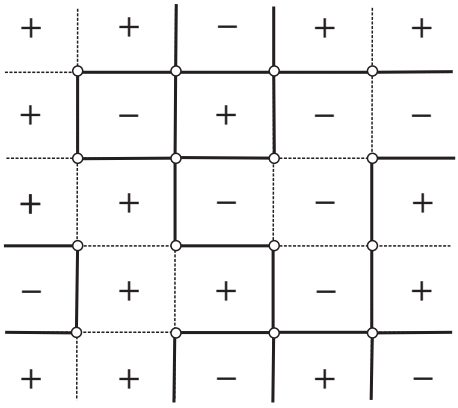

Figure 5: A particular spin configuration on a square lattice, whose vertices and edges are not drawn for clarity. The plus (minus) sign at ith lattice site corresponds to the spin state $\sigma_i = +1$ ($\sigma_i = -1$). The system of solid and broken lines unambiguously determines the corresponding polygon line graph at the dual square lattice (for details see the text).

hexagonal lattice and vice versa. Remembering that N and N_{B} is the total number of vertices and edges of the original lattice, respectively, thence it follows that N_{B} is at the same time the total number of edges of the dual lattice as well (each bond of the dual lattice intersects one and just one bond of the original lattice). If N_{D} denotes the total number of vertices of the dual lattice, N_{D} is in turn also the total number of faces of the original lattice (each face of the original lattice involves one and just one vertex of the dual lattice). Euler's relation for planar graphs[8] then relates the total number of sites of the original and dual lattices with the total number of edges[9]

$$N + N_{\mathrm{D}} = N_{\mathrm{B}}. \tag{3.5}$$

Suppose now some random arrangement of 'up' and 'down' spins on the original lattice, i.e. some particular spin configuration on a whole lattice as displayed in Fig. 5 (the bonds connecting adjacent spins on the original lattice are not drawn for clarity). If the pairs of adjacent spins are unaligned, then draw solid lines between them, otherwise draw broken lines between the pairs of aligned spins. The system of sites, solid and broken lines on the dual lattice creates a configurational graph, which is a subgraph of the full dual lattice

[8]The planar graph is a graph, which can be embedded in the plane so that no edges intersect.

[9]The right-hand-side of Eq. (3.5) is in fact either $N_{\mathrm{B}} + 2$ or $N_{\mathrm{B}} + 1$ for any planar graph, however, in the thermodynamic limit one can use N_{B} instead of them.

graph. The most fundamental property of the configurational graph is that the mutual interchange of each adjacent spins either does not affect the configurational graph, or it causes an even number of changes. The total number of solid and broken lines incident at each site of the dual lattice must be therefore either even or zero. This implies that solid (broken) lines of each configurational graph form a system of closed polygons. So, the configurational graph thus represents a certain kind of polygon line graph. Another important property of the polygon line graph is that the reversal of all spins does not change the configurational graph. It means that two different spin configurations (one is being obtained from the other by reversing all spins) correspond just to one configurational polygon line graph due to invariance $\sigma_i \to -\sigma_i$ (for each i). The partition function of the planar Ising model can be therefore expressed as

$$\mathcal{Z} = 2\exp(\beta J N_{\mathrm{B}}) \sum_{\mathrm{p.g.}} \exp(-n2\beta J), \tag{3.6}$$

where the summation is now performed over all possible polygon subgraphs on a 2D lattice, n denotes the total number of solid lines within each polygon subgraph and the factor 2 comes from the two-to-one mapping between spin and polygon configurations.

Let us take a closer look at another interesting property of the partition function (3.2). By adopting the van der Waerden identity [9]

$$\exp(\beta J \sigma_i \sigma_j) = \cosh(\beta J) + \sigma_i \sigma_j \sinh(\beta J) = \cosh(\beta J)[1 + \sigma_i \sigma_j \tanh(\beta J)] \tag{3.7}$$

and substituting it into Eq. (3.2) one obtains

$$\mathcal{Z} = [\cosh(\beta J)]^{N_{\mathrm{B}}} \sum_{\{\sigma_i\}} \prod_{(i,j)} [1 + \sigma_i \sigma_j \tanh(\beta J)]. \tag{3.8}$$

The product on the right-hand-side of Eq. (3.8) involves in total N_{B} terms (one for each bond), which give after formal multiplication a sum of in total $2^{N_{\mathrm{B}}}$ terms. However, many terms eventually vanish by performing summation over all available spin configurations. For instance, it can be readily proved that all linear terms of the type $\sigma_i \sigma_j \tanh(\beta J)$ will finally disappear when summing over spin states of the spin σ_i or σ_j. The condition, which ensures that the relevant term makes a non-zero contribution to the partition function, can be simply guessed from the validity of the trivial spin identity $\sigma_i^2 = 1$. According to

this, all non-zero terms must necessarily consist of spin variables, which enter into these expressions either even number of times or do not enter into these terms at all. The simplest non-vanishing term for the Ising square lattice is evidently

$$(\sigma_i\sigma_j)(\sigma_j\sigma_k)(\sigma_k\sigma_l)(\sigma_l\sigma_i)\tanh^4(\beta J) = \sigma_i^2\sigma_j^2\sigma_k^2\sigma_l^2\tanh^4(\beta J) = \tanh^4(\beta J), \tag{3.9}$$

which is constituted by the product of four nearest-neighbour interactions (edges) forming an elementary square (the simplest closed polygon) on this lattice. The summation over spin configurations of four spins included in this term consequently gives a factor $2^4\tanh^4(\beta J)$, while the summation over spin states of other spins yields an additional factor 2^{N-4} so that the Boltzmann's factor $2^N\tanh^4(\beta J)$ is finally obtained as the contribution from a single square. It is therefore not difficult to construct the following geometric interpretation of the non-vanishing terms: edges corresponding to interactions present in these terms must create closed polygons so that either no lines or even number of lines meet at each vertex of the lattice. From this point of view, polygon line graphs very similar to those described by the low-temperature series expansion give a non-zero contribution to the partition function. With regard to this, the expression (3.8) for the partition function can be replaced by

$$\mathcal{Z} = 2^N[\cosh(\beta J)]^{N_\mathrm{B}}\sum_{\mathrm{p.g.}}[\tanh(\beta J)]^n, \tag{3.10}$$

where n denotes the total number of full lines constituting the particular polygon graph. It is quite apparent that the summation on the right-hand-side of Eq. (3.10) contains just different powers of the expression $\tanh(\beta J)$. In the limit of high temperatures ($T \to \infty$), the expression $\tanh(\beta J)$ tends to zero and whence, the power expansion into a series $\sum_n[\tanh(\beta J)]^n$ gives very valuable estimate of the partition function in the limit of sufficiently high temperatures (so-called *high-temperature series expansion*).

There is an interesting correspondence between summations to emerge in Eqs. (3.6) and (3.10), since both of them are performed over certain sets of polygon line graphs. The most essential difference between them consists in the fact that the summation in Eq. (3.4) is carried out over polygon graphs on the dual lattice, while the summation in Eq. (3.10) is performed over polygon graphs on the original lattice. It should be stressed, however, that both the final expressions (3.4) and (3.10) for the partition function are

exact when the relevant series is performed up to an infinite order and therefore, they must basically give the same result for the partition function. In the thermodynamic limit, the summations (3.4) and (3.10) yield the same partition function provided that

$$\exp(-2\beta_{\mathrm{D}}J) = \tanh(\beta J), \tag{3.11}$$

$$\frac{\mathcal{Z}(N_{\mathrm{D}},\beta_{\mathrm{D}}J)}{\exp(\beta_{\mathrm{D}}JN_{\mathrm{B}})} = \frac{\mathcal{Z}(N,\beta J)}{2^N[\cosh(\beta J)]^{N_{\mathrm{B}}}}, \tag{3.12}$$

where we have introduced some reciprocal temperature $\beta_{\mathrm{D}} = 1/(k_{\mathrm{B}}T_{\mathrm{D}})$ of the dual lattice and the factor 2 was omitted from the denominator on the left-hand-side of Eq. (3.12) due to its negligible effect in the thermodynamic limit. The connection between two mutually dual lattices (3.11) and (3.12) can also be inverted because of a symmetry in the duality (each from a couple of the mutually dual lattices is dual one to another)

$$\exp(-2\beta J) = \tanh(\beta_{\mathrm{D}}J), \tag{3.13}$$

$$\frac{\mathcal{Z}(N,\beta J)}{\exp(\beta JN_{\mathrm{B}})} = \frac{\mathcal{Z}(N_{\mathrm{D}},\beta_{\mathrm{D}}J)}{2^{N_{\mathrm{D}}}[\cosh(\beta_{\mathrm{D}}J)]^{N_{\mathrm{B}}}}. \tag{3.14}$$

With the help of Eqs. (3.11) and (3.12) [or equivalently Eqs. (3.13) and (3.14)], it is also possible to write this so-called *dual transformation* even in a symmetric form as would be expected from the symmetrical nature of the duality. The relation (3.11) gives after straightforward calculation

$$\sinh(2\beta J)\sinh(2\beta_{\mathrm{D}}J) = 1, \tag{3.15}$$

while the expression (3.12) can be modified by regarding the equality between partition functions $[\mathcal{Z}(N,\beta J) = \mathcal{Z}(N_{\mathrm{D}},\beta_{\mathrm{D}}J)]$, Eqs. (3.11), (3.15) and Euler's relation (3.5) to

$$\begin{aligned} 2^N[\cosh(\beta J)]^{N_{\mathrm{B}}}\exp(-\beta_{\mathrm{D}}JN_{\mathrm{B}}) &= 2^N[\cosh(\beta J)]^{N_{\mathrm{B}}}[\tanh(\beta J)]^{\frac{N_{\mathrm{B}}}{2}} \\ &= 2^N[\sinh(\beta J)]^{\frac{N_{\mathrm{B}}}{2}}[\cosh(\beta J)]^{\frac{N_{\mathrm{B}}}{2}} \\ &= 2^{N-\frac{N_{\mathrm{B}}}{2}}[\sinh(2\beta J)]^{\frac{N_{\mathrm{B}}}{2}} = 2^{\frac{N-N_{\mathrm{D}}}{2}}[\sinh(2\beta J)]^{\frac{N+N_{\mathrm{D}}}{2}} \\ &= \frac{[2\sinh(2\beta J)]^{\frac{N}{2}}}{[2\sinh(2\beta_{\mathrm{D}}J)]^{\frac{N_{\mathrm{D}}}{2}}} = 1. \end{aligned} \tag{3.16}$$

By combining Eq. (3.16) with the relation (3.12), one readily gains another symmetric relationship between the partition functions expressed in terms of the high-temperature

series expansion on the original lattice and the low-temperature series expansion on its dual lattice

$$\frac{\mathcal{Z}(N,\beta J)}{[2\sinh(2\beta J)]^{\frac{N}{2}}}=\frac{\mathcal{Z}(N_{\mathrm{D}},\beta_{\mathrm{D}}J)}{[2\sinh(2\beta_{\mathrm{D}}J)]^{\frac{N_{\mathrm{D}}}{2}}}. \tag{3.17}$$

The existence of an equivalence between the low- and high-temperature series expansions reflects the fundamental property of the partition function, namely, its symmetry with respect to the low and high temperatures. This symmetry means, among other matters, that the partition function at some lower temperature can always be mapped on the equivalent partition function at some certain higher temperature. This mapping is called as the *dual transformation* and the dual lattices are actually connected one to each other by means of the dual transformation. In this respect, the dual lattices are topological representations of the dual transformation and consequently, one says that the dual transformation has a character of the topological transformation.

The mathematical formulation of the dual transformation connecting effective temperatures of the original and its dual lattice is represented (independently of the lattice topology) either by the couple of equivalent Eqs. (3.11) and (3.13), or, respectively, by a single symmetrized relation (3.15). The latter relationship is especially useful for a better understanding of the symmetry of the partition function with respect to the low and high temperatures. It is sufficient to realize that the argument of the function $\sinh(2\beta J)$ must unavoidably decrease when the argument of the other function $\sinh(2\beta_{\mathrm{D}}J)$ increases in order to preserve their constant product required by the dual transformation (3.15). This means that the partition function at some lower temperature, which is obtained for instance from the low-temperature expansion on the dual lattice, is equivalent to the partition function at a certain higher temperature obtained from the high-temperature expansion on the original lattice. It is noteworthy that the dual transformation markedly simplifies the exact enumeration of thermodynamic quantities on different lattices, since it permits to obtain the exact solution of some quantity on arbitrary lattice merely from the corresponding exact result for this quantity on its dual lattice. For instance, the critical point is always accompanied by some singularity or discontinuity in the thermodynamic variables and this non-analyticity is always somehow reflected in the partition function as well. The mapping relation (3.17) clearly shows that the partition function of the

original lattice exhibits a non-analyticity if and only if the partition function of the dual lattice also has a similar non-analyticity at some corresponding temperature satisfying the duality relation (3.15). Besides, the expression (3.17) allows to calculate the partition function of the one of mutually dual lattices merely by substituting the corresponding exact result for the partition function of its dual lattice.

It is worthwhile to remark that the square lattice has an extraordinary position among 2D lattices because of its self-duality. The self-dual property together with the symmetry of the partition function with respect to the low and high temperatures is just enough for determining the critical temperature and other thermodynamic quantities precisely at a critical point. Under the assumption of a single critical point, the same lattice topology ensures that critical parameters must be equal one to each other on both mutually dual square lattices. According to the dual transformation (3.15), the critical temperature of the spin-1/2 Ising model on the square lattice must obey the condition

$$\sinh^2(2\beta_{\mathrm{c}}J) = 1, \tag{3.18}$$

which is consistent with this value of the critical temperature

$$\frac{k_{\mathrm{B}}T_{\mathrm{c}}}{|J|} = \frac{2}{\ln(1+\sqrt{2})}. \tag{3.19}$$

It should be pointed out, however, that the temperature symmetry of the partition function does not suffice for determining critical parameters of 2D lattices like hexagonal and triangular lattices, which are not self-dual.

3.2 Star-triangle transformation

The dual transformation (3.15) maps the hexagonal lattice into the triangular lattice and vice versa and thus, it does not establishes the symmetry between the low- and high-temperature partition function on the same lattice. However, it should be noticed that such a relation can be established even for other (not self-dual) lattices by combining the dual transformation (3.15) with some another transformations. The star-triangle transformation invented by L. Onsager [1] establishes this useful mapping relationship for the couple of dual hexagonal–triangular or Kagomé–diced lattices.

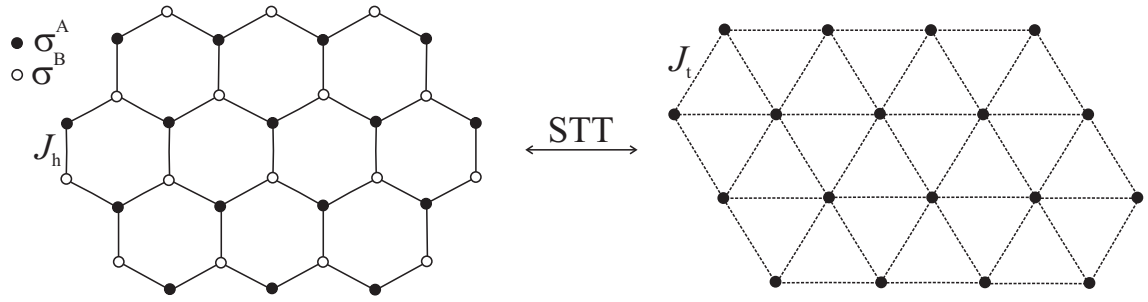

Figure 6: The spin-1/2 Ising model on the hexagonal lattice and its relation to the equivalent spin-1/2 Ising model on the triangular lattice. The equivalence between both models can be established by applying the star-triangle transformation to a half of spins of hexagonal lattice.

Let us consider the spin-1/2 Ising model on the hexagonal lattice. For further convenience, it is advisable to divide the hexagonal lattice into two equivalent interpenetrating triangular sublattices A and B, whose sites are diagrammatically represented in Fig. 6 by full and empty circles, respectively. The division is made in a such way that all nearest neighbours of a site from one sublattice (say A) belong to the other sublattice (B) and vice versa. Owing to this fact, the summation over spin configurations of spins, which belong to the same sublattice, can be performed independently one from each other because there is no direct interaction between the spins from the same sublattice. In this respect, it is very appropriate to write the total Hamiltonian as a sum of site Hamiltonians

$$\mathcal{H} = \sum_{i\in \mathrm{B}}^{N} \mathcal{H}_i, \tag{3.20}$$

where each site Hamiltonian $\mathcal{H}_i$ involves all the interaction terms associated with the ith lattice site belonging to the sublattice B

$$\mathcal{H}_i = -J_{\mathrm{h}} \sigma_i^{\mathrm{B}} (\sigma_j^{\mathrm{A}} + \sigma_k^{\mathrm{A}} + \sigma_l^{\mathrm{A}}). \tag{3.21}$$

In above, the upper index of spin variable specifies the sublattice to which the relevant spin belongs. By the use of Eqs. (3.20) and (3.21), the partition function of the spin-1/2 Ising model on the hexagonal lattice (1.2) can be partially factorized to the form

$$\mathcal{Z}_{\mathrm{hex}} = \sum_{\{\sigma_j^{\mathrm{A}}\}} \prod_{i=1}^{N} \sum_{\sigma_i^{\mathrm{B}}=\pm 1} \exp[\beta J_{\mathrm{h}} \sigma_i^{\mathrm{B}} (\sigma_j^{\mathrm{A}} + \sigma_k^{\mathrm{A}} + \sigma_l^{\mathrm{A}})], \tag{3.22}$$

where the former summation is carried out over all available spin configurations on the sublattice A, the product is over all sites of the sublattice B and the latter summation

accounts for the spin states of one particular spin from the sublattice B. In the consequence of that, it is adequate to consider just one particular spin site from the sublattice B and to sum up over spin degrees of freedom of this site. Each spin from the sublattice B interacts merely with its three nearest-neighbour spins from the sublattice A and hence, this summation gives the Boltzmann's factor

$$\sum_{\sigma_i^{\mathrm{B}}=\pm 1} \exp[\beta J_{\mathrm{h}} \sigma_i^{\mathrm{B}} (\sigma_j^{\mathrm{A}} + \sigma_k^{\mathrm{A}} + \sigma_l^{\mathrm{A}})] = 2\cosh[\beta J_{\mathrm{h}} (\sigma_j^{\mathrm{A}} + \sigma_k^{\mathrm{A}} + \sigma_l^{\mathrm{A}})]$$
$$= A \exp[\beta J_{\mathrm{t}} (\sigma_j^{\mathrm{A}} \sigma_k^{\mathrm{A}} + \sigma_k^{\mathrm{A}} \sigma_l^{\mathrm{A}} + \sigma_l^{\mathrm{A}} \sigma_j^{\mathrm{A}})], \tag{3.23}$$

which is appropriate for substituting by the equivalent expression provided by the *star-triangle transformation*. The physical meaning of the transformation (3.23) is to remove all the interactions associated with a central spin σ_i^{B} of the *star* and to replace them by new effective interactions between three outer spins σ_j^{A}, σ_k^{A} and σ_l^{A} forming the equilateral *triangle*. It is noteworthy that the star-triangle transformation is actually a set of eight equations, which can be obtained from the mapping relation (3.23) by considering all possible spin configurations available to three outer spins from the sublattice A. However, the consideration of available spin configurations leads just to two independent equations, which unambiguously determine the mapping parameters A and J_{t}. This self-consistency condition yields the mapping parameters

$$A = 2[\cosh(3\beta J_{\mathrm{h}})]^{\frac{1}{4}} [\cosh(\beta J_{\mathrm{h}})]^{\frac{3}{4}} \tag{3.24}$$
$$\beta J_{\mathrm{t}} = \frac{1}{4} \ln\Big[\frac{\cosh(3\beta J_{\mathrm{h}})}{\cosh(\beta J_{\mathrm{h}})}\Big]. \tag{3.25}$$

The backward substitution of the transformation (3.23) into the partition function (3.22), which is equivalent with performing the star-triangle transformation for all spins from the sublattice B, yields an exact mapping relationship between the partition functions of the spin-1/2 Ising model on the hexagonal and triangular lattices

$$\mathcal{Z}_{\mathrm{hex}}(2N, \beta J_{\mathrm{h}}) = A^N \mathcal{Z}_{\mathrm{triang}}(N, \beta J_{\mathrm{t}}), \tag{3.26}$$

whose effective temperatures are coupled together through the mapping relation (3.25). As a result, the relation (3.25) established by the use of the star-triangle transformation connects the partition functions of the hexagonal and triangular lattices at two different

effective temperatures in a quite similar way as it does the relation (3.15) provided by the dual transformation. The most crucial difference consists in a profound essence of both mapping relations; the dual transformation is evidently of the topological origin, whereas the star-triangle mapping is the algebraic transformation in its character.

At this stage, let us combine the dual and star-triangle transformations in order to bring insight into the criticality of the spin-1/2 Ising model on the hexagonal and triangular lattices. By employing a set of trivial identities[10], the star-triangle transformation (3.25) should be firstly rewritten as follows

$$\begin{aligned}\exp(4\beta J_{\rm t}) &= \frac{\cosh(3\beta J_{\rm h})}{\cosh(\beta J_{\rm h})} = \frac{\cosh(2\beta J_{\rm h})\cosh(\beta J_{\rm h}) + \sinh(2\beta J_{\rm h})\sinh(\beta J_{\rm h})}{\cosh(\beta J_{\rm h})} \\ &= \cosh(2\beta J_{\rm h}) + \tanh(\beta J_{\rm h})\sinh(2\beta J_{\rm h}) = \cosh(2\beta J_{\rm h}) + 2\sinh^2(\beta J_{\rm h}) \\ &= 2\cosh(2\beta J_{\rm h}) - 1. \end{aligned} \tag{3.27}$$

Furthermore, it is appropriate to combine Eq. (3.27) with one of possible representations of the dual transformation (3.11)

$$\exp(-2\beta' J_{\rm t}) = \tanh(\beta' J_{\rm h}) \tag{3.28}$$

with the aim to eliminate the effective temperature of the one of lattices with equivalent partition functions. For instance, the procedure that eliminates from Eqs. (3.27) and (3.28) the effective temperature of the triangular lattice allows to obtain the symmetrized relationship, which connects the partition function of the spin-1/2 Ising model on the hexagonal lattice at two different temperatures

$$\begin{aligned}[\coth(\beta' J_{\rm h})]^2 &= 2\cosh(2\beta J_{\rm h}) - 1 \\ \frac{\cosh(2\beta' J_{\rm h}) + 1}{\cosh(2\beta' J_{\rm h}) - 1} &= 2\cosh(2\beta J_{\rm h}) - 1 \\ \cosh(2\beta' J_{\rm h}) + 1 &= [2\cosh(2\beta J_{\rm h}) - 1][\cosh(2\beta' J_{\rm h}) - 1] \\ \cosh(2\beta J_{\rm h})\cosh(2\beta' J_{\rm h}) - \cosh(2\beta J_{\rm h}) - \cosh(2\beta' J_{\rm h}) &= 0 \\ \{\cosh(2\beta J_{\rm h}) - 1\}\{\cosh(2\beta' J_{\rm h}) - 1\} &= 1. \end{aligned} \tag{3.29}$$

[10] $\cosh(a \pm b) = \cosh a \cosh b \pm \sinh a \sinh b$, $\cosh 2a = \cosh^2 a + \sinh^2 a$, $\sinh 2a = 2\sinh a \cosh a$, $\cosh^2 a - \sinh^2 a = 1$, $\cosh^2 a = \frac{1+\cosh 2a}{2}$ and $\sinh^2 a = \frac{-1+\cosh 2a}{2}$.

Physically, the relationship (3.29) establishes analogous temperature symmetry of the partition function of the spin-1/2 Ising model on the hexagonal lattice as the dual transformation does for the spin-1/2 Ising model on the self-dual square lattice through the relation (3.15). If there exists just an unique critical point, both temperatures connected via the mapping relation (3.29) must necessarily meet at a critical point due to the same reasons as it was explained in the case of square lattice. So, the critical temperature of the spin-1/2 Ising model on the hexagonal lattice should obey the condition

$$[\cosh(2\beta_{\mathrm{c}}J_{\mathrm{h}}) - 1]^2 = 1, \tag{3.30}$$

which is consistent with this value of the critical temperature

$$\frac{k_{\mathrm{B}}T_{\mathrm{c}}}{|J_{\mathrm{h}}|} = \frac{2}{\ln(2+\sqrt{3})}. \tag{3.31}$$

The same procedure can be repeated once more in order to obtain the critical parameters of the spin-1/2 Ising model on the triangular lattice. Elimination of the effective temperature of the hexagonal lattice from Eqs. (3.27) and (3.28) yields the following symmetric mapping, which relates the partition function of the spin-1/2 Ising model on the triangular lattice at two different temperatures

$$[\exp(4\beta J_{\mathrm{t}}) - 1][\exp(4\beta' J_{\mathrm{t}}) - 1] = 4. \tag{3.32}$$

The latter equation determines the critical condition of the triangular lattice

$$[\exp(4\beta_{\mathrm{c}}J_{\mathrm{t}}) - 1]^2 = 4, \tag{3.33}$$

which locates its exact critical temperature

$$\frac{k_{\mathrm{B}}T_{\mathrm{c}}}{J_{\mathrm{t}}} = \frac{4}{\ln 3}. \tag{3.34}$$

It is noteworthy that the critical temperature of the spin-1/2 Ising model on the triangular lattice (3.34) can be more easily found by substituting the critical condition of the spin-1/2 Ising model on the hexagonal lattice (3.30) to the modified star-triangle transformation (3.27). Note that the same critical temperature is recovered in this way.

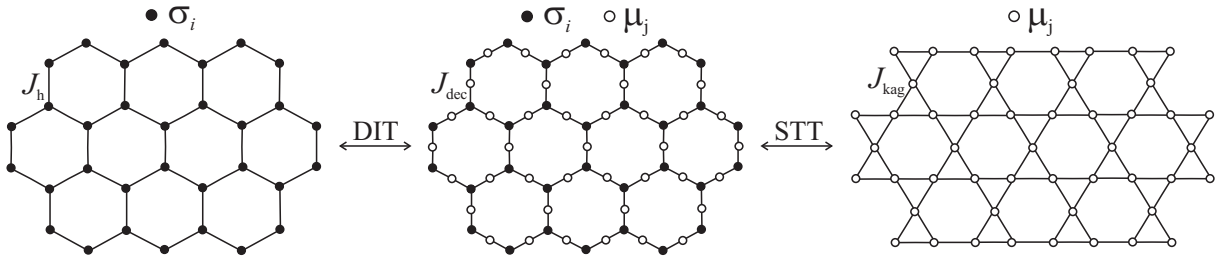

Figure 7: The spin-1/2 Ising model on the hexagonal lattice, decorated hexagonal lattice and Kagomé lattice. The equivalence between all three lattice models can be established by employing the decoration-iteration and star-triangle transformations, respectively.

3.3 Decoration-iteration transformation

Another important mapping transformation, which is purely of algebraic character, represents the decoration-iteration transformation invented by I. Syozi (1951) by solving the spin-1/2 Ising model on the Kagomé lattice [10]. In principle, the approach based on the decoration-iteration transformation enables to obtain an exact solution of the spin-1/2 Ising model on an arbitrary *bond-decorated lattice* from the corresponding exact solution of the simple (undecorated) lattice. The term bond-decorated lattice marks such a lattice, which can be obtained from the simple original lattice (like square, hexagonal or triangular) by placing an additional spin or a cluster of spins on the bonds of this simpler lattice. The sites of the original lattice are then called as *primary* sites, while the sites arising from the decoration procedure are called as *secondary* (decorating) sites. For illustration, Fig. 7 shows the planar topology of the hexagonal lattice, the simply decorated hexagonal lattice and the Kagomé lattice together with the reciprocal relations, which can be established between them by employing algebraic mapping transformations.

Let us consider initially the spin-1/2 Ising model on the decorated hexagonal lattice, which is is shown in the middle of Fig. 7 and is given by the Hamiltonian

$$\mathcal{H}_{\rm dec} = -J_{\rm dec} \sum_{(i,j)}^{3N} \sigma_i \mu_j. \tag{3.35}$$

Above, $\sigma_i = \pm 1$ and $\mu_j = \pm 1$ label Ising spin variables located at the primary and secondary sites of the decorated hexagonal lattice, respectively, the summation runs over all nearest-neighbour spin pairs of the lattice and the total number of primary sites is equal to N. It is convenient to rewrite the total Hamiltonian (3.35) as a sum of bond

Hamiltonians

$$\mathcal{H}_{\mathrm{dec}} = \sum_{j=1}^{3N/2} \mathcal{H}_j, \tag{3.36}$$

where each bond Hamiltonian involves all the interaction terms that include one particular decorating spin site

$$\mathcal{H}_j = -J_{\mathrm{dec}}\mu_j(\sigma_k + \sigma_l). \tag{3.37}$$

By the use of Eqs. (3.36) and (3.37), the partition function (1.2) of the spin-1/2 Ising model on the decorated hexagonal lattice can be partially factorized to the form

$$\mathcal{Z}_{\mathrm{dec}} = \sum_{\{\sigma_i\}} \prod_{j=1}^{3N/2} \sum_{\mu_j=\pm 1} \exp[\beta J_{\mathrm{dec}}\mu_j(\sigma_k + \sigma_l)]. \tag{3.38}$$

In the above expression, the former summation is carried out over all available spin configurations on the primary sites, the product is over all secondary sites and the latter summation accounts for the spin states of the one secondary spin occupying jth bond of the decorated hexagonal lattice. According to Eq. (3.38), the summation over spin degrees of freedom of the decorating sites can be performed independently one from each other, whence it follows that this summation gives the Boltzmann's factor

$$\sum_{\mu_j=\pm 1} \exp[\beta J_{\mathrm{dec}}\mu_j(\sigma_k + \sigma_l)] = 2\cosh[\beta J_{\mathrm{dec}}(\sigma_k + \sigma_l)] = B\exp(\beta J_{\mathrm{h}}\sigma_k\sigma_l). \tag{3.39}$$

which can be successively replaced by the equivalent expression provided by the *decoration-iteration transformation*. The physical meaning of the transformation (3.39) is to remove all interactions associated with the secondary spin μ_j and to substitute them by the effective interaction between two primary spins σ_k and σ_l, which are being its nearest neighbours. It should be emphasized that the decoration-iteration transformation (3.39) has to satisfy the self-consistency condition, i.e. it must hold for any combination of the spin states of the two primary Ising spins σ_k and σ_l. In this respect, the mapping relation (3.39) is in fact a set of four equations, which can be explicitly obtained by considering all possible spin configurations available to the two primary Ising spins. It can be readily proved that a substitution of four possible spin configurations yields from the formula

(3.39) merely two independent equations, which determine the mapping parameters B and βJ_{h}

$$B = 2\sqrt{\cosh(2\beta J_{\mathrm{dec}})}, \tag{3.40}$$

$$\beta J_{\mathrm{h}} = \frac{1}{2}\ln\left[\cosh(2\beta J_{\mathrm{dec}})\right]. \tag{3.41}$$

By applying the decoration-iteration transformation to all the secondary sites, i.e. by substituting the mapping transformation (3.39) into the partition function (3.38), one acquires an exact mapping correspondence between the partition functions of the spin-1/2 Ising model on the decorated hexagonal lattice and simple hexagonal lattice

$$\mathcal{Z}_{\mathrm{dec}}(5N/2, \beta J_{\mathrm{dec}}) = B^{3N/2}\mathcal{Z}_{\mathrm{hex}}(N, \beta J_{\mathrm{h}}) \tag{3.42}$$

whose effective temperatures are connected by means of the relation (3.41). It is quite obvious from Eq. (3.42) that the decorated hexagonal lattice becomes critical if and only if its corresponding hexagonal lattice becomes critical as well. With regard to this, it is sufficient to substitute the exact critical temperature of the hexagonal lattice (3.31) into Eq. (3.41) in order to locate the exact critical point of the decorated hexagonal lattice

$$\frac{k_{\mathrm{B}}T_{\mathrm{c}}}{|J_{\mathrm{dec}}|} = \frac{2}{\ln(2+\sqrt{3}+\sqrt{6+4\sqrt{3}})}. \tag{3.43}$$

It is worthwhile to remark that the decoration-iteration transformation (3.39) is restricted neither by the lattice topology nor by its spatial dimensionality and thus, it can be utilized for obtaining the exact results for arbitrary simply decorated lattice from the known exact solution of the corresponding undecorated lattice.

Now, it is possible to make another vital observation. The total Hamiltonian (3.35) of the spin-1/2 Ising model on the decorated hexagonal lattice can be also formally written as a sum of site Hamiltonians

$$\mathcal{H}_{\mathrm{dec}} = \sum_{i=1}^{N}\mathcal{H}_i, \tag{3.44}$$

each involving all the interaction terms of the one particular primary spin

$$\mathcal{H}_i = -J_{\mathrm{dec}}\sigma_i(\mu_j + \mu_k + \mu_l). \tag{3.45}$$

Substituting Eqs. (3.44) and (3.45) into a statistical definition of the partition function (1.2) allows us to partially factorize the partition function of the spin-1/2 Ising model on the decorated hexagonal lattice and write it in the form

$$\mathcal{Z}_{\rm dec} = \sum_{\{\mu_j\}} \prod_{i=1}^{N} \sum_{\sigma_i=\pm 1} \exp[\beta J_{\rm dec} \sigma_i (\mu_j + \mu_k + \mu_l)]. \tag{3.46}$$

Above, the former summation runs over all available spin configurations on the secondary sites, the product is over all primary sites and the latter summation is carried out over the spin states of the one particular primary spin of the decorated hexagonal lattice. The structure of the partition function (3.46) immediately justifies an application of the familiar star-triangle mapping transformation

$$\begin{aligned} \sum_{\sigma_i=\pm 1} \exp[\beta J_{\rm dec} \sigma_i (\mu_j + \mu_k + \mu_l)] &= 2\cosh[\beta J_{\rm dec}(\mu_j + \mu_k + \mu_l)] \\ &= C \exp[\beta J_{\rm kag}(\mu_j \mu_k + \mu_k \mu_l + \mu_l \mu_j)], \end{aligned} \tag{3.47}$$

which satisfies the self-consistency condition provided that

$$C = 2[\cosh(3\beta J_{\rm dec})]^{\frac{1}{4}} [\cosh(\beta J_{\rm dec})]^{\frac{3}{4}}, \tag{3.48}$$

$$\beta J_{\rm kag} = \frac{1}{4} \ln \left[\frac{\cosh(3\beta J_{\rm dec})}{\cosh(\beta J_{\rm dec})} \right] = \frac{1}{4} \ln \left[2\cosh(2\beta J_{\rm dec}) - 1 \right]. \tag{3.49}$$

The star-triangle transformation maps the spin-1/2 Ising model on the decorated hexagonal lattice into the spin-1/2 Ising model on the Kagomé lattice once it is performed at all primary sites. As a matter of fact, it is easy to derive the following exact mapping correspondence between the partition functions of both these models by a direct substitution of the star-triangle mapping (3.47) into the relation (3.46)

$$\mathcal{Z}_{\rm dec}(5N/2, \beta J_{\rm dec}) = C^N \mathcal{Z}_{\rm kag}(3N/2, \beta J_{\rm kag}). \tag{3.50}$$

At this stage, it is possible to combine the decoration-iteration mapping with the star-triangle transformation in order to express the partition function of the spin-1/2 Ising model on the Kagomé lattice in terms of the corresponding partition function of the spin-1/2 Ising model on the hexagonal lattice. The mapping relations (3.42) and (3.50) provide this useful connection between the partition functions of the spin-1/2 Ising model on the

hexagonal and Kagomé lattices

$$\mathcal{Z}_{\mathrm{kag}}(3N/2,\beta J_{\mathrm{kag}}) = \left(\frac{B^{\frac{3}{2}}}{C}\right)^{N} \mathcal{Z}_{\mathrm{hex}}(N,\beta J_{\mathrm{h}}) \\ = 2^{N}\left\{\frac{\exp(6\beta J_{\mathrm{h}})[\exp(2\beta J_{\mathrm{h}})+1]}{[2\exp(4\beta J_{\mathrm{h}})+\exp(2\beta J_{\mathrm{h}})-1]^{3}}\right\}^{\frac{1}{4}} \mathcal{Z}_{\mathrm{hex}}(N,\beta J_{\mathrm{h}}), \quad (3.51)$$

whereas Eqs. (3.41) and (3.49) relate the effective temperatures of the hexagonal and Kagomé lattices with the equal partition function

$$\beta J_{\mathrm{kag}} = \frac{1}{4}\ln\left[2\exp(2\beta J_{\mathrm{h}})-1\right]. \quad (3.52)$$

Substituting the exact critical temperature of the spin-1/2 Ising model on the hexagonal lattice (3.31) to the mapping relation (3.52) yields the exact critical temperature of the spin-1/2 Ising model on the Kagomé lattice

$$\frac{k_{\mathrm{B}}T_{\mathrm{c}}}{J_{\mathrm{kag}}} = \frac{4}{\ln(3+2\sqrt{3})}. \quad (3.53)$$

Before concluding, let us compare the obtained critical temperatures corresponding to the order-disorder phase transition of the spin-1/2 Ising model on several lattices. For this purpose, the Table 2 enumerates the critical temperatures of the spin-1/2 Ising model on all three regular planar lattices – hexagonal, square and triangular, which can be regarded as the only possible particular tilings that entirely cover the plane with the same regular polygon (hexagon, square and triangle, respectively). The critical point of the semi-regular Kagomé lattice, which consists of two kinds of regularly alternating polygons (hexagons and triangles) is especially interesting from the academic point of view, since this lattice represents the only semi-regular tiling, which has all sites as well as all bonds equivalent quite similarly as a triad of the aforementioned regular lattices. It can be easily understood from the Table 2 that the greater the coordination number (the number of nearest neighbours) of the planar lattice, the higher the critical temperature of its order-disorder transition. Accordingly, the cooperativity of spontaneous ordering

Table 2: Critical temperatures of the spin-1/2 Ising model on several planar lattices.

	hexagonal	kagomé	square	triangular
$k_{\mathrm{B}}T_{\mathrm{c}}/J$	1.51865	2.14332	2.26919	3.64096

seems to be very closely connected with such a topological feature as being the lattice's coordination number. On the other hand, the coordination number by itself does not entirely determine the critical temperature as it can be clearly seen from a comparison of the critical temperatures of the square and Kagomé lattices having the same coordination number. It turns out that the irregular lattices composed of more regular polygons always have lower critical temperature than their regular counterparts with the same averaged coordination number. Thus, it might be concluded that the cooperativity is strongly related also to other topological features of planar lattices. Note that such an information cannot be elucidated from the approximate methods that usually predict the same critical temperature for all lattices with the same coordination numbers.

3.4 Transfer-matrix approach

Even although the dual, star-triangle and decoration-iteration transformations provide several rigorous results for the spin-1/2 Ising model on the planar lattices, they do not solve this problem completely as they afford exact results precisely at a critical point alone. In this regard, sophisticated mathematical methods are needed in order to obtain a complete closed-form exact solution of 2D Ising model in a whole temperature range. Here, we shall show some crucial points of the transfer-matrix approach when applying it to the spin-1/2 Ising model on the simple square lattice. It is noteworthy, however, that the procedure to be explained in what follows can be used to obtain the exact solution of the spin-1/2 Ising model on an arbitrary planar lattice in the qualitatively same manner as explained below for the case of square lattice.

Let us consider the spin-1/2 Ising model on the square lattice, which consists of r rows and c columns and is defined through the Hamiltonian

$$\mathcal{H} = -J \left(\sum_{i=1}^{r} \sum_{j=1}^{c} \sigma_{i,j}\sigma_{i+1,j} + \sum_{i=1}^{r} \sum_{j=1}^{c} \sigma_{i,j}\sigma_{i,j+1} \right). \tag{3.54}$$

Apparently, the total Hamiltonian (3.54) is constituted by two kinds of summations. The former summation is carried out over all interactions between the nearest-neighbouring spins from adjacent rows of the square lattice, while the latter one takes into account all interactions between the nearest-neighbouring spins from adjacent columns. As usual,

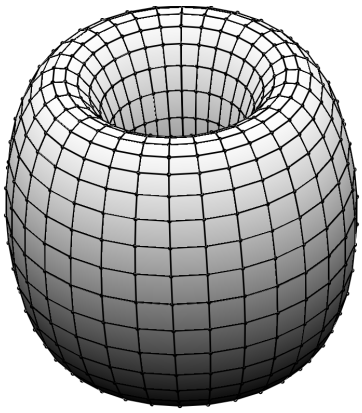

Figure 8: The square lattice wrapped on a torus ensures periodic (cyclic) boundary conditions in both horizontal as well as vertical directions.

the periodic boundary conditions simplifying further treatment are imposed by

$$\sigma_{r+1,j} = \sigma_{1,j}, \qquad \text{where} \quad j = 1, 2, \ldots, c; \tag{3.55}$$

$$\sigma_{i,c+1} = \sigma_{i,1}, \qquad \text{where} \quad i = 1, 2, \ldots, r. \tag{3.56}$$

It is noteworthy that the periodicity of the square lattice, which is ensured by the conditions (3.55) and (3.56), is equivalent to wrapping the square lattice on a torus in such a way that the cth column is coupled to the first column and the rth row is coupled to the first row (Fig. 8). This is the statistical-mechanical definition of the spin-1/2 Ising model on the square lattice with periodic boundary conditions in both horizontal and vertical directions, which is in principle sufficient for evaluating its partition function. It should be noted, however, that the accurate evaluation of the partition function of any 2D Ising model is an extremely difficult task, since it demands a considerable knowledge of sophisticated mathematics required for understanding of the exact solution in its full details.

First, let us denote the overall spin configuration of the jth column of spins by

$$\mu_j = (\sigma_{1,j}, \sigma_{2,j}, \ldots, \sigma_{r,j}), \tag{3.57}$$

which has in total 2^r possible spin configurations (the variable μ_j can be viewed as one 'column' macrospin with in total 2^r possible microstates). The total Hamiltonian (3.54) can be then written as a sum of two terms, namely, the interaction energy of individual

columns and the interaction energy between adjacent columns. The interaction energy pertain to the jth column of spins is

$$\mathcal{H}_1(\mu_j) = -J\sum_{i=1}^{r}\sigma_{i,j}\sigma_{i+1,j}, \tag{3.58}$$

while the interaction energy between the jth and $(j+1)$st column is given by

$$\mathcal{H}_2(\mu_j,\mu_{j+1}) = -J\sum_{i=1}^{r}\sigma_{i,j}\sigma_{i,j+1}. \tag{3.59}$$

With all this in mind, the total Hamiltonian (3.54) can be rewritten as a sum of both these contributions

$$\mathcal{H}(\mu) = \sum_{j=1}^{c}\left[\mathcal{H}_1(\mu_j) + \mathcal{H}_2(\mu_j,\mu_{j+1})\right] \tag{3.60}$$

and it can be further symmetrized upon

$$\mathcal{H}(\mu) = \sum_{j=1}^{c}\left\{\frac{1}{2}\left[\mathcal{H}_1(\mu_j) + \mathcal{H}_1(\mu_{j+1})\right] + \mathcal{H}_2(\mu_j,\mu_{j+1})\right\}. \tag{3.61}$$

Furthermore, it is very appropriate to substitute Eq. (3.61) to a statistical definition of the partition function (1.2) in order to gain the relation

$$\begin{aligned}\mathcal{Z} &= \sum_{\mu_1}\sum_{\mu_2}\dots\sum_{\mu_c}\exp\left(\sum_{j=1}^{c}\left\{-\frac{\beta}{2}\left[\mathcal{H}_1(\mu_j)+\mathcal{H}_1(\mu_{j+1})\right] - \beta\mathcal{H}_2(\mu_j,\mu_{j+1})\right\}\right)\\ &= \sum_{\mu_1}\sum_{\mu_2}\dots\sum_{\mu_c}\prod_{j=1}^{c}\exp\left\{-\frac{\beta}{2}\left[\mathcal{H}_1(\mu_j)+\mathcal{H}_1(\mu_{j+1})\right] - \beta\mathcal{H}_2(\mu_j,\mu_{j+1})\right\}.\end{aligned} \tag{3.62}$$

The structure of the relation (3.62) implies that the partition function of the spin-1/2 Ising model on the square lattice can be formally calculated following the standard procedure based on the transfer-matrix method

$$\mathcal{Z} = \sum_{\mu_1}\sum_{\mu_2}\dots\sum_{\mu_c}T(\mu_1,\mu_2)T(\mu_2,\mu_3)\dots T(\mu_c,\mu_1) = \sum_{\mu_1}T^c(\mu_1,\mu_1) = \mathrm{Tr}(T^c), \tag{3.63}$$

with the relevant transfer matrix $T(\mu_j,\mu_{j+1})$ depending on the two nearest-neighbouring 'column' macrospins μ_j and μ_{j+1}

$$\begin{aligned}T(\mu_j,\mu_{j+1}) &= \exp\left\{-\frac{\beta}{2}\left[\mathcal{H}_1(\mu_j)+\mathcal{H}_1(\mu_{j+1})\right] - \beta\mathcal{H}_2(\mu_j,\mu_{j+1})\right\}\\ &= \exp\left[\frac{\beta J}{2}\left(\sum_{i=1}^{r}\sigma_{i,j}\sigma_{i+1,j} + \sum_{i=1}^{r}\sigma_{i,j+1}\sigma_{i+1,j+1}\right) + \beta J\sum_{i=1}^{r}\sigma_{i,j}\sigma_{i,j+1}\right]\end{aligned} \tag{3.64}$$

As a matter of fact, the final result to be presented in Eq. (3.63) indicates that the partition function of the spin-1/2 Ising model on the square lattice can be calculated as a trace of the matrix T^c, which is eventually equal to a sum over all eigenvalues of the $2^r \times 2^r$ transfer matrix $T(\mu_j, \mu_{j+1})$ raised to the cth power

$$\mathcal{Z} = \mathrm{Tr}(T^c) = \sum_{j=1}^{2^r} \lambda_j^c. \tag{3.65}$$

In the thermodynamic limit, the Helmholtz free energy normalized per one site can be largely simplified by sorting the eigenvalues of the transfer matrix $T(\mu_j, \mu_{j+1})$ in descending order $\lambda_1 > \lambda_2 \geq \ldots \geq \lambda_{2^r}$, actually,

$$\begin{aligned}
\mathcal{F} &= -k_{\mathrm{B}}T \lim_{r\to\infty} \lim_{c\to\infty} \frac{1}{rc} \ln \mathcal{Z} = -k_{\mathrm{B}}T \lim_{r\to\infty} \lim_{c\to\infty} \frac{1}{rc} \ln \left(\lambda_1^c + \lambda_2^c + \ldots + \lambda_{2^r}^c\right) \\
&= -k_{\mathrm{B}}T \lim_{r\to\infty} \frac{1}{r} \ln \lambda_1 - k_{\mathrm{B}}T \lim_{r\to\infty} \lim_{c\to\infty} \frac{1}{rc} \ln \left[1 + \sum_{k=1}^{2^r} \left(\frac{\lambda_k}{\lambda_1}\right)^c\right] \\
&= -k_{\mathrm{B}}T \lim_{r\to\infty} \frac{1}{r} \ln \lambda_1.
\end{aligned} \tag{3.66}$$

In this way, the finding of the exact solution for the spin-1/2 Ising model on the square lattice essentially reduces to finding of the largest eigenvalue of the transfer matrix $T(\mu_j, \mu_{j+1})$. It should be stressed, nevertheless, that the exact solution of the spin-1/2 Ising model on the square lattice requires the finding of the largest eigenvalue of the $2^r \times 2^r$ transfer matrix $T(\mu_j, \mu_{j+1})$ by letting r tend to infinity unlike the finding of the largest eigenvalue of the simple 2×2 transfer matrix corresponding to the spin-1/2 Ising chain. This is an origin of major difficulties to be present by solving any planar Ising model.

The largest eigenvalue of the transfer matrix, which corresponds to the spin-1/2 Ising model on the square lattice, was firstly derived in the highly celebrated Onsager's paper [1] by the use of Lie algebra and group representation. It is worthy to note that the original Onsager's work as well as many of its subsequent simplifications offered by the Pfaffian method or other combinatorial approaches are mathematically too intricate to follow them within this elementary course. Therefore, we shall henceforth restrict ourselves merely to stating the final result of this rather cumbersome derivation. The largest eigenvalue of the transfer matrix (3.64) is

$$\lambda_1 = [2\sinh(2\beta J)]^{\frac{r}{2}} \exp\left[\frac{1}{2}(\alpha_1 + \alpha_3 + \ldots + \alpha_{2r-1})\right], \tag{3.67}$$

where α_k is defined by

$$\cosh(\alpha_k) = \coth(2\beta J)\cosh(2\beta J) - \cos\left(\frac{\pi k}{r}\right). \tag{3.68}$$

By adopting Eq. (3.67), the Helmholtz free energy (3.66) per one site can be modified to

$$\mathcal{F} = -k_{\mathrm{B}}T \lim_{r\to\infty} \frac{1}{r} \ln \lambda_1 = -\frac{k_{\mathrm{B}}T}{2} \ln\left[2\sinh(2\beta J)\right] - k_{\mathrm{B}}T \lim_{r\to\infty} \frac{1}{2r} \sum_{k=1}^{r} \alpha_{2k-1}. \tag{3.69}$$

In the thermodynamic limit ($r \to \infty$), the sum appearing in Eq. (3.69) can be substituted by the integral so that

$$\mathcal{F} = -\frac{k_{\mathrm{B}}T}{2} \ln\left[2\sinh(2\beta J)\right] - \frac{k_{\mathrm{B}}T}{2\pi} \int_0^{\pi} \mathrm{arccosh}\left[\coth(2\beta J)\cosh(2\beta J) - \cos\theta\right] \mathrm{d}\theta. \tag{3.70}$$

The expression (3.70) can be further simplified by the use of identity

$$\mathrm{arccosh}|x| = \frac{1}{\pi} \int_0^{\pi} \ln[2(x - \cos\phi)] \mathrm{d}\phi, \tag{3.71}$$

which consecutively yields from Eq. (3.70) the formula

$$\begin{aligned} \mathcal{F} = &- \frac{k_{\mathrm{B}}T}{2} \ln\left[2\sinh(2\beta J)\right] - \frac{k_{\mathrm{B}}T}{2} \ln 2 \\ &- \frac{k_{\mathrm{B}}T}{2\pi^2} \int_0^{\pi}\int_0^{\pi} \ln\left[\coth(2\beta J)\cosh(2\beta J) - \cos\theta - \cos\phi\right] \mathrm{d}\theta\mathrm{d}\phi. \end{aligned} \tag{3.72}$$

The formula (3.72) can finally be symmetrized to

$$\begin{aligned} \mathcal{F} = &- k_{\mathrm{B}}T \ln 2 \\ &- \frac{k_{\mathrm{B}}T}{2\pi^2} \int_0^{\pi}\int_0^{\pi} \ln\left\{\left[\cosh(2\beta J)\right]^2 - \sinh(2\beta J)[\cos\theta + \cos\phi]\right\} \mathrm{d}\theta\mathrm{d}\phi. \end{aligned} \tag{3.73}$$

The above equation represents the famous Onsager's result determining the Helmholtz free energy of the spin-1/2 Ising model on the square lattice. It should be remarked that the exact results for other thermodynamic quantities can be obtained from Eq. (3.73) after straightforward but usually lengthy calculation by the use of standard thermodynamical-statistical relations. For simplicity, we shall merely list the exact expression for the spontaneous magnetization, which represents the order parameter for ferromagnetic materials.

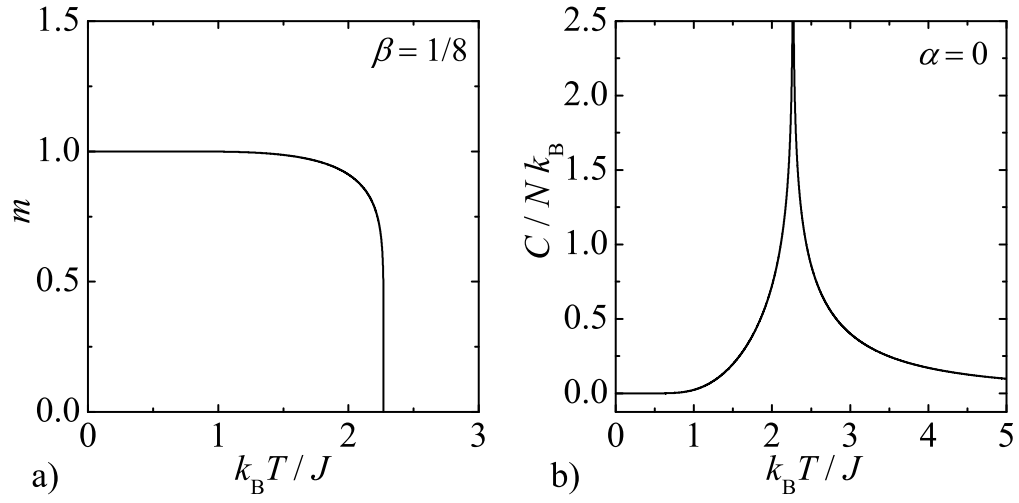

Figure 9: a) Spontaneous magnetization of the spin-1/2 Ising model on the square lattice as a function of the dimensionless temperature; b) Temperature dependence of the specific heat in an absence of the external magnetic field. The logarithmic divergence in the specific heat can be observed at the critical temperature.

Even though the final expression for the spontaneous magnetization of the spin-1/2 Ising model on the square lattice is surprisingly simple

$$m = \begin{cases} \left[1 - \dfrac{1}{(\sinh 2\beta J)^4}\right]^{\frac{1}{8}} & \text{if } T < T_{\mathrm{c}}, \\ 0 & \text{if } T \geq T_{\mathrm{c}}, \end{cases} \tag{3.74}$$

its derivation is regrettably complex[11]. It can be easily understood from Eq. (3.74) that the spontaneous magnetization is zero at and above the critical temperature, while it monotonically increases by decreasing the temperature until its saturation value is reached at the absolute zero temperature (see Fig. 9a). The non-zero spontaneous magnetization means that there is an excess of spins, which are spontaneously pointing in the same spatial direction below some (critical) temperature. In other words, the spins have a

[11] Note that the exact expression for the spontaneous magnetization cannot be straightforwardly derived by differentiating the Helmholtz free energy with respect to the external magnetic field (2.28) and consecutively taking the limit of vanishing external field, since there is no exact expression for the Helmholtz free energy in a presence of the external magnetic field. In this regard, some indirect method must be employed in order to derive the spontaneous magnetization (3.74) in a similar way as firstly done by C. N. Yang [11] in his pioneering work published in 1952.

tendency to align themselves in the same spatial direction and if we randomly choose one spin from the lattice, then, it is more likely that the spin is pointing in the direction of the spontaneous magnetization than in the opposite direction. It is noteworthy that this rather peculiar long-range correlation occurs spontaneously without being enforced by some external field of force such as the magnetic field. A presence of the order-disorder phase transition is independently verified also by the temperature dependence of the specific heat (see Fig. 9b), which exhibits a marked logarithmic divergence in a vicinity of the critical temperature.

We shall end up the present section with several concluding remarks. First, it is worthwhile to remark that changing the dimensionality of a magnetic lattice (from 1D to 2D) has such a dramatic effect upon the phase transitions and critical phenomena. Even although 2D Ising model seems to be extraordinary simple model, it should be emphasized that the exact solution of 2D Ising model in a presence of the external magnetic field is still unresolved problem, yet. Note furthermore that this exact solution would be of fundamental importance as it would clarify the dependence of the magnetization on the magnetic field or it would permit the derivation of the exact closed-form expression for the zero-field susceptibility as a function of the temperature. What is even much worse, we even do not know whether such a calculation can be in principle performed.

3.5 Ising model and insulating magnetic materials

Even although the Ising model has been originally developed to model essential aspects of magnetic materials, throughout the years it has found manifold applications in seemingly diverse research areas. Actually, there are several physical motivations why to explore the Ising model and its manifold variants, which have proved their usefulness in the realm of statistical physics as suitable models for investigating the order-disorder phenomena in binary alloys, the lattice gas models capturing liquid–gas transitions, the models clarifying a phase separation in liquid mixtures, the models explaining an adsorption of gas atoms on a solid surface, the models elucidating cooperative phenomena in various biological and chemical systems such as DNA, allosteric enzymes, hemoglobine, myoglobine, etc. Here, we shall discuss in particular perhaps its most important connection with the insulating

magnetic materials.

For many years was Ising model regarded just as a pure theoretical simplification without any detailed correspondence to a specific material[12]. First insulating magnetic materials, which behave rather similarly to the corresponding Ising model, have indeed been discovered almost a half century after Wilhelm Lenz suggested to his postgraduate student Ernst Ising to solve this simple model of magnetism [12]. Apart from this inconvenience, there are currently two wide families of insulating magnetic materials that are usually recognized as Ising-like materials generally meeting the microscopic Hamiltonian based on the Ising model. First class of the Ising-like materials involves several *rare-earth compounds* such as dysprosium ethylsulfate nonahydrate $Dy(C_2H_5SO_4)_3.9H_2O$, dysprosium aluminum garnet $Dy_3Al_5O_{12}$, dysprosium phosphate $DyPO_4$, lithium-holmium fluoride $LiHoF_4$, lithium-terbium fluoride $LiTbF_4$ (see [13] and references therein). In this class of materials, the only carriers of magnetic moment are rare-earth elements (Dy, Ho, Tb) that interact among themselves almost entirely through dipolar forces and other non-dipolar interactions are generally weak. Because the dipole-dipole interaction decays rather rapidly with a distance (as a third power of distance), the interaction between spatially distant rare-earth ions can frequently be ignored. Therefore, it is often sufficient to consider merely the interaction between nearest-neighbour rare-earth ions and to neglect all other interactions with more distant neighbours (Ising-like criterion). However, it should be nevertheless pointed out that the magnetic dipole-dipole interaction is in fact a long-range interaction and hence, the interactions with distant neighbours can occasionally be at an origin of more complex behaviour. Thus, the most suitable rare-earth compounds for representing Ising-like materials are those, where interactions with more distant neighbours almost completely cancel out and the nearest-neighbour interaction makes the most significant contribution to the overall magnetic behaviour. Even if there could exist clear differences between the ideal Ising model and the real magnetic substances, the agreement between theoretical predictions and relevant experimental data is then found to be very satisfactory [13, 14].

[12]The application of models presuming a fully localized magnetic moments to conducting metals such as iron or nickel is unjustifiable for fundamental reasons.

More sophisticated representatives of the Ising-like materials represent insulating magnetic materials from the family of *polymeric coordination compounds*. Partly by accident, but in most cases by a careful choice of magnetic substances from an immense reservoir of polymeric coordination compounds, it is often possible to find magnetic materials whose magnetic properties resemble quite closely those predicted by the Ising model and its various variants [14]. In this wide class of compounds, the most important interaction between magnetic centers (usually transition-metal elements) represents a superexchange interaction mediated via intervening non-magnetic atom(s). Unfortunately, there is no general theory, which would admit a straightforward calculation of the parameter J related to the pairwise exchange interaction between metal centers and hence, the coupling constant J must be determined just as a self-adjustable parameter from a comparison with relevant experimental data of a specific material. It is noteworthy, however, that the strength of exchange interaction depends very sensitively on a distance (it decays like r^{-10} or even more rapidly [15]) as it bears a direct relationship with an effective overlap between the wave functions of magnetic metal centers and the ones of non-magnetic atoms mediating the superexchange interaction between them[13]. In this respect, the polymeric coordination compounds satisfy even much better the necessary (but not sufficient) criterion of the Ising-like material, which demands a predominant nearest-neighbour interaction and weak further-neighbour interactions.

The most crucial limitation for obtaining Ising-like material from the class of polymeric coordination compounds thus lies in the fact that the exchange interaction is extremely anisotropic within the Ising model description (this model contains just one spatial component of spin operators), while the superexchange mechanism gives rise to a wholly isotropic exchange interaction. According to this, the Heisenberg model (containing all three spatial components of spin operators) is in general much more appropriate for describing the real magnetic materials from this wide family of compounds. However, the effective anisotropic exchange interaction need not arise from the interaction mechanism, but it may have a close connection to different sources of magnetic anisotropy such as

[13]There is a rule that each additional intervening atom reduces the strength of exchange interaction hundred times.

spin-orbit interaction, crystal-field effect, dipolar interaction and so on. In such a case, the application of Ising model is justified even if it still represents a certain oversimplification of the real system (there does not exist infinite magnetic anisotropy in nature). Notwithstanding of this objection, the overall agreement between theoretical predictions derived from Ising model and experimental measurements performed on several cobalt-based coordination compounds, as for instance $Co(pyridine)_2Cl_2$, K_2CoF_4, Rb_2CoF_4, Cs_3CoX_5 (X = F, Cl, Br), is generally found very satisfactory [14].

It should be also remarked that all magnetic compounds from both the families of Ising-like materials are in reality three-dimensional crystals, however, some of them can effectively possess the low-dimensional magnetic structure on behalf of the lack of an appreciable magnetic interaction in one or more spatial directions. As a matter of fact, the magnetic and crystallographic lattice can significantly differ especially when the carriers of magnetic moment are largely separated along some spatial direction(s). In the consequence of that, the magnetic lattice then becomes low-dimensional due to the short-range character of magnetic interactions. The reliability of exactly solved low-dimensional Ising models in representing real-world insulating magnetic materials has been checked with appreciable success even if some healthy skepticism is always appropriate if one is seeking true understanding of real materials [13].

Finally, let us briefly comment on a connection between the effective spin Hamiltonian of the usual spin-1/2 Ising model defined with the help of Ising spin variables $\sigma_i = \pm 1$

$$\mathcal{H} = -\sum_{(i,j)} J_{ij}\sigma_i\sigma_j - \sum_i H\sigma_i \tag{3.75}$$

and the effective spin Hamiltonian describing the real insulating magnetic materials. It should be stressed, nevertheless, that the spin-1/2 particles have quantized intrinsic angular momentum with the eigenvalues $S = \pm\hbar/2$ in opposite to the simple Ising spin variables $\sigma_i = \pm 1$ (it is tacitly presumed that the Planck's constant $\hbar$ is set to unity and the eigenvalues $\pm 1/2$ are rescaled to ± 1). In addition, each magnetic moment m_i (rather than spin S_i) possesses some magnetostatic Zeeman's energy if a spin-1/2 particle is placed in an external magnetic field B. According to the magneto-mechanical parallelism, there is a simple correspondence between a spin angular momentum and its

corresponding magnetic moment and this correspondence can be expressed through the relation $m_i = g\mu_{\mathrm{B}} S_i$ (g is Landé g-factor and μ_{B} is Bohr magneton). With all this in mind, is is much more precise to define the spin-1/2 Ising model through the Hamiltonian

$$\mathcal{H} = -\sum_{(i,j)} R_{ij} S_i S_j - \sum_i g\mu_{\mathrm{B}} B S_i. \tag{3.76}$$

It should be pointed out, however, that both Hamiltonians (3.75) and (3.76) are essentially equivalent on assumption that

$$J_{ij} = R_{ij}\hbar^2/4 \qquad \text{and} \qquad H = g\mu_{\mathrm{B}} B\hbar/2, \tag{3.77}$$

whereas it is much more appropriate to work with some scaled dimensionless variables rather than with the real physical quantities multiplied by several constant factors.

4 Ising model on Bethe lattice

In spite of its conceptual simplicity the spin-1/2 Ising model on any 2D lattice is in general intractable problem in a presence of the external magnetic field and hence, one does not have a direct access from this simple lattice-statistical model to a rigorous investigation of the magnetization process of insulating magnetic materials. From this perspective, it appears worthwhile to investigate the spin-1/2 Ising model defined on lattices, which may closely resemble a magnetic behaviour of the planar Ising models in a magnetic field but they are still exactly solvable. To this special class of exactly solved Ising lattices belong the ones denoting a deep interior of recursively built trees.

4.1 Cayley tree versus Bethe lattice

The Cayley tree denotes a recursively built tree developed from a node forming its zeroth generation, to which q different sites of the first generation are connected if one considers the recursively built tree with the coordination number q. Next, other $q-1$ sites of the second generation are connected to each site of the first generation and this procedure is then recursively repeated up to infinity. For better illustration, a part of the recursively built Cayley tree with the particular value of the coordination number $q = 3$ is schematically depicted in Fig. 10. If the total number of sites of the jth generation is labeled as N_j, then, one acquires the following sequence of the total number of sites for the recursively built generations

$$N_0 = 1,\ N_1 = q,\ N_2 = q(q-1),\ N_3 = q(q-1)^2,\ \ldots,\ N_n = q(q-1)^{n-1}. \tag{4.1}$$

It is quite obvious that the total number of sites of the individual generations form a geometric series with the coefficient q and the common ratio between adjacent terms $q-1$, hence, the total number of sites of the whole Cayley tree equals

$$N_t = \sum_{j=0}^{n} N_j = 1 + q\frac{(q-1)^n - 1}{q-2}. \tag{4.2}$$

In the thermodynamic limit $n \to \infty$ of the infinitely large Cayley tree the total number of sites of the last generation forms non-negligible fraction with respect to the total number

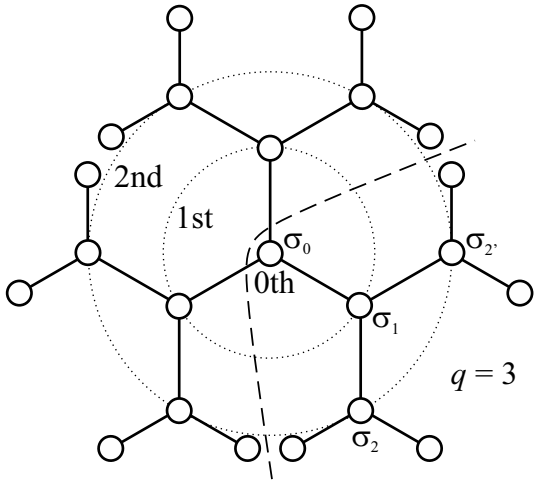

Figure 10: A schematic illustration of a small portion of the Cayley tree with the coordination number $q = 3$, which is composed from the nodal site occupied by the Ising spin σ_0 and three successive generations. The Bethe lattice denotes an interior of the Cayley tree obtained by neglecting boundary sites from the last generation, i.e. in this particular case it consists only from a central node and first two generations connected by dotted circles. A broken line demarcates one individual branch of the Bethe lattice.

of sites of the whole Cayley tree

$$\lim_{n\to\infty} \frac{N_n}{N_t} = \frac{q-2}{q-1}. \tag{4.3}$$

For instance, the boundary sites of the Cayley tree with the coordination number $q = 3$ form 50% of all lattice sites and this fraction becomes greater as the coordination number q increases. Owing to this fact, the lattice-statistical behaviour of the spin-1/2 Ising model defined on such a recursively built tree will crucially depend on whether or not the boundary sites from the last generation are taken into consideration what is in sharp contrast with the standard planar lattices where the number of boundary sites is negligible with respect to the total number of sites as they follow the scaling law $\propto 1/\sqrt{N_t}$. In the consequence of that, the spin-1/2 Ising model on the whole Cayley tree does not display a finite-temperature phase transition because all sites from the last generation are only singly coordinated [16, 17, 18], while the spin-1/2 Ising model defined solely on a deep interior of infinitely large Cayley tree does show a finite-temperature phase transition [19]. For this reason, the deep interior of infinitely large Cayley tree is traditionally called as the Bethe lattice in order to unambiguously discern both particular cases. In the following

we will focus our attention to a detailed analysis of the spin-1/2 Ising model on the Bethe lattice, which could approximate a magnetic behaviour of the planar Ising model with the same coordination number assuming an ideal crystal without any boundaries.

4.2 Exact recursion relations

Let us start by considering the Hamiltonian of the spin-1/2 Ising model on the Bethe lattice with the coordination number q

$$\mathcal{H} = -J \sum_{(i,j)} \sigma_i \sigma_j - H \sum_i \sigma_i, \tag{4.4}$$

which takes into account the nearest-neighbour interaction J between the Ising spins $\sigma_i = \pm 1$ placed in the external magnetic field H. For the sake of simplicity, we will consider the particular case with the ferromagnetic coupling constant $J > 0$, while a few comments will be mentioned at the end of our discussion also for the antiferromagnetic case with $J < 0$. The partition function of the spin-1/2 Ising model on the Bethe lattice can be defined as follows

$$\mathcal{Z} = \sum_{\{\sigma\}} \exp(-\beta \mathcal{H}) = \sum_{\{\sigma\}} \exp\left(\beta J \sum_{(i,j)} \sigma_i \sigma_j + \beta H \sum_i \sigma_i \right), \tag{4.5}$$

where $\beta = 1/(k_{\mathrm{B}} T)$, k_{B} is Boltzmann's constant, T is the absolute temperature and the summation $\sum_{\{\sigma\}}$ is carried out over all possible states of the Ising spins of the Bethe lattice. To proceed further with the calculation one may take advantage of the fact that the Bethe lattice can be split into q different branches originating from the central spin σ_0 and the summation over spin states within individual branches can be performed independently of each other due to a nonexistence of an interaction between any pair of spins from different branches (see Fig. 10). In this respect, the partition function of the spin-1/2 Ising model on the Bethe lattice can be rewritten into this equivalent form

$$\mathcal{Z} = \sum_{\sigma_0 = \pm 1} \exp\left(\beta H \sigma_0\right) \left[g_n(\sigma_0)\right]^q = \exp\left(\beta H\right) \left[g_n(+1)\right]^q + \exp\left(-\beta H\right) \left[g_n(-1)\right]^q . \tag{4.6}$$

In above, the expression $g_n(\sigma_0)$ denotes the partition function of one individual branch composed of n generations starting from the central spin σ_0, which can be recursively

defined through the partition function $g_{n-1}(\sigma_1)$ of one of its subbranches with $n-1$ generations having the central spin σ_1 (see Fig. 10 for the relevant notation)

$$\begin{aligned} g_n(\sigma_0) &= \sum_{\sigma_1=\pm 1} \exp\left(\beta J\sigma_0\sigma_1 + \beta H\sigma_1\right)\left[g_{n-1}(\sigma_1)\right]^{q-1} \\ &= \exp\left(\beta J\sigma_0 + \beta H\right)\left[g_{n-1}(+1)\right]^{q-1} + \exp\left(-\beta J\sigma_0 - \beta H\right)\left[g_{n-1}(-1)\right]^{q-1}. \end{aligned} \quad (4.7)$$

After substituting two available states of the central spin $\sigma_0 = \pm 1$ into Eq. (4.7) one gets the following couple of equations

$$\begin{aligned} g_n(+1) &= \exp\left(\beta J + \beta H\right)\left[g_{n-1}(+1)\right]^{q-1} + \exp\left(-\beta J - \beta H\right)\left[g_{n-1}(-1)\right]^{q-1}; \\ g_n(-1) &= \exp\left(-\beta J + \beta H\right)\left[g_{n-1}(+1)\right]^{q-1} + \exp\left(\beta J - \beta H\right)\left[g_{n-1}(-1)\right]^{q-1}; \end{aligned} \quad (4.8)$$

which determines the partition function of one individual branch of n generation with the central spin being in the spin state $\sigma_0 = +1$ or -1, respectively. By dividing the couple of equations (4.8) one may introduce the relative ratio $x_n = \frac{g_n(-1)}{g_n(+1)}$ between the partition functions of one branch of n generations having the central spin two available spin states $\sigma_0 = +1$ and -1

$$x_n = \frac{g_n(-1)}{g_n(+1)} = \frac{\exp\left(-\beta J+\beta H\right)\left[g_{n-1}(+1)\right]^{q-1} + \exp\left(\beta J-\beta H\right)\left[g_{n-1}(-1)\right]^{q-1}}{\exp\left(\beta J+\beta H\right)\left[g_{n-1}(+1)\right]^{q-1} + \exp\left(-\beta J-\beta H\right)\left[g_{n-1}(-1)\right]^{q-1}}, \quad (4.9)$$

which can be further simplified into a more compact form when defining the relative ratio $x_{n-1} = \frac{g_{n-1}(-1)}{g_{n-1}(+1)}$ between the partition functions of the subbranch of $n-1$ generations

$$x_n = \frac{\exp\left(-\beta J + \beta H\right) + \exp\left(\beta J - \beta H\right) x_{n-1}^{q-1}}{\exp\left(\beta J + \beta H\right) + \exp\left(-\beta J - \beta H\right) x_{n-1}^{q-1}}. \quad (4.10)$$

The equation (4.10) represents the central result of our calculation, because it determines the relative ratio between the partition functions of n and $n-1$ generations. It is clear that the equation (4.10) can be solved recursively by the method of successive iterations and thus, this relative ratio can be easily found even in the thermodynamic limit $n \to \infty$ when it converges to the so-called *stable fixed point*. It can be found that there exist two stable fixed points at sufficiently low temperatures with $x_\infty < 1$ and $x_\infty > 1$, whereas there is only one stable fixed point $x_\infty = 1$ at high enough temperatures. It will be convincingly evidenced hereafter that two former stable fixed points at $x_\infty < 1$ and $x_\infty > 1$ correspond to a ferromagnetic long-range order with two opposite values of the

spontaneous magnetization $m > 0$ and $m < 0$, while the latter stable fixed point at $x_\infty = 1$ is pertinent to a disordered paramagnetic state with zero spontaneous magnetization $m = 0$.

In the following we will demonstrate how the magnetization can be expressed solely in terms of the relative ratio x_n corresponding to the stable fixed point of the recursive relations (4.10). In the thermodynamic limit $n \to \infty$ all spins of the Bethe lattice are equivalent and the magnetization per site can be accordingly calculated as the statistical mean value of the central spin

$$m \equiv \langle \sigma_0 \rangle = \frac{1}{\mathcal{Z}} \sum_{\{\sigma\}} \sigma_0 \exp(-\beta \mathcal{H}). \tag{4.11}$$

The partition function $\mathcal{Z}$ of the spin-1/2 Ising model on the Bethe lattice can be evaluated from Eq. (4.6) and the similar relation can be also derived for the other expression

$$\begin{aligned} \sum_{\{\sigma\}} \sigma_0 \exp(-\beta \mathcal{H}) &= \sum_{\sigma_0 = \pm 1} \exp(\beta H \sigma_0)\, \sigma_0 \left[g_n(\sigma_0)\right]^q \\ &= \exp(\beta H) \left[g_n(+1)\right]^q - \exp(-\beta H) \left[g_n(-1)\right]^q . \end{aligned} \tag{4.12}$$

Substituting Eqs. (4.6) and (4.12) into the definition (4.11) one obtains for the magnetization the following result

$$m = \frac{\exp(\beta H) \left[g_n(+1)\right]^q - \exp(-\beta H) \left[g_n(-1)\right]^q}{\exp(\beta H) \left[g_n(+1)\right]^q - \exp(-\beta H) \left[g_n(-1)\right]^q}, \tag{4.13}$$

which can be further re-expressed in terms of the relative ratio x_n given by Eq. (4.10)

$$m = \frac{\exp(\beta H) - \exp(-\beta H)\, x_n^q}{\exp(\beta H) + \exp(-\beta H)\, x_n^q}. \tag{4.14}$$

The exact result for the magnetization of the spin-1/2 Ising model on the Bethe lattice can be obtained from Eq. (4.14) when substituting therein the relative ratio x_n, which corresponds to the stable fixed point of the exact recursion relation (4.10). In the thermodynamic limit $n \to \infty$ the solution for the exact recursion relation (4.10) converges to the stable fixed point with the specific value to be further denoted for the sake of simplicity as $x = \lim_{n \to \infty} x_n$. Bearing this in mind, the formulas (4.10) and (4.14) for the exact recursion relation and the magnetization can be rewritten in this compact form

$$x = \frac{\exp(-\beta J + \beta H) + \exp(\beta J - \beta H)\, x^{q-1}}{\exp(\beta J + \beta H) + \exp(-\beta J - \beta H)\, x^{q-1}} \tag{4.15}$$

and

$$m = \frac{\exp(\beta H) - \exp(-\beta H)\, x^q}{\exp(\beta H) + \exp(-\beta H)\, x^q}. \tag{4.16}$$

It is worth noticing that the exact recursion relation (4.15) is invariant under the transformation $x \to 1/x$ and $H \to -H$, while the respective formula (4.16) for the magnetization satisfies the fundamental property $m(x, H) = -m(1/x, -H)$ ensuring that the magnetization is odd function of the external magnetic field. Instead of iterative solution of the exact recursion relation (4.15) one may alternatively solve a single polynomial equation of degree q in order to determine the fixed points x of the exact recursion relations

$$\mathrm{e}^{-\beta J-\beta H} x^q - \mathrm{e}^{\beta J-\beta H} x^{q-1} + \mathrm{e}^{\beta J+\beta H} x - \mathrm{e}^{-\beta J+\beta H} = 0. \tag{4.17}$$

The polynomial equation (4.17) may have up to q different real roots and it is therefore important to find a thermodynamically stable solution with the lowest Gibbs free energy. In the thermodynamic limit $n \to \infty$ one may take advantage of the fact that the recursion parameter converges to the stable fixed point $x \equiv x_n \cong x_{n-1}$ and the same holds true for the partition function of the branch of n generations having the central spin in the spin-up state $g(+1) \equiv g_n(+1) \cong g_{n-1}(+1)$. Bearing all this in mind, the following expression can be obtained from Eq. (4.6) for the Gibbs free energy

$$\mathcal{G} = -q k_{\mathrm{B}} T \ln\left[g(+1)\right] - k_{\mathrm{B}} T \ln\left(\mathrm{e}^{\beta H} + \mathrm{e}^{-\beta H} x^q\right). \tag{4.18}$$

One may consequently eliminate from Eq. (4.18) the particular value of the partition function $g(+1)$ by making use of Eq. (4.8) in order to get the final expression for the Gibbs free energy of the spin-1/2 ising model on the Bethe lattice

$$\mathcal{G} = \frac{q}{q-2} k_{\mathrm{B}} T \ln\left(\mathrm{e}^{\beta J+\beta H} + \mathrm{e}^{-\beta J-\beta H} x^{q-1}\right) - k_{\mathrm{B}} T \ln\left(\mathrm{e}^{\beta H} + \mathrm{e}^{-\beta H} x^q\right), \tag{4.19}$$

which is entirely expressed in terms of the recursion parameter x unambiguously given by the polynomial equation (4.17). The particular value of the Gibbs free energy (4.19) assigned to each real root of the polynomial equation (4.17) can be subsequently regarded as a conclusive criterion whether a given solution is thermodynamically stable or not.

4.3 Spontaneous order and critical point

In the following part we will focus our attention on the zero-field limit ($H = 0$) of the ferromagnetic spin-1/2 Ising model on the Bethe lattice, which displays at sufficiently low temperatures a spontaneous long-range order that terminates at a critical point. In the absence of the external magnetic field the exact results for the recursion relation (4.15) and the magnetization (4.16) can be simplified to the following expressions

$$x = \frac{\mathrm{e}^{-\beta J} + \mathrm{e}^{\beta J} x^{q-1}}{\mathrm{e}^{\beta J} + \mathrm{e}^{-\beta J} x^{q-1}} \tag{4.20}$$

and

$$m = \frac{1 - x^q}{1 + x^q}. \tag{4.21}$$

It is worthwhile to recall that the exact recursion relation (4.20) is still invariant under the transformation $x \to 1/x$ and the spontaneous magnetization satisfies the condition $m(x, H = 0) = -m(1/x, H = 0)$. If the exact recursion relation (4.20) has a solution affording nonzero magnetization $m \neq 0$, the aforementioned properties automatically guarantee two equivalent solutions for x and $1/x$ with the same absolute value of the spontaneous magnetization. It is quite clear that the two inverse solutions x and $1/x$ correspond to a spontaneous ferromagnetic order with either positive or negative magnetization, whereby the solution with $x < 1$ gives $m > 0$ and the one with $x > 1$ provides $m < 0$, respectively. It can be readily proved, moreover, that the exact recursion relation (4.20) also has a paramagnetic solution $x = 1$, which is consistent with existence of a disordered phase with zero spontaneous magnetization $m = 0$.

In the zero-temperature asymptotic limit $T \to 0$ one gets from Eq. (4.20) two solutions $x \to 0$ and $x \to \infty$, which imply a perfect spontaneous ferromagnetic long-range order with $m = +1$ and $m = -1$, respectively. It can be easily verified that these two ordered solutions 'symmetrically' distributed with respect to a disorder point $x = 1$ move closer to each other upon increasing of temperature until they completely coalesce at a certain temperature, which determines a critical temperature associated with a breakdown of the spontaneous ferromagnetic long-range order. To support this statement it is useful to rewrite the exact recursion relation (4.20) into the form of a polynomial equation with

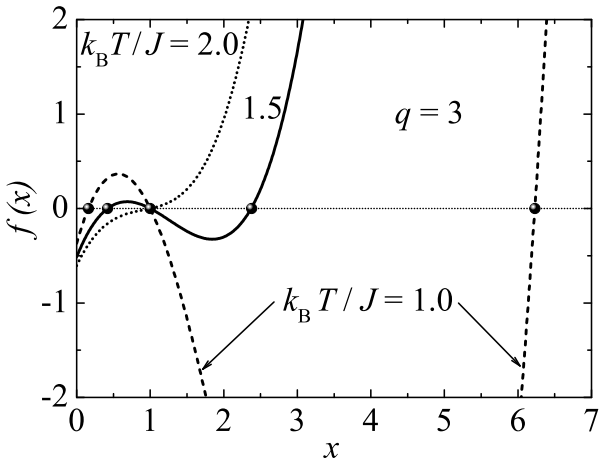

Figure 11: The polynomial function $f(x)$ versus the recursive parameter x for the spin-1/2 Ising model on the Bethe lattice with the coordination number $q = 3$ at three different temperatures $k_B T/J = 1.0$, 1.5 and 2.0. The intercept points of the polynomial function $f(x)$ with the special value $f(x) = 0$ visualized as black balls determine algebraic solutions of the polynomial equation (4.22), which correspond to the stable fixed points of the recursion relation (4.20).

respect to the recursion parameter x

$$f(x) = \mathrm{e}^{-\beta J} x^q - \mathrm{e}^{\beta J} x^{q-1} + \mathrm{e}^{\beta J} x - \mathrm{e}^{-\beta J} = 0. \tag{4.22}$$

A typical dependence of the polynomial function $f(x)$ on the recursion parameter x is plotted in Fig. 11 for the spin-1/2 Ising model on the Bethe lattice with the coordination number $q = 3$ at three different temperatures. It actually follows from Fig. 11 and previous argumentation that all three roots of the polynomial equation (4.22) are gradually shifting closer to each other upon increasing of temperature until they complete coalesce at the critical temperature, which means that the critical point of the ferromagnetic spin-1/2 Ising model on the Bethe lattice can be obtained from an inflection point of the polynomial equation (4.22)

$$\left(\frac{\mathrm{d}f(x)}{\mathrm{d}x}\right)_{x=1,T=T_c} = 0 \qquad \text{and} \qquad \left(\frac{\mathrm{d}^2 f(x)}{\mathrm{d}x^2}\right)_{x=1,T=T_c} = 0. \tag{4.23}$$

After performing the differentiation of the polynomial equation (4.22) with respect to the relative ratio x at the critical point one obtains two expressions

$$\frac{\mathrm{d}f(x)}{\mathrm{d}x} = q\mathrm{e}^{-\beta J} x^{q-1} - (q-1)\mathrm{e}^{\beta J} x^{q-2} + \mathrm{e}^{\beta J},$$

$$\frac{\mathrm{d}^2 f(x)}{\mathrm{d}x^2} = q(q-1)\mathrm{e}^{-\beta J}x^{q-2} - (q-1)(q-2)\mathrm{e}^{\beta J}x^{q-3}, \tag{4.24}$$

which provide for the inflection point (4.23) of the polynomial equation (4.22) a unique condition directly determining the critical point

$$q\mathrm{e}^{-\beta_{\mathrm{c}} J} - (q-2)\mathrm{e}^{\beta_{\mathrm{c}} J} = 0. \tag{4.25}$$

The solution of the critical condition (4.25) gives the following exact result for the critical temperature of the ferromagnetic spin-1/2 Ising model on the Bethe lattice

$$\mathrm{e}^{2\beta_{\mathrm{c}} J} = \frac{q}{q-2} \Longleftrightarrow \frac{k_{\mathrm{B}} T_{\mathrm{c}}}{J} = \frac{2}{\ln\left(\frac{q}{q-2}\right)}. \tag{4.26}$$

At this stage, it appears worthwhile to compare the critical temperatures of the ferromagnetic spin-1/2 Ising model on the Bethe lattice with the respective exact critical temperatures of the ferromagnetic spin-1/2 Ising model on the regular planar lattices such as hexagonal, square or triangular lattice compiled in Table 2. The spin-1/2 Ising model on the Bethe lattice has the following values of the critical temperatures $k_{\mathrm{B}}T_{\mathrm{c}}/J \approx 1.82048$ for $q = 3$, $k_{\mathrm{B}}T_{\mathrm{c}}/J \approx 2.88539$ for $q = 4$ and $k_{\mathrm{B}}T_{\mathrm{c}}/J \approx 4.93261$ for $q = 6$, which exceed only by 19%, 27% and 35% the exact critical temperatures of the spin-1/2 Ising model on the hexagonal, square and triangular lattice with the same values of the coordination number q. From this point of view, the exact results for the spin-1/2 Ising model on the Bethe lattice are quite superior with respect to the conventional mean-field theory $k_{\mathrm{B}}T_{\mathrm{c}}^{\mathrm{MFA}}/J = q$, which overestimates the respective exact critical temperatures of the spin-1/2 Ising model on the hexagonal, square and triangular lattice by 98%, 76% and 65%, respectively. The exact solution of the spin-1/2 Ising model on Bethe lattice can be therefore regarded as a useful approximation to the true behaviour of the spin-1/2 Ising model on the regular planar lattices, which can be additionally performed in a presence of the external magnetic field.

Last but not least, let us investigate in somewhat more detail typical temperature dependence of the spontaneous magnetization of the ferromagnetic spin-1/2 Ising model on the Bethe lattice. To this end, one may directly use the formula (4.21) that expresses the spontaneous magnetization of the ferromagnetic spin-1/2 Ising model on the Bethe lattice in terms of the single parameter x determined either by the stable fixed point of

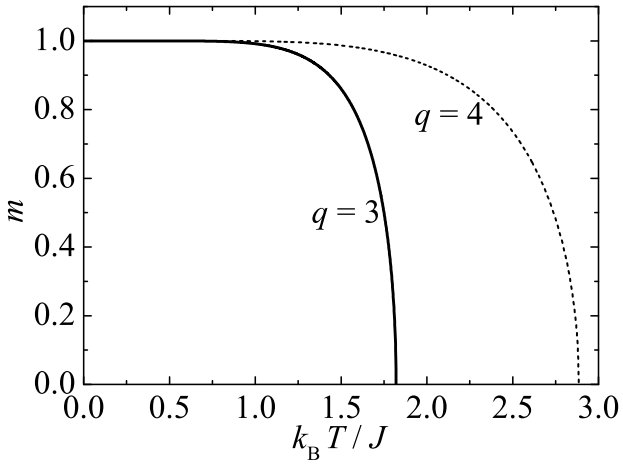

Figure 12: The temperature dependence of the spontaneous magnetization of the spin-1/2 Ising model on the Bethe lattice with the coordination numbers $q = 3$ and $q = 4$ as obtained from the formula (4.21) by considering the root x_+ of the polynomial equation (4.22) given by Eqs. (4.27) and (4.28), respectively.

the exact recursion relation (4.20) or the polynomial equation (4.22). To provide a more complete understanding we have rigorously solved the polynomial equation (4.22) for the particular case of the spin-1/2 Ising model on the Bethe lattice with the coordination number $q = 3$ having the following three roots

$$x_{\mp} = \frac{1}{2}\left[\mathrm{e}^{2\beta J} - 1 \pm \sqrt{(\mathrm{e}^{2\beta J} - 3)\,(\mathrm{e}^{2\beta J} + 1)}\right], \qquad x_0 = 1. \tag{4.27}$$

It can be easily understood from Eq. (4.27) that the solutions $x_{\mp}$ are real only if the inequality $\mathrm{e}^{2\beta J} \geq 3$ is satisfied, which is in concordance with a stability condition of the fixed points $x_{\mp}$ below the critical temperature $k_{\mathrm{B}}T/J \leq k_{\mathrm{B}}T_{\mathrm{c}}/J = 2/\ln 3 \approx 1.82048$. The solutions $x_{\mp}$ can be thus straightforwardly connected with the occurrence of nonzero spontaneous magnetization below the critical temperature, whereby two inversely equal roots $x_- = 1/x_+$ eventually provide the same absolute value of the spontaneous magnetization with the following sign convention $m \geq 0$ for x_+ and $m \leq 0$ for x_-, respectively.

For better illustration, temperature variations of the positive solution for the spontaneous magnetization of the ferromagnetic spin-1/2 Ising model on the Bethe lattice with the coordination numbers $q = 3$ and $q = 4$ are plotted in Fig. 12. It directly follows from Eq. (4.27) that two inversely equal roots $x_{\mp}$ affording the ferromagnetic long-range

order with nonzero spontaneous magnetization coalesce due to a vanishing argument of the respective square root at the critical temperature with the third root $x_0 = 1$, which corresponds to a disordered (paramagnetic) state with zero spontaneous magnetization. This result in turn implies a power-law decay of the spontaneous magnetization with the critical exponent $\beta = 1/2$ from the standard Ising universality class in a vicinity of the critical temperature. Above the critical temperature the two roots $x_{\mp}$ become complex and hence, there exists only one stable fixed point $x_0 = 1$ corresponding to the disordered state with zero spontaneous magnetization. It should be mentioned that the aforedescribed features do not hold specifically only for the ferromagnetic spin-1/2 Ising model on the Bethe lattice with the coordination number $q = 3$, but they represent generic feature of the ferromagnetic spin-1/2 Ising model on the Bethe lattice with arbitrary coordination number q. As a matter of fact, the polynomial equation (4.22) for the particular case of the spin-1/2 Ising model on the Bethe lattice with the coordination number $q = 4$ has the following four roots

$$x_{\mp} = \frac{1}{2}\left(\mathrm{e}^{2\beta J} \pm \sqrt{\mathrm{e}^{4\beta J} - 4}\right), \qquad x_0 = 1, \qquad x_1 = -1, \tag{4.28}$$

among which the last negative solution $x_1 = -1$ is unphysical as the ratio between two partition functions must be nonnegative. From this point of view, one may also repeat the same argumentation for the spin-1/2 Ising model on the Bethe lattice with the coordination number $q = 4$, which displays the spontaneous ferromagnetic order below the critical temperature $k_{\mathrm{B}}T/J \leq k_{\mathrm{B}}T_{\mathrm{c}}/J = 2/\ln 2 \approx 2.88539$ being consistent with the temperature range $\mathrm{e}^{4\beta J} > 4$ ensuring real values of two inversely equal roots $x_{\mp}$.

4.4 Other applications of the method

Let us conclude the section concerned with the exact solution of the spin-1/2 Ising model on the Bethe lattice with a few comments on advantages and disadvantages of the method of exact recursion relations. It has been already mentioned that the main advantage of the method of exact recursion relations is that it may be easily applied to the spin-1/2 Ising model in a presence of the external magnetic field and thus, one gets reasonable approximation to the true magnetic behaviour of the spin-1/2 Ising model on regular

planar lattices in a magnetic field currently inaccessible to any exact analytical method. It should be also stressed that the method of exact recursion relations is by no means restricted to the ferromagnetic spin-1/2 Ising model on the Bethe lattice but it may be relatively easily adapted also to a more complex spin-S Ising models in a magnetic field (including Blume-Capel and Blume-Emery-Griffiths models), which have up to date persisted all attempts aimed at their exact analytical solution when formulated on any 2D lattice even in zero magnetic field.

A few statements are also in order as far as the antiferromagnetic spin-1/2 Ising model on the Bethe lattice is concerned. Although all results presented in this section are valid also for the spin-1/2 Ising model on the Bethe lattice with the antiferromagnetic coupling constant $J < 0$, the iterative solution of the exact recursion relations (4.10) in zero magnetic field and low enough temperatures does not converge to a unique stable fixed point but it bifurcates instead. This property is a direct consequence of the antiferromagnetic (Néel) long-range order when the local magnetizations on odd and even generations of the Bethe lattice have opposite signs. The problem of solving the antiferromagnetic spin-1/2 Ising model on the Bethe lattice can be nevertheless simply avoided by introducing two different relative ratios x_{2n-1}, x_{2n} and associated local magnetizations for odd and even generations, which consequently define a couple of two mutually interconnected recursive relations that still may be exactly solved iteratively. Notwithstanding of this complication, the critical temperature of the antiferromagnetic spin-1/2 Ising model on the Bethe lattice is completely identical with the exact result (4.26) derived for the ferromagnetic spin-1/2 Ising model on the Bethe lattice. Similarly, the staggered magnetization of the antiferromagnetic spin-1/2 Ising model on the Bethe lattice behaves alike the uniform magnetization of the ferromagnetic spin-1/2 Ising model on the Bethe lattice. The same statements of course holds also for the more general antiferromagnetic spin-S Ising models.

On the other hand, it should be pointed out that the antiferromagnetic Ising model on the Bethe lattice cannot in principle capture a magnetic behaviour of the antiferromagnetic Ising model on close-packed lattices such as kagomé or triangular lattice, which are subject to a geometric spin frustration and therefore do not display antiferomagnetic long-range order at sufficiently low temperatures. The Bethe lattice by construction does

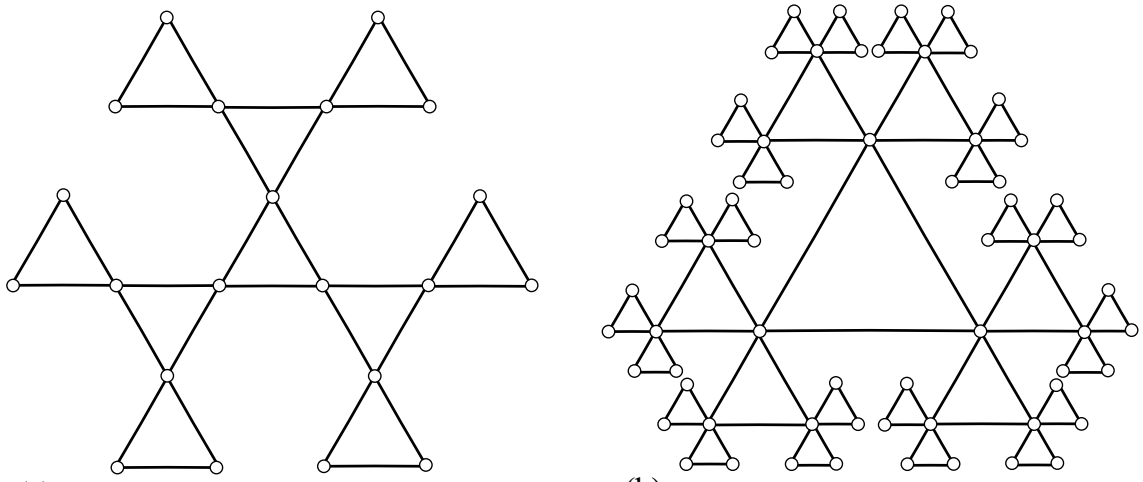

Figure 13: A schematic illustration of first three generations of two recursively built Husimi trees, which may bring insight into a geometric spin frustration of the antiferromagnetic Ising model on the kagomé (a) and triangular (b) lattice, respectively.

not contain any closed polygon and thus, it is incapable of predicting absence of the antiferromagnetic long-range order due to a geometric spin frustration. This drawback can be however avoided by considering more complex recursive lattices, which can be developed from a deep interior of recursively built trees involving closed polygons that are still available to the method of exact recursion relations. The perhaps most famous example of this type represent triangular Husimi lattices schematically illustrated in Fig. 13 for two particular values of the ramification number $r = 2$ and $r = 3$, which could approximate the magnetic behaviour of the antiferromagnetic Ising models on kagomé and triangular lattices, respectively.

Exercises

1. Calculate the nearest-neighbour pair correlation function for the ferromagnetic spin-1/2 Ising model on the Bethe lattice.

2. With the help of Eq. (4.19) calculate and draw temperature dependencies of the Gibbs free energy, entropy and specific heat of the ferromagnetic spin-1/2 Ising model on the Bethe lattice.

3. Solve iteratively the exact recursion relations for the antiferromagnetic spin-1/2 Ising model on the Bethe lattice and show presence of bifurcation.

4. Find the critical point of the ferromagnetic spin-1 Ising model on the Bethe lattice.

5. Calculate the critical temperature for the ferromagnetic spin-1/2 Ising model on the Husimi lattices shown in Fig. 13. Compare the calculated critical temperatures with the exact critical temperatures of the ferromagnetic spin-1/2 Ising model on the kagomé and triangular lattice and the ferromagnetic spin-1/2 Ising model on the Bethe lattice.

5 Exactly soluble Heisenberg models

The Heisenberg model [20] is being another valuable microscopic model, which is worthwhile to study partly on account of an interesting quantum behaviour it displays and partly due to the fact that it represents more realistic model of insulating magnetic materials than the Ising model. The Heisenberg model can be defined through the Hamiltonian

$$\hat{\mathcal{H}} = -J \sum_{(i,j)} \hat{\mathbf{S}}_i \cdot \hat{\mathbf{S}}_j = -J \sum_{(i,j)} \left(\hat{S}_i^x \hat{S}_j^x + \hat{S}_i^y \hat{S}_j^y + \hat{S}_i^z \hat{S}_j^z \right), \tag{5.1}$$

where the summation is usually restricted to nearest-neighbour spin pairs only, the parameter J then labels the exchange interaction between the nearest-neighbouring spins and $\hat{S}_i^\alpha$ ($\alpha = x, y, z$) denotes spatial components of a spin operator at ith lattice point. It is quite obvious from the definition (5.1) that the Heisenberg model contains all three spatial components of a spin operator in contrast to the Ising model, which contains just one spatial component of each spin operator involved in its Hamiltonian. It should be remarked that this is an origin of insurmountable mathematical complexities to emerge by rigorous solving of the Heisenberg model, since different spatial components of the same spin operator do not commute with each other. Owing to this fact, it is much more difficult to attain the exact solution of 1D Heisenberg model in comparison with that one of its corresponding Ising model. The non-commutability between the relevant spin operators vanishes in the limit of infinite spin and this special limiting case is therefore called as the classical Heisenberg model.

5.1 Classical Heisenberg chain

In this part, let us explicitly evaluate the partition function and other important quantities of 1D classical Heisenberg model. It is worthy to mention that the approach developed hereafter closely follows the original exact treatment invented by M. E. Fisher (1964) [21]. First, let us write the Hamiltonian of 1D classical Heisenberg model on the open chain consisting of $(N+1)$ spins S of infinite magnitude ($S \to \infty$)

$$\hat{\mathcal{H}} = -J_S \sum_{i=1}^{N} \hat{\mathbf{S}}_{i-1} \cdot \hat{\mathbf{S}}_i. \tag{5.2}$$

Next, it is advisable to introduce the unit vector operator $\hat{\mathbf{s}}_i = \hat{\mathbf{S}}_i/S$ with the following commutation rules between its spatial components

$$[\hat{s}_i^x, \hat{s}_i^y] = i\hat{s}_i^z/S, \quad [\hat{s}_i^y, \hat{s}_i^z] = i\hat{s}_i^x/S \quad \text{and} \quad [\hat{s}_i^z, \hat{s}_i^x] = i\hat{s}_i^y/S. \tag{5.3}$$

In the limit $S \to \infty$, the different spatial components of the unit vector operators commute and thus, the Hamiltonian (5.2) can be rewritten to the classical form

$$\hat{\mathcal{H}} = -J \sum_{i=1}^{N} \hat{\mathbf{s}}_{i-1} \cdot \hat{\mathbf{s}}_i \tag{5.4}$$

by a mere rescaling of the nearest-neighbour exchange coupling $J = J_S S^2$. The partition function of this classical 1D spin system can be consequently written as

$$\mathcal{Z} = \int \frac{\mathrm{d}\Omega_0}{4\pi} \int \frac{\mathrm{d}\Omega_1}{4\pi} \dots \int \frac{\mathrm{d}\Omega_N}{4\pi} \exp\left(\beta J \sum_{i=1}^{N} \hat{\mathbf{s}}_{i-1} \cdot \hat{\mathbf{s}}_i\right), \tag{5.5}$$

where $\mathrm{d}\Omega_i$ is the element of solid angle for the unit vector $\mathbf{s}_i$. The integrals appearing in the above expression can easily be separated by introducing the spherical coordinates θ_i and ϕ_i for each unit vector $\mathbf{s}_i$ in a such way that they are referred to the previous unit vector $\mathbf{s}_{i-1}$ as a zenith axis

$$\mathcal{Z} = \int \frac{\mathrm{d}\Omega_0}{4\pi} \prod_{i=1}^{N} \int \frac{\mathrm{d}\Omega_i}{4\pi} \exp\left(\beta J \hat{\mathbf{s}}_{i-1} \cdot \hat{\mathbf{s}}_i\right) = \prod_{i=1}^{N} \int_0^{2\pi} \int_0^{\pi} \exp\left(\beta J \cos\theta_i\right) \sin\theta_i \mathrm{d}\theta_i \mathrm{d}\phi_i. \tag{5.6}$$

If the integration over the azimuthal angle ϕ_i is followed by the integration over the zenith angle θ_i, the partition function (5.6) of 1D classical Heisenberg chain simplifies to

$$\mathcal{Z} = \left(\frac{\sinh \beta J}{\beta J}\right)^N. \tag{5.7}$$

It can be easily understood that the above expression is invariant under the transformation $J \to -J$, what means that the classical Heisenberg model has the same partition function regardless of whether ferromagnetic or antiferromagnetic interaction is assumed. In the thermodynamic limit ($N \to \infty$), the reduced Helmholtz free energy becomes

$$\mathcal{F} = -k_\mathrm{B}T \lim_{N\to\infty} \frac{1}{N} \ln \mathcal{Z} = k_\mathrm{B}T \ln(\beta J) - k_\mathrm{B}T \ln(\sinh \beta J), \tag{5.8}$$

while the internal energy per one spin reduces to

$$\mathcal{U} = -\lim_{N\to\infty} \frac{1}{N} \frac{\partial \ln \mathcal{Z}}{\partial \beta} = k_\mathrm{B}T - J \coth \beta J. \tag{5.9}$$

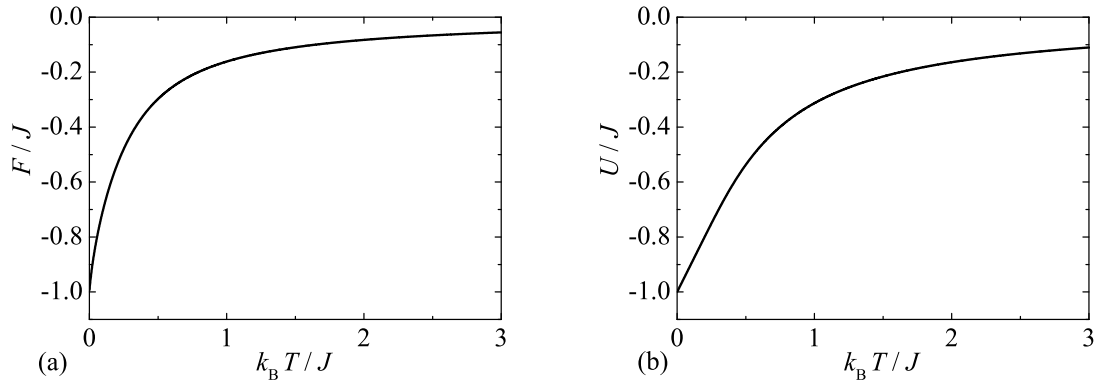

Figure 14: Temperature dependencies of the Helmholtz free energy (a) and the internal energy (b) of the classical Heisenberg chain as given by Eqs. (5.8) and (5.9), respectively.

Temperature dependencies of the Helmholtz free energy (5.8) and the internal energy (5.9) of the classical Heisenberg chain are for better illustration depicted in Fig. 14. It is quite clear from this figure that both these thermodynamic potentials monotonically increase upon rising temperature. While the temperature-induced rise of the internal energy is in agreement with general expectations, the Helmholtz free energy should contrarily decrease upon increasing of temperature in opposite to what is observed. This thermodynamically unacceptable behaviour will have important consequences on the entropy of the classical Heisenberg chain. To illustrate the case, let us derive the exact analytical expression for the entropy

$$\mathcal{S} = -\frac{\partial \mathcal{F}}{\partial T} = k_{\mathrm{B}} \left[1 + \ln \left(\frac{\sinh \beta J}{\beta J} \right) - \beta J \coth \beta J \right] \tag{5.10}$$

and the specific heat

$$\mathcal{C} = \frac{\partial \mathcal{U}}{\partial T} = k_{\mathrm{B}} \left[1 - \left(\frac{\beta J}{\sinh \beta J} \right)^2 \right]. \tag{5.11}$$

It can be readily checked from Eqs. (5.10) and (5.11) that the entropy diverges $\mathcal{S} \to -\infty$ and the specific heat tends to constant value $\mathcal{C} \to k_{\mathrm{B}}$ by approaching the absolute zero temperature $T \to 0$ K and these claims are in obvious contradiction with both Nernst's as well as Planck's formulations of the third law of thermodynamics. To support the aforementioned statements, temperature variations of the entropy and the specific heat of the classical Heisenberg chain as obtained from Eqs. (5.10) and (5.11) are displayed in Fig. 15. It is quite obvious from this figure that the entropy is indeed negative in the

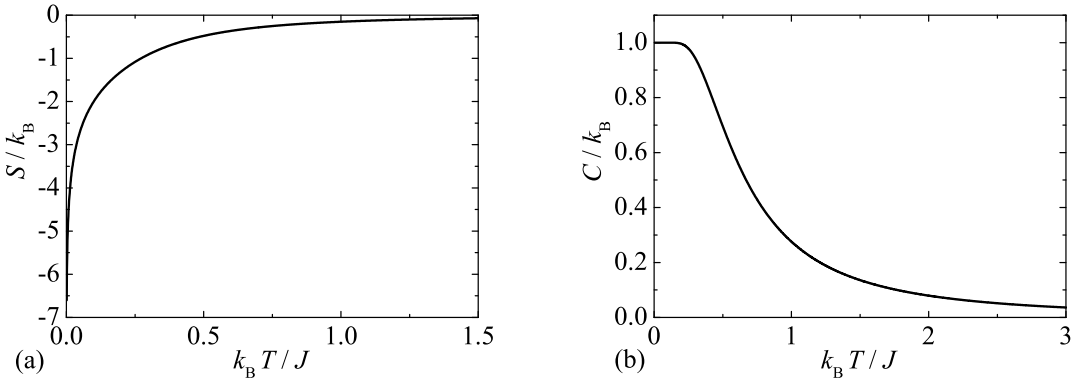

Figure 15: Temperature dependencies of the entropy (a) and the specific heat (b) of the classical Heisenberg chain as given by Eqs. (5.10) and (5.11), respectively.

whole temperature region when it rises from minus infinity and tends to zero in the limit of infinite temperature, while the specific heat monotonically decreases from its nonzero zero-temperature asymptotic value upon increasing of temperature. It should be nevertheless mentioned that all these unrealistic features of basic thermodynamic quantities are quite typical for any classical spin model.

5.2 Majumdar-Ghosh model

The crucial step, which enables to obtain the exact solution for the classical Heisenberg chain in a relatively straightforward manner, represents a validity of the commutation rules (5.3) that permits a simple factorization of the interaction terms in the relevant expression of the partition function (5.6). On the other hand, it is worthwhile to remark that the commutability between different spatial components of the spin operator (to emerge just in the limit $S \to \infty$) disables an onset of quantum fluctuations, which basically change magnetic as well as thermodynamic properties of the Heisenberg chain with a finite spin. Generally, the lower the spin value, the stronger the influence of quantum fluctuations on basic characteristics of the quantum Heisenberg model should be expected.

In this part, we shall focus in particular on the ground-state behaviour of the spin-1/2 Heisenberg chain with both nearest-neighbour as well as next-nearest-neighbour interactions (see Fig. 16) [22]. Interestingly, the addition of a special next-nearest-neighbour interaction facilitates obtaining the exact solution compared to the simple spin-1/2 Heisen-

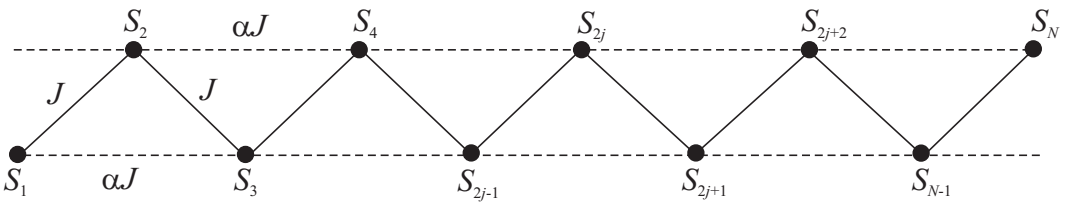

Figure 16: The 'railroad-trestle' geometry of the spin-1/2 Heisenberg chain with the nearest-neighbour interaction J and the next-nearest-neighbour interaction αJ. The 'zig-zag' bonds (solid lines) are referred to nearest-neighbour interactions and horizontal bonds (broken lines) to the next-nearest-neighbour ones. The periodic boundary conditions are assumed for simplicity.

berg chain with the nearest-neighbour interaction only, which can be exactly treated merely by a rather cumbersome Bethe ansatz method [23]. Let us begin by introducing the general Hamiltonian for the spin-1/2 Heisenberg chain with the nearest-neighbour and next-nearest-neighbour interactions

$$\hat{\mathcal{H}} = J \sum_{j=1}^{N} \left(\hat{\mathbf{S}}_j \cdot \hat{\mathbf{S}}_{j+1} + \alpha \hat{\mathbf{S}}_j \cdot \hat{\mathbf{S}}_{j+2} \right), \tag{5.12}$$

whereas the cyclic boundary conditions $S_{N+1} \equiv S_1$ and $S_{N+2} \equiv S_2$ are imposed for simplicity (these are equivalent to joining both chain ends). Notice that the general Hamiltonian (5.12) reduces to the Majumdar-Ghosh model by restricting the next-nearest-neighbour interaction precisely to a half of the nearest-neighbour interaction ($\alpha = 1/2$)

$$\hat{\mathcal{H}}_{\mathrm{MG}} = J \sum_{j=1}^{N} \hat{\mathbf{S}}_j \cdot \hat{\mathbf{S}}_{j+1} + \frac{J}{2} \sum_{j=1}^{N} \hat{\mathbf{S}}_j \cdot \hat{\mathbf{S}}_{j+2}. \tag{5.13}$$

Under this circumstance, it is very convenient to relate the Hamiltonian of the Majumdar-Ghosh model (5.13) with the trial Hamiltonian

$$\hat{\mathcal{H}}_{\mathrm{t}} = \frac{J}{4} \sum_{j=1}^{N} \left(\hat{\mathbf{S}}_j + \hat{\mathbf{S}}_{j+1} + \hat{\mathbf{S}}_{j+2} \right)^2 = J \sum_{j=1}^{N} \hat{\mathbf{S}}_j \cdot \hat{\mathbf{S}}_{j+1} + \frac{J}{2} \sum_{j=1}^{N} \hat{\mathbf{S}}_j \cdot \hat{\mathbf{S}}_{j+2} + \frac{3}{4} J \sum_{j=1}^{N} \hat{\mathbf{S}}_j^2 \tag{5.14}$$

According to quantum mechanics, the square of spin angular momentum is an integral of motion (i.e. it commutes with the Hamiltonian) and thus, it is possible to write the following relation $\hat{\mathbf{S}}_j^2 = S(S+1) = 3/4$ for the particular spin case $S = 1/2$. With regard to this, the third sum in the Hamiltonian (5.14) represents merely a constant factor

$$\hat{\mathcal{H}}_{\mathrm{t}} = J \sum_{j=1}^{N} \hat{\mathbf{S}}_j \cdot \hat{\mathbf{S}}_{j+1} + \frac{J}{2} \sum_{j=1}^{N} \hat{\mathbf{S}}_j \cdot \hat{\mathbf{S}}_{j+2} + \frac{9}{16} JN. \tag{5.15}$$

The comparison between Eqs. (5.13) and (5.15) relates the Hamiltonian of Majumdar-Ghosh model to the trial Hamiltonian through the simple relationship

$$\hat{\mathcal{H}}_{\mathrm{MG}} = \hat{\mathcal{H}}_{\mathrm{t}} - \frac{9}{16}NJ. \tag{5.16}$$

It is quite obvious from Eq. (5.16) that eigenvalues of the Majumdar-Ghosh model (5.13) can be obtained from eigenvalues of the trial Hamiltonian (5.15) by a mere shift of these energy levels by the constant $-9NJ/16$. Of course, the ground state of the Majumdar-Ghosh model is unambiguously given just by the lowest-energy eigenvalue and hence, it is of particular interest to search for the lowest-lying eigenvalue of the trial Hamiltonian (5.15). Because of the validity of inequality

$$\left(\hat{\mathbf{S}}_j + \hat{\mathbf{S}}_{j+1} + \hat{\mathbf{S}}_{j+2}\right)^2 \geq \left[S(S+1)\right]_{S=\frac{1}{2}} = \frac{3}{4} \tag{5.17}$$

the eigenvalues of the trial Hamiltonian (5.15) must obey the condition

$$E_{\mathrm{t}} \geq \frac{3}{16}NJ. \tag{5.18}$$

By combining the inequality (5.18) with the relation (5.16), all eigenvalues of the Majumdar-Ghosh model have to obey the condition

$$E_{\mathrm{MG}} \geq E_{\mathrm{GS}} \equiv -\frac{3}{8}NJ. \tag{5.19}$$

It is quite apparent from the above relation that the lowest-energy (ground-state) eigenvalue of the Majumdar-Ghosh model must have the energy $E_{\mathrm{GS}} = -3NJ/8$.

To gain a deeper insight into the ground-state spin arrangement, let us firstly focus on the possible eigenstates of the simple spin-1/2 Heisenberg dimer model defined through the Hamiltonian

$$\hat{\mathcal{H}}_{\mathrm{d}} = J\hat{\mathbf{S}}_1 \cdot \hat{\mathbf{S}}_2. \tag{5.20}$$

By remembering that the spatial components of both spin operators $\hat{\mathbf{S}}_j \equiv (\hat{S}_j^x, \hat{S}_j^y, \hat{S}_j^z)$ $(j = 1, 2)$ are given within the usual representation by standard Pauli matrices

$$\hat{S}_j^x = \frac{1}{2}\begin{pmatrix} 0 & 1 \\ 1 & 0 \end{pmatrix}_j, \quad \hat{S}_j^y = \frac{1}{2}\begin{pmatrix} 0 & -i \\ i & 0 \end{pmatrix}_j, \quad \hat{S}_j^z = \frac{1}{2}\begin{pmatrix} 1 & 0 \\ 0 & -1 \end{pmatrix}_j, \tag{5.21}$$

the Hamiltonian (5.20) of the spin-1/2 Heisenberg dimer model can be transcribed to the following matrix representation

$$\langle\gamma|\hat{\mathcal{H}}_{\mathrm{d}}|\alpha\rangle = \begin{pmatrix} \langle\uparrow\uparrow|\hat{\mathcal{H}}_{\mathrm{d}}|\uparrow\uparrow\rangle & \langle\uparrow\downarrow|\hat{\mathcal{H}}_{\mathrm{d}}|\uparrow\uparrow\rangle & \langle\downarrow\uparrow|\hat{\mathcal{H}}_{\mathrm{d}}|\uparrow\uparrow\rangle & \langle\downarrow\downarrow|\hat{\mathcal{H}}_{\mathrm{d}}|\uparrow\uparrow\rangle \\ \langle\uparrow\uparrow|\hat{\mathcal{H}}_{\mathrm{d}}|\uparrow\downarrow\rangle & \langle\uparrow\downarrow|\hat{\mathcal{H}}_{\mathrm{d}}|\uparrow\downarrow\rangle & \langle\downarrow\uparrow|\hat{\mathcal{H}}_{\mathrm{d}}|\uparrow\downarrow\rangle & \langle\downarrow\downarrow|\hat{\mathcal{H}}_{\mathrm{d}}|\uparrow\downarrow\rangle \\ \langle\uparrow\uparrow|\hat{\mathcal{H}}_{\mathrm{d}}|\downarrow\uparrow\rangle & \langle\uparrow\downarrow|\hat{\mathcal{H}}_{\mathrm{d}}|\downarrow\uparrow\rangle & \langle\downarrow\uparrow|\hat{\mathcal{H}}_{\mathrm{d}}|\downarrow\uparrow\rangle & \langle\downarrow\downarrow|\hat{\mathcal{H}}_{\mathrm{d}}|\downarrow\uparrow\rangle \\ \langle\uparrow\uparrow|\hat{\mathcal{H}}_{\mathrm{d}}|\downarrow\downarrow\rangle & \langle\uparrow\downarrow|\hat{\mathcal{H}}_{\mathrm{d}}|\downarrow\downarrow\rangle & \langle\downarrow\uparrow|\hat{\mathcal{H}}_{\mathrm{d}}|\downarrow\downarrow\rangle & \langle\downarrow\downarrow|\hat{\mathcal{H}}_{\mathrm{d}}|\downarrow\downarrow\rangle \end{pmatrix}$$
$$= \begin{pmatrix} J/4 & 0 & 0 & 0 \\ 0 & -J/4 & J/2 & 0 \\ 0 & J/2 & -J/4 & 0 \\ 0 & 0 & 0 & J/4 \end{pmatrix} \tag{5.22}$$

with the four orthogonal spin states used as basis states

$$|\uparrow\uparrow\rangle = \begin{pmatrix} 1 \\ 0 \end{pmatrix}_1 \begin{pmatrix} 1 \\ 0 \end{pmatrix}_2, \qquad |\uparrow\downarrow\rangle = \begin{pmatrix} 1 \\ 0 \end{pmatrix}_1 \begin{pmatrix} 0 \\ 1 \end{pmatrix}_2,$$
$$|\downarrow\uparrow\rangle = \begin{pmatrix} 0 \\ 1 \end{pmatrix}_1 \begin{pmatrix} 1 \\ 0 \end{pmatrix}_2, \qquad |\downarrow\downarrow\rangle = \begin{pmatrix} 0 \\ 1 \end{pmatrix}_1 \begin{pmatrix} 0 \\ 1 \end{pmatrix}_2. \tag{5.23}$$

The straightforward diagonalization of the Hamiltonian (5.22) yields a complete spectrum of eigenvalues and subsequently, the standard procedure can be utilized for attaining its corresponding eigenfunctions, as well. In this way, one easily finds the complete set of eigenvalues and eigenfunctions

$$E_0 = -\frac{3}{4}J, \qquad |\Psi_0\rangle = \frac{1}{\sqrt{2}}\left(|\uparrow\downarrow\rangle - |\downarrow\uparrow\rangle\right) \tag{5.24}$$
$$E_1 = \frac{1}{4}J, \qquad |\Psi_1\rangle = |\uparrow\uparrow\rangle \tag{5.25}$$
$$E_2 = \frac{1}{4}J, \qquad |\Psi_2\rangle = \frac{1}{\sqrt{2}}\left(|\uparrow\downarrow\rangle + |\downarrow\uparrow\rangle\right) \tag{5.26}$$
$$E_3 = \frac{1}{4}J, \qquad |\Psi_3\rangle = |\downarrow\downarrow\rangle. \tag{5.27}$$

The nature of overall spectrum of eigenenergies is quite surprising, since it consists of one non-degenerate energy level (singlet), which is separated from a three-fold degenerate energy level (triplet) by the so-called singlet–triplet energy gap $\Delta E_{\mathrm{s-t}} = J$. Note that the singlet–triplet structure of eigenenergies is in obvious contrast with simple intuitive expectations that would rather predict two different kinds of two-fold degenerate eigenstates;

two ferromagnetic ones with the energy $J/4$ and respectively, two antiferromagnetic ones with the energy -$J/4$. Both the ferromagnetic states $|\uparrow\uparrow\rangle$ and $|\downarrow\downarrow\rangle$ are eigenstates of the Heisenberg model and they actually have the energy $J/4$. Contrary to this, none of two antiferromagnetic eigenstates (5.24) and (5.26) (if one spin is pointing 'up', then the other one is necessarily pointing 'down') do not possess the classically predicted energy -$J/4$ and what is even more surprising, they do not even have the same energy. The only plausible explanation for the energy difference between both antiferromagnetic eigenstates lies evidently in an influence of quantum fluctuations, which lift the degeneracy of antiferromagnetic eigenstates owing to the fact that the simple antiferromagnetic states $|\uparrow\downarrow\rangle$ and $|\downarrow\uparrow\rangle$ are not eigenstates of the Heisenberg model. Bearing this in mind, one may conclude that it is much more intriguing to investigate antiferromagnetic rather than ferromagnetic Heisenberg models, because the latter ones usually exhibit semi-classical spin order not affected by quantum effects.

Under the assumption of antiferromagnetic interaction $J > 0$, the lowest energy level of the spin-1/2 Heisenberg dimer model with two spins 1 and 2 is fully characterized by the antisymmetric *singlet-dimer* eigenfunction for which we shall introduce the abbreviated notation

$$|\Psi_0\rangle = \frac{1}{\sqrt{2}}\left(|\uparrow\downarrow\rangle - |\downarrow\uparrow\rangle\right) = [1,2]. \tag{5.28}$$

Now, let us try to construct the lowest-energy eigenfunction of the Majumdar-Ghosh model by a mere considering of the singlet-dimer eigenfunctions (5.28). The Heisenberg chain with the nearest-neighbour and next-nearest-neighbour interactions can be completely covered with the singlet-dimer states in two different ways, which are diagrammatically shown in Fig. 17 and mathematically can be expressed as

$$|\mathrm{I}\rangle = [1,2][3,4]\ldots[2j-1,2j]\ldots = \prod_{j=1}^{N/2}[2j-1,2j], \tag{5.29}$$

and respectively

$$|\mathrm{II}\rangle = [2,3][4,5]\ldots[2j,2j+1]\ldots = \prod_{j=1}^{N/2}[2j,2j+1]. \tag{5.30}$$

Our next aim is to investigate whether $|\mathrm{I}\rangle$ and $|\mathrm{II}\rangle$ are actually eigenfunctions of the

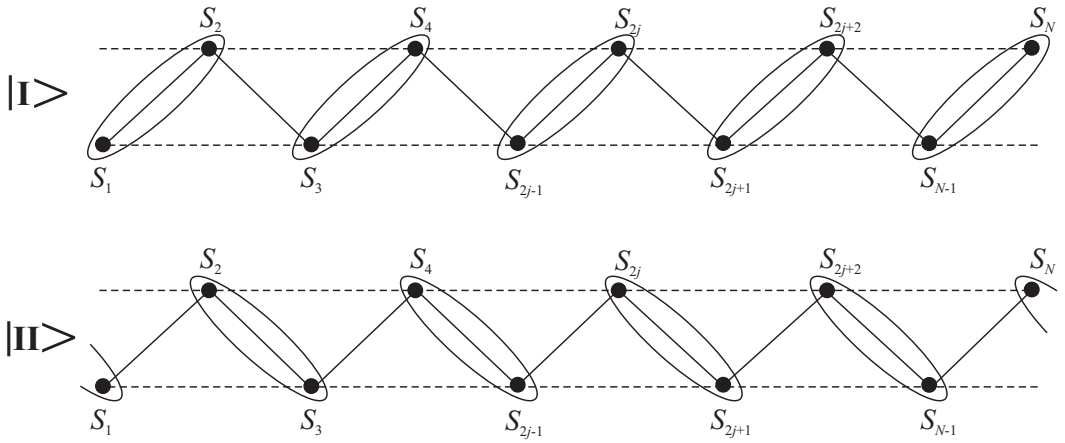

Figure 17: Two possible eigenstates of the Majumdar-Ghosh model, which can be constructed just from the singlet-dimer states. Ellipses denote the singlet-dimer state (5.28).

Majumdar-Ghosh model and if yes, whether they determine the lowest-energy eigenstate (ground state). For simplicity, we shall merely prove that $|\mathrm{I}\rangle$ is indeed the lowest-energy eigenstate with the ground-state energy $E_{\mathrm{GS}} = -3NJ/8$ (the proof for $|\mathrm{II}\rangle$ is essentially the same). First, let us examine an impact of spin operators $\hat{\mathbf{S}}_{2j-1} \cdot \hat{\mathbf{S}}_{2j}$, $\hat{\mathbf{S}}_{2j} \cdot \hat{\mathbf{S}}_{2j+1}$, $\hat{\mathbf{S}}_{2j-1} \cdot \hat{\mathbf{S}}_{2j+1}$ and $\hat{\mathbf{S}}_{2j} \cdot \hat{\mathbf{S}}_{2j+2}$ on the singlet-dimer states $[2j-1, 2j]$ creating $|\mathrm{I}\rangle$. After straightforward but a little bit lengthy calculation

$$\hat{\mathbf{S}}_{2j-1} \cdot \hat{\mathbf{S}}_{2j}[2j-1, 2j] = -\frac{3}{4}[2j-1, 2j], \tag{5.31}$$

$$\hat{\mathbf{S}}_{2j} \cdot \hat{\mathbf{S}}_{2j+1}[2j-1, 2j][2j+1, 2j+2] = \frac{1}{8}\Big(2|\uparrow\uparrow\downarrow\downarrow\rangle + 2|\downarrow\downarrow\uparrow\uparrow\rangle - |\uparrow\downarrow\uparrow\downarrow\rangle - |\uparrow\downarrow\downarrow\uparrow\rangle - |\downarrow\uparrow\uparrow\downarrow\rangle - |\downarrow\uparrow\downarrow\uparrow\rangle\Big)_{2j-1,2j,2j+1,2j+2}, \tag{5.32}$$

$$\hat{\mathbf{S}}_{2j-1} \cdot \hat{\mathbf{S}}_{2j+1}[2j-1, 2j][2j+1, 2j+2] = -\frac{1}{8}\Big(2|\uparrow\uparrow\downarrow\downarrow\rangle + 2|\downarrow\downarrow\uparrow\uparrow\rangle - |\uparrow\downarrow\uparrow\downarrow\rangle - |\uparrow\downarrow\downarrow\uparrow\rangle - |\downarrow\uparrow\uparrow\downarrow\rangle - |\downarrow\uparrow\downarrow\uparrow\rangle\Big)_{2j-1,2j,2j+1,2j+2}, \tag{5.33}$$

$$\hat{\mathbf{S}}_{2j} \cdot \hat{\mathbf{S}}_{2j+2}[2j-1, 2j][2j+1, 2j+2] = -\frac{1}{8}\Big(2|\uparrow\uparrow\downarrow\downarrow\rangle + 2|\downarrow\downarrow\uparrow\uparrow\rangle - |\uparrow\downarrow\uparrow\downarrow\rangle - |\uparrow\downarrow\downarrow\uparrow\rangle - |\downarrow\uparrow\uparrow\downarrow\rangle - |\downarrow\uparrow\downarrow\uparrow\rangle\Big)_{2j-1,2j,2j+1,2j+2}, \tag{5.34}$$

one indeed finds that $|\mathrm{I}\rangle$ is one of the eigenfunctions of the Hamiltonian (5.13) and moreover, its corresponding eigenenergy is equal to the lowest possible (ground-state) energy

$$E_{\mathrm{I}} = \langle \mathrm{I}|\hat{\mathcal{H}}_{\mathrm{MG}}|\mathrm{I}\rangle = \frac{1}{2}NJ\langle \mathrm{I}|\hat{\mathbf{S}}_{2j-1} \cdot \hat{\mathbf{S}}_{2j}|\mathrm{I}\rangle = -\frac{3}{8}NJ = E_{\mathrm{GS}}. \tag{5.35}$$

Apparently, the dimer product states $|\mathrm{I}\rangle$ and $|\mathrm{II}\rangle$ are ground states of the Majumdar-Ghosh model and in the consequence of that, the spin system is completely disordered as

the correlation function between two different spins (with exception of those which create singlet dimers) is identically equal to zero even within the ground state

$$\langle \hat{\mathbf{S}}_j \cdot \hat{\mathbf{S}}_k \rangle = \langle \mathrm{I} | \hat{\mathbf{S}}_j \cdot \hat{\mathbf{S}}_k | \mathrm{I} \rangle = 0. \tag{5.36}$$

Notwithstanding of this fact the Majumdar-Ghosh model peculiarly exhibits a special kind of perfect ordering, which is called as a *valence-bond crystal* or equivalently as a *singlet-dimer product state*. It should be noticed that the valence-bond crystal can be characterized by the non-zero dimer–dimer correlation between four spins creating two different singlet dimers. In our case, the dimer–dimer correlation function is equal to

$$\langle (\hat{\mathbf{S}}_{2j-1} \cdot \hat{\mathbf{S}}_{2j})(\hat{\mathbf{S}}_{2k-1} \cdot \hat{\mathbf{S}}_{2k}) \rangle = \langle \mathrm{I} | (\hat{\mathbf{S}}_{2j-1} \cdot \hat{\mathbf{S}}_{2j})(\hat{\mathbf{S}}_{2k-1} \cdot \hat{\mathbf{S}}_{2k}) | \mathrm{I} \rangle = \frac{9}{16}. \tag{5.37}$$

5.3 Variational method

It is worthwhile to remark that an exact ground state with character of the valence-bond crystal can be found in several geometrically frustrated quantum Heisenberg spin models and it does not represent very special feature of the Majumdar-Ghosh model only. A quite natural question thus arises whether one may prove existence of the exact singlet-dimer ground state of a given quantum Heisenberg spin model by employing some relatively simple and easily adaptable method. Using the variational principle Shastry and Sutherland were capable of proving the exact singlet-dimer ground state for a two-dimensional Heisenberg square lattice with additional diagonal interaction [24] and this calculation procedure has been further put forward by Bose when considering several other geometrically frustrated Heisenberg spin chains and lattices [25]. In the following part we will clarify the general scheme of the variational method and illustrate its basic ideas by considering the particular example of a spin-1/2 Heisenberg diamond chain.

Let us begin with a few general comments on the variational principle. It well known that the ground-state energy E_0 of any quantum-mechanical system defined through the Hamiltonian $\hat{\mathcal{H}}$ is bounded from above by the variational energy

$$E_0 \leq \varepsilon \equiv \langle \phi | \hat{\mathcal{H}} | \phi \rangle, \tag{5.38}$$

which is nothing else as a mean value of the Hamiltonian calculated for some trial (variational) wave vector $|\phi\rangle$ depending generally on a set of variational parameters.

If the eigenenergies E_i of the Hamiltonian $\hat{\mathcal{H}}$ formally obtained by solving the eigenvalue problem $\hat{\mathcal{H}}|\Psi_i\rangle = E_i|\Psi_i\rangle$ are sorted in ascending order with respect to its subscript $E_0 \leq E_1 \leq \ldots \leq E_N$, then, the ground-state energy naturally represents a lower bound of the overall energy spectrum $E_0 \leq E_i$ of a given quantum-mechanical system. Of course, the relevant eigenvalue problem is in general not tractable, but an exact ground state can be rigorously determined whenever one finds a lower bound of the ground-state energy that coincides with an upper bound. The principal question is thus how to effectively find a lower bound of the ground-state energy. To this end, one may at first split the total Hamiltonian $\hat{\mathcal{H}}$ of a quantum-mechanical system into local Hamiltonians of its subsystems $\hat{\mathcal{H}} = \sum_j \hat{\mathcal{H}}_j$. The ground-state energy can be formally expressed as the mean value of the Hamiltonian $E_0 = \langle\Psi_0|\hat{\mathcal{H}}|\Psi_0\rangle$ calculated with the help of the corresponding (unknown) eigenvector, which may be alternatively regarded as the variational eigenvector for the local Hamiltonians of its subsystems

$$E_0 = \langle\Psi_0|\sum_j \hat{\mathcal{H}}_j|\Psi_0\rangle = \sum_j \langle\Psi_0|\hat{\mathcal{H}}_j|\Psi_0\rangle \geq \sum_j \varepsilon_j^0. \tag{5.39}$$

In the last step of derivation of the inequality (5.39) we have applied term-by-term the variational principle for each local Hamiltonian. If one compares the left-hand-side and right-hand-side of the inequality (5.39) the ground-state energy of a quantum-mechanical system is bounded from below by a sum of lowest energies of all its constituent subsystems and from above by any energy eigenvalue

$$E_i \geq E_0 \geq \sum_j \varepsilon_j^0. \tag{5.40}$$

The exact ground state can be accordingly found whenever one finds the eigenstate of the Hamiltonian whose eigenenergy directly equals to a sum of the lowest-energy eigenvalues of its constituent subsystems, i.e. $E_i = \sum_j \varepsilon_j^0$.

5.4 Heisenberg diamond chain

To illustrate applicability of the variational arguments presented in the previous paragraph let us consider a spin-1/2 Heisenberg diamond chain in a presence of the magnetic field,

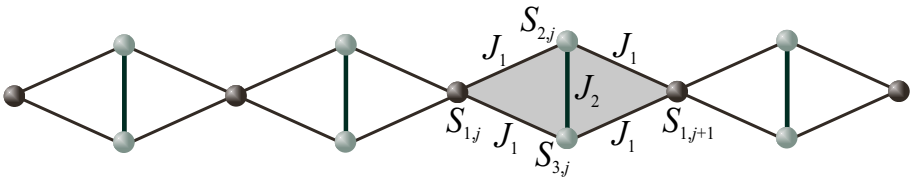

Figure 18: A schematic illustration of the spin-1/2 Heisenberg diamond chain defined by the Hamiltonian (5.41). A shaded diamond cell is composed from two Heisenberg spin triangles defined through the local cluster Hamiltonians $\hat{\mathcal{H}}_{j,\alpha}$ given by Eq. (5.42).

which is schematically illustrated in Fig. 18 and mathematically defined through the Hamiltonian

$$\hat{\mathcal{H}} = J_1 \sum_{j=1}^{N} (\hat{\mathbf{S}}_{1,j} + \hat{\mathbf{S}}_{1,j+1}) \cdot (\hat{\mathbf{S}}_{2,j} + \hat{\mathbf{S}}_{3,j}) + J_2 \sum_{j=1}^{N} \hat{\mathbf{S}}_{2,j} \cdot \hat{\mathbf{S}}_{3,j} - H \sum_{j=1}^{N} \sum_{i=1}^{3} \hat{S}^z_{i,j}. \tag{5.41}$$

In above, $\hat{\mathbf{S}}_{i,j}$ $(i = 1, 2, 3; j = 1, \ldots, N)$ denotes spin-1/2 operator assigned to a lattice site given by two subscripts, the first subscript determines spins from a given unit cell and the second subscript specifies the unit cell itself. The coupling constant $J_1 > 0$ stands for the antiferromagnetic interaction between nearest-neighbor monomeric $(S_{1,j})$ and dimeric $(S_{2,j},\ S_{3,j})$ spins, while the coupling constant $J_2 > 0$ accounts for the antiferromagnetic interaction between the dimeric spins $S_{2,j}$ and $S_{3,j}$ that is responsible for a geometric spin frustration. The Zeeman term $H \geq 0$ accounts for an effect of the external magnetic field and finally, the periodic boundary condition is imposed for simplicity $S_{1,N} \equiv S_{1,1}$.

The total Hamiltonian (5.41) can be decomposed into a sum of the local cluster Hamiltonians $\hat{\mathcal{H}} = \sum_{j=1}^{N} \sum_{\alpha=0,1} \hat{\mathcal{H}}_{j,\alpha}$ given by the following definition

$$\hat{\mathcal{H}}_{j,\alpha} = J_1 \hat{\mathbf{S}}_{1,j+\alpha} \cdot (\hat{\mathbf{S}}_{2,j} + \hat{\mathbf{S}}_{3,j}) + \frac{J_2}{2} \hat{\mathbf{S}}_{2,j} \cdot \hat{\mathbf{S}}_{3,j} - \frac{H}{2} (\hat{S}^z_{1,j+\alpha} + \hat{S}^z_{2,j} + \hat{S}^z_{3,j}). \tag{5.42}$$

It is quite clear that two local cluster Hamiltonians $\hat{\mathcal{H}}_{j,\alpha}$ defined for $\alpha = 0$ or 1 by Eq. (5.42) correspond to the spin-1/2 Heisenberg triangular clusters schematically shown in Fig. 18 by two shaded triangles. Note furthermore that the factor 1/2 at the last two terms of the Hamiltonian (5.42) avoids double counting of the coupling constant J_2 and the Zeeman's term H, which are symmetrically split into two adjacent local cluster Hamiltonians. To proceed further with the calculation one should find the lowest-energy eigenstate of the Heisenberg spin triangle given by Eq. (5.42). A full diagonalization of

the Hamiltonian (5.42) of the spin-1/2 Heisenberg triangle can be easily accomplished within Kambe projection method, which allows to express the relevant Hamiltonian in terms of the total spin operator of triangle $\hat{\mathbf{S}}_t = \hat{\mathbf{S}}_{1,j+\alpha} + \hat{\mathbf{S}}_{2,j} + \hat{\mathbf{S}}_{3,j}$, its z-component $\hat{S}^z_t = \hat{S}^z_{1,j+\alpha} + \hat{S}^z_{2,j} + \hat{S}^z_{3,j}$ and the composite spin operator of pair $\hat{\mathbf{S}}_p = \hat{\mathbf{S}}_{2,j} + \hat{\mathbf{S}}_{3,j}$. The Hamiltonian (5.42) of the spin-1/2 Heisenberg triangle can be subsequently re-expressed with the help of these three auxiliary spin operators

$$\hat{\mathcal{H}}_{j,\alpha} = -\frac{3}{8}J_1 - \frac{3}{8}J_2 + \frac{J_1}{2}\hat{\mathbf{S}}_t^2 + \frac{J_2 - 2J_1}{4}\hat{\mathbf{S}}_p^2 - \frac{H}{2}\hat{S}^z_t. \tag{5.43}$$

It directly follows from Eq. (5.43) that the Hamiltonian of the spin-1/2 Heisenberg triangle commutes with all three auxiliary spin operators involved therein $[\hat{\mathcal{H}}_{j,\alpha}, \hat{\mathbf{S}}_t^2] = [\hat{\mathcal{H}}_{j,\alpha}, \hat{\mathbf{S}}_p^2] = [\hat{\mathcal{H}}_{j,\alpha}, \hat{S}^z_t] = 0$, which means that the Hamiltonian has a common set of eigenvectors with the auxiliary spin operators and the respective quantities correspond to conserved quantities with well defined quantum spin numbers. A full energy spectrum of the spin-1/2 Heisenberg triangle can be thus readily expressed in terms of the eigenvalues of the auxiliary spin operators

$$\varepsilon_{j,\alpha}(S_t, S_p, S^z_t) = -\frac{3}{8}J_1 - \frac{3}{8}J_2 + \frac{J_1}{2}S_t(S_t+1) + \frac{J_2 - 2J_1}{4}S_p(S_p+1) - \frac{H}{2}\hat{S}^z_t. \tag{5.44}$$

All available combinations of the quantum spin numbers S_p, S_p and S^z_t are dictated by basic composition rules known for angular spin momentum. The respective quantum spin number of the pair may achieve only two values $S_p = 0$ or 1, whereby the respective quantum spin number of the triangle has a single value $S_t = 1/2$ for $S_p = 0$ and two available values $S_t = 1/2$ and 3/2 for $S_p = 1$. The z-component of the quantum spin number of the triangle may acquire the set of values $S^z_t = -S_t, -S_t+1, \ldots, S_t$ depending on the choice of the quantum spin number S_t. It could be easily understood from Eq. (5.44) that the lowest-energy eigenstate should have equal values of the total spin of the triangle and its z-component $S_t = S^z_t$, which basically limits a possible number of the lowest-energy eigenstates to the following three candidates

$$\varepsilon_{j,\alpha}(1/2, 0, 1/2) = -\frac{3}{8}J_2 - \frac{1}{4}H, \tag{5.45}$$

$$\varepsilon_{j,\alpha}(1/2, 1, 1/2) = -J_1 + \frac{1}{8}J_2 - \frac{1}{4}H, \tag{5.46}$$

$$\varepsilon_{j,\alpha}(3/2, 1, 3/2) = \frac{1}{2}J_1 + \frac{1}{8}J_2 - \frac{3}{4}H. \tag{5.47}$$

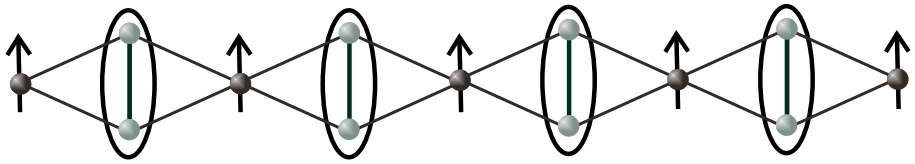

Figure 19: A schematic illustration of the monomer-dimer ground state of the spin-1/2 Heisenberg diamond chain given by the eigenvector (5.48). Ovals represent the singlet-dimer state defined by Eq. (5.28).

The eigenstate of the spin-1/2 Heisenberg triangle with the eigenenergy $\varepsilon_{j,\alpha}(1/2,0,1/2)$ becomes the lowest-energy eigenstate on assumption that the inequalities $\varepsilon_{j,\alpha}(1/2,0,1/2) < \varepsilon_{j,\alpha}(1/2,1,1/2)$ and $\varepsilon_{j,\alpha}(1/2,0,1/2) < \varepsilon_{j,\alpha}(3/2,1,3/2)$ are simultaneously satisfied what delimits a stability region of this lowest-energy eigenstate to the parameter space $J_2 > 2J_1$ and $H < J_1 + J_2$. Moreover, the zero value of the quantum spin number $S_p = 0$ in turn implies the singlet state (5.28) between the dimeric spins $S_{2,j}$ and $S_{3,j}$ within the aforementioned eigenstate. This finding is indeed consistent with absence of any spin-spin correlation between monomeric and dimeric spins as manifested in the eigenenergy (5.45) through absence of any term depending on the coupling constant J_1. Hence, it is quite plausible to conjecture that the relevant ground state of the spin-1/2 Heisenberg diamond chain in the highly frustrated parameter region $J_2 > 2J_1$ and $H < J_1 + J_2$ is given by the eigenvector with character of the monomer-dimer state

$$|\mathrm{MD}\rangle = \prod_{j=1}^{N} |\uparrow_{1,j}\rangle \otimes \frac{1}{\sqrt{2}}(|\uparrow_{2,j}\downarrow_{3,j}\rangle - |\downarrow_{2,j}\uparrow_{3,j}\rangle), \tag{5.48}$$

which represents a product state consisting of the fully polarized monomeric spins and the singlet state of the dimeric spins (see Fig. 19 for graphical illustration). It can be actually proved that the monomer-dimer state given by the eigenvector (5.48) is true eigenstate of the Hamiltonian (5.41) of the spin-1/2 Heisenberg diamond chain with the respective eigenenergy $E_{MD} = -3NJ_2/4 - NH/2$, which is in the parameter region $J_2 > 2J_1$ and $H < J_1 + J_2$ equal to a sum of the lowest energies $E = \sum_{j=1}^{N} \sum_{\alpha=0,1} \varepsilon_{j,\alpha}(1/2,0,1/2)$ of the spin-1/2 Heisenberg triangles. According to the requirements (5.40) of the variational principle, the equality between the eigenenergy of the eigenstate of the whole spin-1/2 Heisenberg diamond chain with the sum of lowest energies of its constituent parts (spin triangles) represent sufficient condition for an exact proof of the relevant ground state.

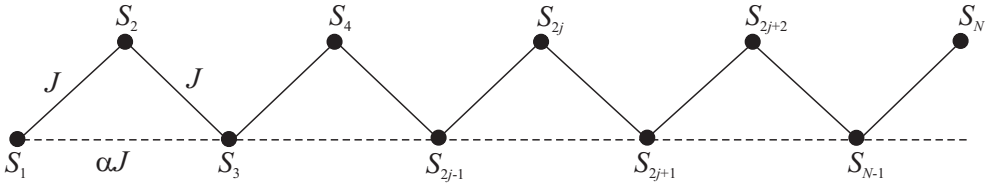

Figure 20: The spin-1/2 Heisenberg sawtooth (Δ) chain.

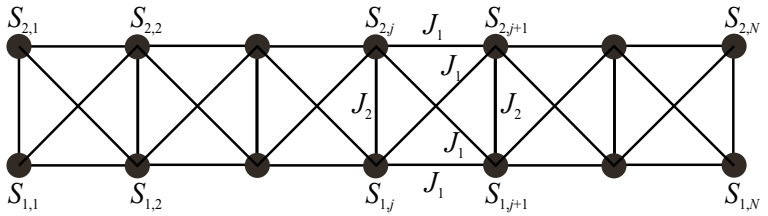

Figure 21: The fully frustrated spin-1/2 Heisenberg two-leg ladder.

Exercises

1. Calculate a complete spectrum of eigenvalues and eigenfunctions of the spin-1/2 XYZ Heisenberg dimer model given by the Hamiltonian

$$\hat{\mathcal{H}}_{\mathrm{XYZ}} = J_{\mathrm{X}} \hat{S}_1^x \hat{S}_2^x + J_{\mathrm{Y}} \hat{S}_1^y \hat{S}_2^y + J_{\mathrm{Z}} \hat{S}_1^z \hat{S}_2^z.$$

How the overall spectrum of eigenenergies changes by introducing a spatial anisotropy $J_{\mathrm{X}} = J_{\mathrm{Y}} \neq J_{\mathrm{Z}}$ or $J_{\mathrm{X}} \neq J_{\mathrm{Y}} \neq J_{\mathrm{Z}}$ in the exchange interaction?

2. Prove the validity of relations (5.31)-(5.34).

3. Search for the lowest-energy eigenstate of the spin-1/2 Heisenberg antiferromagnet on the sawtooth (Δ) chain [26] by following the same procedure as used for the Majumdar-Ghosh model. The investigated model system is defined through the Hamiltonian

$$\hat{\mathcal{H}}_{\Delta} = J \sum_{j=1}^{N} \hat{\mathbf{S}}_j \cdot \hat{\mathbf{S}}_{j+1} + J\alpha \sum_{j=1}^{N/2} \hat{\mathbf{S}}_{2j-1} \cdot \hat{\mathbf{S}}_{2j}$$

and is schematically shown in Fig. 20.

4. By making use of the variational principle find an exact ground state of the fully frustrated spin-1/2 Heisenberg two-leg ladder [27], which is defined through the Hamiltonian

$$\hat{\mathcal{H}} = J_1 \sum_{j=1}^{N} (\hat{\mathbf{S}}_{1,j} + \hat{\mathbf{S}}_{2,j}) \cdot (\hat{\mathbf{S}}_{1,j+1} + \hat{\mathbf{S}}_{2,j+1}) + J_2 \sum_{j=1}^{N} \hat{\mathbf{S}}_{1,j} \cdot \hat{\mathbf{S}}_{2,j} - H \sum_{j=1}^{N} (\hat{S}_{1,j}^z + \hat{S}_{2,j}^z)$$

and is schematically shown in Fig. 21.

6 Ice-type models

In this section, we shall consider a certain class of exactly solvable models, which exhibit perhaps the most interesting phase transitions and critical phenomena among all exactly solved models. The common feature of all these so-called *ice-type* models is that they are based on Pauling's (1938) [28] and Slater's (1941) [29] phenomenological description of cooperative effects closely associated with the hydrogen bonding.

6.1 Six-vertex models

6.1.1 Ice model

Before introducing the ice model, let us firstly make few remarks about the water molecule (H_2O), which represents the constituent particle of the ice. It is well known fact that each water molecule contains two equivalent O–H covalent bonds, which arise from the spin pairing of 1s electrons of two hydrogen atoms and two sp_3 hybridized electrons of the oxygen atom, respectively. It should be mentioned that the oxygen has besides two electrons, which take part by constituting two covalent bonds, another four sp_3 hybridized electrons that reside two so-called *lone-pair* orbitals. The lobes of lone-pair orbitals are mirror images with respect to the H–O–H plane with the angle between them about 120°. The H–O–H angle between two covalent bonds is 104.5° and the length of each of them is 0.096 nm. Owing to these facts, the geometry of the water molecule can be roughly regarded as a slightly deformed tetrahedron having the oxygen atom at its center, whereas two hydrogens and two lone-pair orbitals are situated at its corners (see Fig. 22a). Since the electronegativity[14] of the oxygen is much larger than the electronegativity of the hydrogen, both spin paired electrons creating O–H covalent bond are shifted closer to the oxygen atom. Accordingly, there is an excess of a negative charge at the oxygen atom and its lone-pair orbitals, while there is an excess of a positive charge at both hydrogen atoms. This charge distribution is responsible for the fact that the water molecule is highly *polar*, since the geometry of the water molecule is not linear. In other words, the water molecule has on behalf of its spatial geometry a rather strong *electric dipole moment*.

[14]The electronegativity is a physical quantity, which measures ability of atoms to attract electrons.

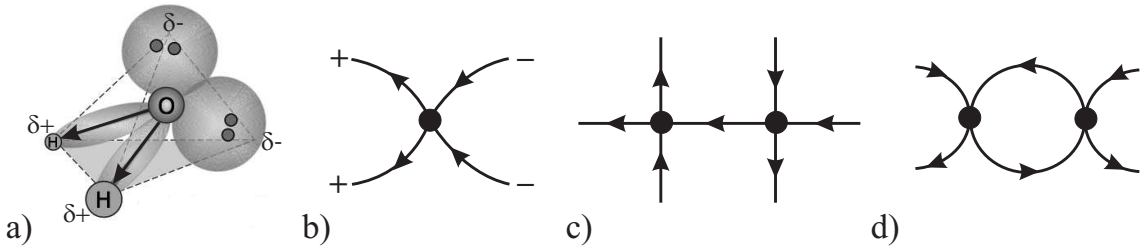

Figure 22: a) The tetrahedron geometry of water molecule; b) The arrow convention specifying a polarity of the water molecule: arrows always point inwards (outwards) positively (negatively) charged corners of the water molecule; c)-d) The hydrogen-bonded water molecules, which are held together by means of one or two hydrogen bonds, respectively.

When two different water molecules come in a sufficiently close contact, it becomes quite obvious that very specific highly-oriented interactions, which are called as *hydrogen bonds*, can lower the overall electrostatic energy of this complex. It is quite apparent that this occurs just when the hydrogen atoms of one water molecule (i.e. the corners of tetrahedron with the effective positive charge) are directed towards the lobes of lone-pair orbitals of the oxygen atom of other water molecule (i.e. the corners of tetrahedron with the effective negative charge). If the hydrogen bond is being formed, the hydrogen atom is situated at a link between two oxygen atoms, whereas the oxygen involved in the covalent bonding is being much closer to the hydrogen atom than the one involved in the hydrogen bonding. Evidently, any water molecule might in principle form at best four hydrogen bonds with other water molecules. Ice is a molecular crystal of water molecules, which condensates predominantly due to the hydrogen bonds formed between constituent water molecules. It is therefore possible to have the solid hydrogen-bonded water crystal (ice), where the water molecules are arranged to form 3D network of corner-sharing tetrahedrons and the centers of these tetrahedrons (i.e. the position of the oxygen atoms) form 3D diamond-like lattice. 3D diamond-like ice crystal indeed occurs in the temperature range between -120°C and -140°C and is known as ice Ic. It is worthwhile to remark that the usual ice I, which is stable under the normal conditions (atmospheric pressure and temperatures slightly below 0°C), has a wurtzite-like structure that is also tetrahedrally coordinated. Each water molecule is tetrahedrally bonded to other four water molecules in both these polymorphs of ice and consequently, there are in total six

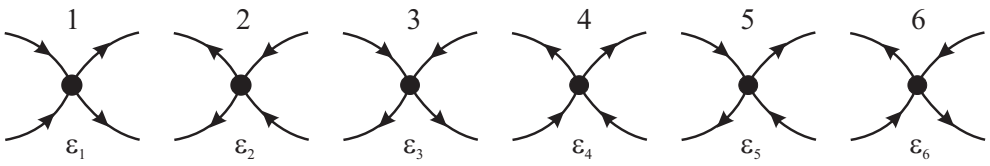

Figure 23: Six possible arrow arrangements satisfying the ice rule.

different orientations available for each molecule of the ice crystal depending on where the covalent and hydrogen bonds are situated[15].

Now, let us construct the possible model of ice. First, it is very convenient to introduce an *arrow* convention that specifies the polarity of the water molecule. As we have already explained in above, the water molecule can be regarded as a slightly deformed tetrahedron with two kinds of charged corners; the two corners occupied by hydrogen atoms are positively charged, whereas the other two corners (where the lone-pair orbitals of the oxygen are directed) are negatively charged. This charge arrangement can be redrawn to the plane as displayed in Fig. 22b. The simple arrow convention can be introduced through this rule: *let an arrow always point inwards (outwards) a positively (negatively) charged corner*. Apparently, there must be precisely one single arrow on each bond between two water molecules when the hydrogen bonding takes place in between them (Fig. 22c-d). The complete hydrogen-bonded network can be thus represented by a graph whose vertices label the centers of water molecules (i.e. their oxygen atoms) and there is one and just one arrow on each edge of this graph. Of course, the two arrows must point inwards and the remaining two outwards from a vertex in agreement with the tetrahedron model of water molecule with two positively and two negatively charged corners. The Pauling's claim [28] 'two arrows pointing inwards and two arrows pointing outwards from a vertex' is also known as *ice rule*, which consequently leads just to six available arrow configurations with equal energies conveniently set to zero $\varepsilon_1 = \ldots = \varepsilon_6 = 0$. The model based on six available arrow configurations depicted in Fig. 23 is therefore called also as the *six-vertex model*. Another basic assumption of the six-vertex model is that the overall energy is given by a simple sum over all individual vertex energies, what means that the overall energy is obtained by summing over individual energies of all water molecules.

[15]There is a large number of polymorphs of ice to be stable at higher pressures, however, each of them has every water molecule hydrogen-bonded to other four water molecules.

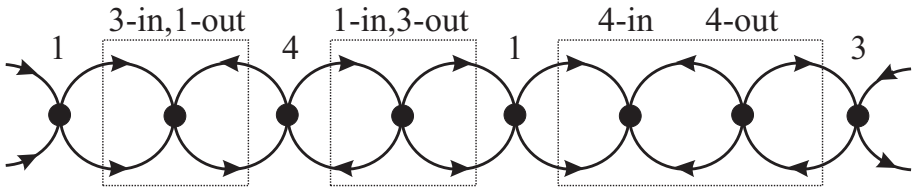

Figure 24: The simplest 1D ice model of double hydrogen-bonded water molecules. The vertices denote positions of oxygen atoms and the arrows specify the hydrogen bonding between the nearest-neighbouring water molecules. Broken lines demarcate vertices (hydrogen molecules) with forbidden arrow configuration.

At this stage, we shall define 1D model representing the simplest possible ice model, which obeys the Pauling's ice rule 'two in, two out arrows'. The geometry of 1D ice model of N water molecules is schematically illustrated in Fig. 24. In this figure, each vertex denotes the oxygen position of one water molecule and the arrows placed on edges of this graph specify the polarity of water molecules. It is quite obvious from Fig. 24 that the nearest-neighbouring water molecules are bind together through two hydrogen bonds. Accordingly, the simple observation can be made for each pair of hydrogen-bonded water molecules: if one water molecule is directed towards the other one by the same kind of tetrahedron corners (both corners are either positively or negatively charged), then the other water molecule must be oriented with respect to the former one by the complementary charged tetrahedron corners to enable the hydrogen bonding between them. This claim has far-reaching consequences on possible arrow configurations of 1D ice model. As a matter of fact, once two arrows are pointing likewise on the same side of a certain vertex, then the Pauling's ice rule demands all the other vertices with the same arrow configuration on the same side. As a result, there are just two possible macrostates that involve first two microstates from Fig. 23: the one with all arrows pointing to the right and the other one with all arrows pointing to the left (see Fig. 25a-b).

Besides, there also exists the second type of macrostates that are composed solely of another four microstates having two different arrow orientations on the same side of each vertex (the last four microstates depicted in Fig. 23). It is quite clear from Figs. 23 and 25c that if one of these microstates is chosen at a certain vertex, then there are just two different possibilities how to arrange an arrow configuration of each its nearest-

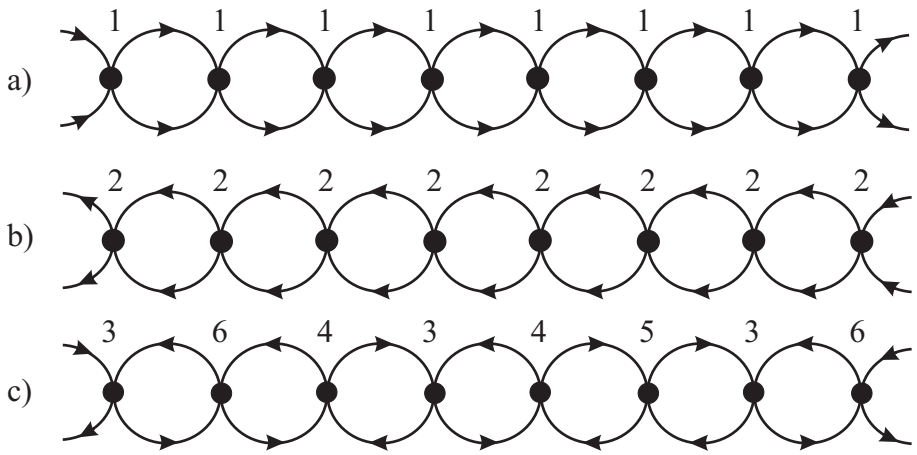

Figure 25: Several possible macrostates of 1D ice model, which are constructed merely by the use of allowed arrow configurations shown in Fig. 23.

neighbouring vertex. With regard to this, one can generally set up another 2^N macrostates by employing four microstates of a vertex, which have two different arrows (one in and one out) on each side. Since the configurational energy is assumed to be the sum of individual vertex energies and each vertex energy is equal to zero, it follows from (1.3) that the overall internal energy of each possible macrostate is zero and thus, $\mathcal{U} = 0$. According to Eq. (1.2), the partition function enumerates the number of microstates accessible to the macrosystem. It becomes quite apparent from the aforementioned arguments that the partition function of 1D ice model must be equal to $\mathcal{Z} = 2 + 2^N$. Then, the entropy can be simply obtained by substituting these final results for the partition function and the internal energy to the relation (1.4). This straightforward procedure yields the entropy $\mathcal{S} = k_{\mathrm{B}} \ln(2 + 2^N)$, which is consistent with the famous Boltzmann's result

$$\mathcal{S} = k_{\mathrm{B}} \ln \Omega \tag{6.1}$$

that evaluates the entropy in terms of the number of available microstates Ω corresponding to the macrostate in the thermal equilibrium. The Helmholtz free energy, internal energy and entropy reduce in the thermodynamic limit to extraordinary simple expressions

$$\mathcal{F} = -Nk_{\mathrm{B}}T \ln 2, \qquad \mathcal{U} = 0 \qquad \text{and} \qquad \mathcal{S} = Nk_{\mathrm{B}} \ln 2. \tag{6.2}$$

It is quite evident from Eq. (6.2) that all temperature derivatives of the Helmholtz free energy are continuous functions of the temperature and hence, the 'linear' ice displayed

in Fig. 24 cannot exhibit any phase transition and/or a marked critical point. Moreover, the molar entropy (6.2) of linear ice $\mathcal{S}_{\text{linear}} = R \ln 2 = 5.763$ JK^{-1}mol^{-1} is in obvious contradiction with the experimentally measured value $\mathcal{S}_{\text{exp}} = R \ln 1.507 = 3.409$ JK^{-1}mol^{-1}.

The main reason for this discrepancy lies evidently in the hydrogen-bonding of the linear ice, whose water molecules are bonded by a couple of hydrogen bonds to two nearest-neighbouring water molecules. Contrary to this, each water molecule is hydrogen-bonded to four different water molecules in the real ice. The simplest plausible ice model of the completely hydrogen-bonded water crystal thus represents 2D ice model on a square lattice, since this lattice has the appropriate coordination number ensuring hydrogen bonding to four different water molecules. However, the evaluation of the partition function in a closed form is an extremely difficult task for the 'square' ice and this problem has been exactly solved by sophisticated mathematical procedure developed by E. H. Lieb in 1967 [30]. It is noteworthy that the Lieb's exact result for the residual entropy of square ice $\mathcal{S}_{\text{square}} = \frac{3}{2} R \ln \frac{4}{3} = 3.588$ JK^{-1}mol^{-1} is strikingly close to the rough Pauling's estimate based on simple heuristic arguments [28]. Anyway, the crude Pauling's explanation of the residual entropy of square ice is one of the most accurate estimations in the condensed matter physics at all and it can be made in the following way. By neglecting the boundary effects, the square lattice of N vertices has in total $2N$ edges and there are merely 2 arrow orientations allowed per each its edge. So, there exist in total 2^{2N} different arrow configurations by covering all edges of the square lattice precisely by one arrow. However, some of these arrow configurations violate the ice rule and thus, the additional factor $\frac{6}{16}$ must be taken into consideration because only 6 from 16 possible vertex configurations are allowed for each vertex according to the ice rule. In this respect, the partition function of the square ice model reads

$$\mathcal{Z} = 2^{2N} \left(\frac{6}{16} \right)^N = \left(\frac{3}{2} \right)^N , \tag{6.3}$$

which gives in the thermodynamic limit the entropy $\mathcal{S}_{\text{Pauling}} = R \ln \frac{3}{2} = 3.371$ JK^{-1}mol^{-1}. This value of residual entropy is remarkably close to the Lieb's exact result for the entropy of the square ice [30] and what is still more surprising, it is even closer to the experimentally measured value than the Lieb's exact result.

6.1.2 KDP model of ferroelectrics

Potassium dihydrogen phosphate KH_2PO_4, to be further abbreviated as KDP, is an important representative of hydrogen-bonded ferroelectric crystals with a sharp phase transition at $T_c = 123$ K. Below this critical temperature, KDP is a *ferroelectric* with the non-zero spontaneous polarization even in zero external electric field, while it becomes *paraelectric* without any spontaneous polarization above and at the critical temperature. This is a generic feature of a large number of ferroelectric crystals in which hydrogen ions are located between bulky anion groups (like phosphate group in KDP) so that the ferroelectric crystal is in fact a hydrogen-bonded lattice with the positions of large anion groups as lattice vertices. It turns out that the equilibrium positions of hydrogen ions are closer to one of two bulky anions and this leads to an onset of the non-zero spontaneous polarization at sufficiently low temperatures. In this respect, the position of hydrogen ions determines a state of the ferroelectric crystal. It is noteworthy that the ferroelectric crystals with the outstanding order of hydrogen ions like KDP can be specified by the rule analogous to Pauling's ice rule [28], which disallows so-called charged configurations connected with the hydrogen bonding to the anionic part of the constituent molecule. It means that this simple electrostatic picture excludes the configurations with the lack or excess of hydrogen ions leading to a charge accumulation, which consequently increases the overall electrostatic energy of the ferroelectric crystal. In this part, we shall provide an accurate solution for 1D analogue of KDP model, which was suggested for the hydrogen-bonded ferroelectric crystals by J. C. Slater in 1941 [29]. It should be remarked that the exact treatment presented hereafter closely follows the ingenious and fairly simple derivation developed by J. F. Nagle (1968) [31].

Let us consider 1D chain of KDP molecules (vertices), which are joined by double hydrogen bonds as schematically illustrated in Fig. 26. In this figure, the potassium cations K^+ are denoted by open circles, the hydrogen ions H^+ are represented by filled circles and the positions of the phosphate anions PO_4^{3-} are represented by tetrahedra. 1D ferroelectric crystal of KDP is held together by hydrogen bonds, whereas each pair of nearest-neighbouring phosphate groups is joined through two hydrogen bonds. The basic assumption is that the energy of 1D KDP model consists of the sum of single phosphate

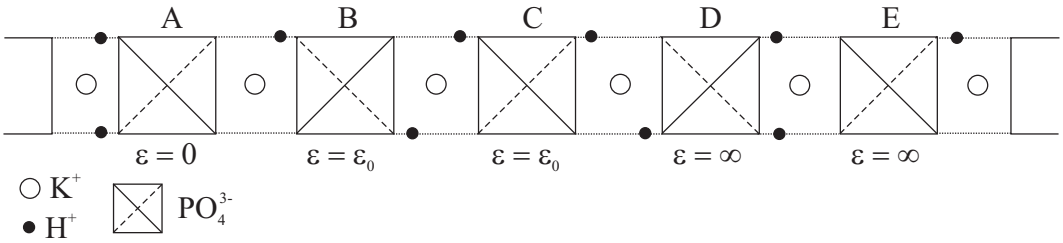

Figure 26: The linear crystal of KDP molecules. The potassium cations K^+ are denoted by large open circles, the hydrogen ions H^+ by small filled circles and the phosphate groups PO_4^{3-} are represented by tetrahedra.

group energies, which are assigned according to the Slater's rules [29]:

- if a phosphate group has two hydrogen cations close by on the same side, such as the group A in Fig. 26, then, it possesses zero energy $\varepsilon = 0$;
- if a phosphate group has two hydrogen cations close by on two different sides, such as the groups B and C in Fig. 26, then, it possesses a finite amount of energy $\varepsilon = \varepsilon_0 > 0$;
- if a phosphate group has zero, one, three or four hydrogen cations close by, such as the groups D and E in Fig. 26, then, it possesses infinite energy $\varepsilon \to \infty$.

Notice that all aforementioned energy assignments have a plausible explanation in a simple electrostatic picture of 1D ferroelectric crystal constituted by charged K^+, H^+ and PO_4^{3-} ions (see Fig. 26). First, it should be realized that a negative charge of the phosphate group is balanced by a positive charge of one potassium and two hydrogen cations in order to ensure the electroneutrality condition of each KDP molecule. However, it should be also mentioned that the mass of the phosphate group as well as the one of the potassium cation are much larger than the mass of the hydrogen cation. Hence, it follows that the phosphate groups and the potassium cations can just barely change their rigid positions in a crystal, while the hydrogen cations can change their lattice positions the most easily because of their light mass. Obviously, the third rule energetically prohibits all configurations with other than two hydrogen cations nearby each phosphate group, since this would lead to a net accumulation of charge that should cost a large amount of electrostatic energy. Therefore, the infinite energy is assigned to these *ionized* states,

which are consequently completely disregarded within this approximation. It is somewhat more difficult to explain the assignment of higher energy to the phosphate groups of B and C type in comparison with the phosphate group A, because the hydrogen cations are closer together just in the phosphate group A. It is therefore necessary to consider also the electrostatic repulsion between the potassium and hydrogen cations in order to shed light on the energy difference between the configurations with two hydrogen cations nearby the phosphate group. Namely, two hydrogen cations are effectively shielded from the electrostatic force of the larger potassium cation by the bulky asymmetric phosphate group A and moreover, the potassium cation has a tendency to move closer to the phosphate anion in order to enhance its distance with respect to the closest pair of hydrogen ions. This mechanism cannot evidently occur in the phosphate groups B and C, which have the hydrogen cations on both sides of the phosphate group and the potassium cations have a tendency to lie in a center of the hydrogen bonds between the two nearest-neighbouring phosphate groups.

Now, let us define 1D KDP model of ferroelectric crystal, which obeys the aforementioned rules and consists of N KDP molecules. For convenience, let us also consider the periodic boundary conditions so that 1D chain becomes a ring. The partition function of 1D KDP model reads

$$\mathcal{Z} = \sum_{\text{config.}} \exp\left(-\beta \sum_{i=1}^{N} \varepsilon_i\right) = \sum_{\text{config.}} \prod_{i=1}^{N} \exp(-\beta\varepsilon_i), \tag{6.4}$$

where the first summation is carried out over all possible configurations of the hydrogen ions in the closed chain and the second summation runs over configurational energies of all phosphate groups assigned according to the aforedescribed rules. The position of hydrogen ions (hydrogen bonding) determines the overall configurational energy of the phosphate groups, which are being on the left-hand-side and right-hand-side with respect to them. Altogether, there exist in total six possible microstates around each phosphate group (vertex), which are diagrammatically shown in Fig. 27 together with their configurational energies. That is why the ferroelectric KDP model is also called as the *six-vertex model*. In view of further manipulation, it is very appropriate to reformulate the six-vertex model in terms of the arrow representation, which is introduced through Fig. 28. The arrow

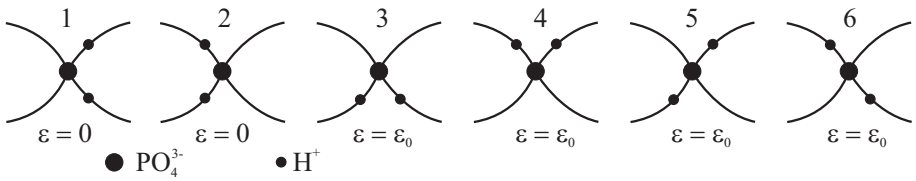

Figure 27: Six possible microstates of KDP molecule, which have two hydrogen ions (small filled circles) close by the bulky phosphate group (vertices = large filled circles).

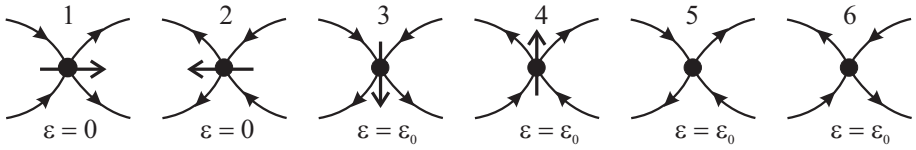

Figure 28: The arrow representation of the six possible microstates depicted in Fig. 27. The greatest arrow illustrates the overall dipole moment of each configuration.

representation of the six-vertex model can be obtained following this rule: if the hydrogen is close by (i.e. forms a covalent bond with) the phosphate group, then draw an arrow pointing outwards a vertex, otherwise draw an arrow pointing inwards a vertex. In such a way, six possible hydrogen configurations depicted in Fig. 27 can be redrawn with the help of six arrow configurations shown in Fig. 28.

It is not very difficult to obtain the exact solution of the model under investigation by employing the transfer-matrix approach invented by J. F. Nagle [31]. Let us choose a pair of hydrogen bonds joining the $(i-1)$st and ith phosphate groups (vertices). This pair of hydrogen bonds might have four different hydrogen (arrow) configurations LL_{i-1}, LR_{i-1}, RL_{i-1} and RR_{i-1}, where L and R refer to the position of hydrogen ions on the left side and right side of the bond, respectively. Accordingly, the hydrogen position L corresponds to an arrow configuration pointing inwards the former $(i-1)$st vertex, whereas the hydrogen position R corresponds to an arrow configuration pointing inwards the latter ith vertex. At this stage, it is appropriate to introduce the transfer matrix

$$T \equiv \mathrm{e}^{-\beta\varepsilon_i} = \begin{pmatrix} T(LL_{i-1}, LL_i) & T(LL_{i-1}, LR_i) & T(LL_{i-1}, RL_i) & T(LL_{i-1}, RR_i) \\ T(LR_{i-1}, LL_i) & T(LR_{i-1}, LR_i) & T(LR_{i-1}, RL_i) & T(LR_{i-1}, RR_i) \\ T(RL_{i-1}, LL_i) & T(RL_{i-1}, LR_i) & T(RL_{i-1}, RL_i) & T(RL_{i-1}, RR_i) \\ T(RR_{i-1}, LL_i) & T(RR_{i-1}, LR_i) & T(RR_{i-1}, RL_i) & T(RR_{i-1}, RR_i) \end{pmatrix}, \quad (6.5)$$

which acquires the following explicit form if one takes into account configurational energies

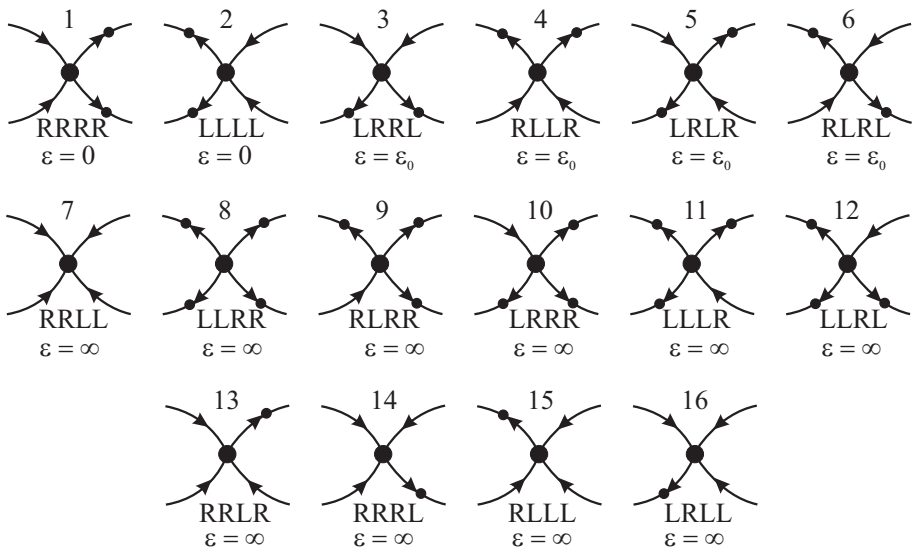

Figure 29: The hydrogen and arrow representations of all sixteen microstates, whose Boltzmann's weights act as the entries of the transfer matrix (6.5).

assigned to the individual microstates of the KDP model according to Fig. 29

$$T \equiv \exp(-\beta\varepsilon_i) = \begin{pmatrix} 1 & 0 & 0 & 0 \\ 0 & \exp(-\beta\varepsilon_0) & \exp(-\beta\varepsilon_0) & 0 \\ 0 & \exp(-\beta\varepsilon_0) & \exp(-\beta\varepsilon_0) & 0 \\ 0 & 0 & 0 & 1 \end{pmatrix}. \tag{6.6}$$

Apparently, the rows of the transfer matrix (6.5) determine the arrow configuration joining $(i-1)$st and ith vertices, while its columns determine the arrow configuration joining ith and $(i+1)$st vertices. In this way, the transfer matrix (6.5) unambiguously determines the configuration of hydrogen ions (arrows) on both sides of the ith phosphate group (vertex) and thus, it also determines its available energies and Boltzmann's factors. In the consequence of that, the entries of the transfer matrix (6.6) are nothing but the Boltzmann's factors, which are associated with the particular arrow (hydrogen ion) configurations. All sixteen configurations serving as the entries of the transfer matrix (6.5) are displayed in Fig. 29 together with their configurational energies. As one can see from this figure, ten from sixteen configurations have zero Boltzmann's weights owing to the infinite energy of forbidden ionized states. The remaining six configurations with the non-zero Boltzmann's factors correspond to the allowed configurations (Figs. 27 and 28) satisfying the Slater's rules.

When the substitution of the transfer matrix (6.5) to Eq. (6.4) is successively followed by the multiplication of all transfer matrices being equivalent to the summation over all allowed configurations of the common hydrogen bonds, the partition function of 1D KDP model can be expressed as a trace over the final result of this matrix product

$$\mathcal{Z} = \mathrm{Tr}\left[T^N(\varepsilon_1, \varepsilon_2, \varepsilon_3, \varepsilon_4, \varepsilon_5, \varepsilon_6)\right] = \sum_{i=1}^{4} \lambda_i^N \tag{6.7}$$

and this trace is simply equal to a sum over all eigenvalues of the transfer matrix (6.5) raised to the Nth power. The sought eigenvalues of the transfer matrix (6.5) can readily be calculated by solving the secular determinant

$$\begin{vmatrix} 1-\lambda & 0 & 0 & 0 \\ 0 & \exp(-\beta\varepsilon_0)-\lambda & \exp(-\beta\varepsilon_0) & 0 \\ 0 & \exp(-\beta\varepsilon_0) & \exp(-\beta\varepsilon_0)-\lambda & 0 \\ 0 & 0 & 0 & 1-\lambda \end{vmatrix} = 0, \tag{6.8}$$

which yields after straightforward calculation a complete spectrum of eigenvalues

$$\lambda_{1,2} = 1, \quad \lambda_3 = 2\exp(-\beta\varepsilon_0), \quad \text{and} \quad \lambda_4 = 0. \tag{6.9}$$

Regarding this, the canonical partition function of the 1D KDP model is simply obtained by substituting the eigenvalues (6.9) to Eq. (6.7)

$$\mathcal{Z} = 2 + 2^N \exp(-\beta N\varepsilon_0). \tag{6.10}$$

From here onward, all thermodynamic quantities follow straightforwardly. As a matter of fact, the Helmholtz free energy can be obtained from Eq. (1.4)

$$\mathcal{F} = -k_\mathrm{B}T \ln\left[2 + 2^N \exp(-\beta N\varepsilon_0)\right], \tag{6.11}$$

while the internal energy can be the most readily obtained by adopting Eq. (1.3)

$$\mathcal{U} = N\varepsilon_0 \frac{2^N \exp(-\beta N\varepsilon_0)}{2 + 2^N \exp(-\beta N\varepsilon_0)}. \tag{6.12}$$

It can be easily shown from Eqs. (6.11) and (6.12) that 1D KDP model exhibits in the thermodynamic limit ($N \to \infty$) very peculiar phase transition. Consider for instance

the internal energy $\mathcal{U}$. It immediately follows from Eq. (6.12) that the internal energy normalized per one KDP molecule is given by

$$\frac{\mathcal{U}}{N\varepsilon_0} = \lim_{N\to\infty} \frac{2^N \exp(-\beta N\varepsilon_0)}{2 + 2^N \exp(-\beta N\varepsilon_0)} = \begin{cases} 0 & \text{if} \quad \exp(\beta\varepsilon_0) > 2; \\ 1 & \text{if} \quad \exp(\beta\varepsilon_0) < 2. \end{cases} \tag{6.13}$$

Thus, there exist two temperature intervals, where the internal energy of 1D KDP model has two completely different values

$$\text{if} \quad \frac{k_{\mathrm{B}}T}{\varepsilon_0} < \frac{1}{\ln 2} \quad \text{then} \quad \mathcal{U}_1 = 0, \tag{6.14}$$

$$\text{if} \quad \frac{k_{\mathrm{B}}T}{\varepsilon_0} > \frac{1}{\ln 2} \quad \text{then} \quad \mathcal{U}_2 = N\varepsilon_0. \tag{6.15}$$

According to this, the temperature $k_{\mathrm{B}}T_{\mathrm{c}} = \varepsilon_0/\ln 2$ represents a critical temperature at which the internal energy changes discontinuously. The abrupt change of the internal energy is being a typical feature of the first-order (discontinuous) phase transitions, so it is of particular interest to look at the entropy change of this phase transition. The entropy can be easily obtained from Eq. (1.4)

$$\mathcal{S} = \frac{\mathcal{U}}{T} + k_{\mathrm{B}} \ln \mathcal{Z} = \frac{N\varepsilon_0}{T} \frac{2^N \exp(-\beta N\varepsilon_0)}{2 + 2^N \exp(-\beta N\varepsilon_0)} + k_{\mathrm{B}} \ln \left[2 + 2^N \exp(-\beta N\varepsilon_0)\right]. \tag{6.16}$$

Evidently, Eq. (6.16) predicts for two temperature intervals, where the macrosystem has two different internal energies, also two different entropies

$$\text{if} \quad \frac{k_{\mathrm{B}}T}{\varepsilon_0} < \frac{1}{\ln 2} \quad \text{then} \quad \frac{\mathcal{S}_1}{Nk_{\mathrm{B}}} = 0, \tag{6.17}$$

$$\text{if} \quad \frac{k_{\mathrm{B}}T}{\varepsilon_0} > \frac{1}{\ln 2} \quad \text{then} \quad \frac{\mathcal{S}_2}{Nk_{\mathrm{B}}} = \ln 2. \tag{6.18}$$

Owing to this fact, even smooth temperature change over the temperature interval containing the critical point $k_{\mathrm{B}}T_{\mathrm{c}} = \varepsilon_0/\ln 2$ leads to an abrupt change of the entropy $\Delta\mathcal{S} = \mathcal{S}_2 - \mathcal{S}_1 = Nk_{\mathrm{B}} \ln 2$. Therefore, the finite amount of the latent heat $\mathcal{L} = T_{\mathrm{c}}\Delta\mathcal{S} = Nk_{\mathrm{B}}T_{\mathrm{c}} \ln 2 = N\varepsilon_0$ must be either absorbed or released at a critical point of the first-order phase transition from the low- to high-temperature phase or vice versa. Note that standard thermodynamical-statistical relations can be used for calculating other important thermodynamical properties of ferroelectrics such as spontaneous polarization, specific heat, enthalpy, etc.

Now, let us bring a deeper insight into the phase transitions and critical phenomena of 1D KDP model by detailed analysis of its available macrostates. If the asymmetric configuration with two hydrogen cations on the same side of a certain vertex (in other words, the arrow configuration with two inwards pointing arrows on the same side of a certain vertex) is selected, then, all the other vertices must necessarily have the same asymmetric configuration around them. In the consequence of that, the two asymmetric microstates with zero energy cannot be mixed with the other four microstates with non-zero energy ε_0 in order to form some macrostate. As a result, there exist just two possible macrostates containing merely the asymmetric microstates with zero energy; the one with all vertices having inward pointing arrows from the left-hand-side and the other one with all vertices having inward pointing arrows from the right-hand-side (see Fig. 25a-b). The overall energy of both these macrostates is certainly zero and this corresponds to two Boltzmann's factors equal to unity. On the other hand, if the configuration with two hydrogen cations on two different sides of a certain vertex (in other words, the arrow configuration with two inwards pointing arrows on two different sides of a certain vertex) is chosen, then, there are always two possibilities how to arrange the configuration of hydrogen ions (arrows) on its nearest-neighbouring vertices. Therefore, there exists the second type of macrostates, which are constituted by to a certain extent random arrangement of the four microstates with non-zero energy ε_0 (see Fig. 25c). In this respect, we have in total another 2^N macrostates with the overall energy $N\varepsilon_0$ (each of them consists of N microstates with the energy ε_0) and thus, these macrostates contribute to the partition function by the Boltzmann's factor $2^N \exp(-\beta N\varepsilon_0)$. In this way, we have recovered the partition function (6.10) without performing the extended calculation relying on the transfer-matrix approach.

At first sight, the results presented in this section seem to be in contradiction with the well known fact that 1D models with short-range forces cannot exhibit a phase transition towards a spontaneously ordered phase. However, it should be stressed that one of the conditional assumptions of this dictum is that the potential arising from short-range forces cannot be singular. It is quite obvious that 1D KDP model based on the Slater's rules violates this assumption due to the assignment of infinite energy to ionized phosphate

groups, which do not have precisely two hydrogen ions close by. In this respect, it could be expected that more realistic energy assignment with a rather strong but finite vertex energies should resolve this problem (see the modified Takagi's KDP model discussed below). What is even more surprising, the ingenious and rather complex exact solutions of 2D Slater's KDP model achieved by B. Sutherland [32] and E. H. Lieb [33] have confirmed a presence of the analogous first-order phase transition to emerge at the same critical temperature in 2D Slater's KDP model on the square lattice as well.

6.2 Sixteen-vertex model

Let us modify Slater's 1D KDP model by considering more realistic energy assignments to ionized configurations of the phosphate group. Of course, the energy of the phosphate group with other than two hydrogen cations close by must necessarily increase due to a net accumulation of charge, which costs an additional amount of electrostatic energy. Takagi's 1D KDP model of hydrogen-bonded ferroelectrics [34] relies on a plausible assumption that the once ionized configurations with one or three hydrogen cations in the close vicinity of the phosphate group have the energy $\varepsilon_1 \gg \varepsilon_0$, while the twice ionized configurations with zero or four hydrogen cations nearby the phosphate group have roughly twice as large energy $\varepsilon_2 = 2\varepsilon_1$. For illustration, Fig. 15 shows all sixteen available configurations together with their corresponding configurational energies. With regard to this, there are no forbidden configurations within Takagi's KDP model and the model is essentially the *sixteen-vertex model*.

The exact solution of the Takagi's 1D KDP model can be acquired by adopting the approach, which was invented by J. F. Nagle (1968) [31] to obtain the exact solution of the Slater's 1D KDP model as explained in the preceding part. The most crucial difference consists in the modified Boltzmann's weights, which are schematically depicted in Fig. 30 and which change the entries of the transfer matrix (6.5) to

$$T \equiv \exp(-\beta\varepsilon_i) = \begin{pmatrix} 1 & \exp(-\beta\varepsilon_1) & \exp(-\beta\varepsilon_1) & \exp(-2\beta\varepsilon_1) \\ \exp(-\beta\varepsilon_1) & \exp(-\beta\varepsilon_0) & \exp(-\beta\varepsilon_0) & \exp(-\beta\varepsilon_1) \\ \exp(-\beta\varepsilon_1) & \exp(-\beta\varepsilon_0) & \exp(-\beta\varepsilon_0) & \exp(-\beta\varepsilon_1) \\ \exp(-2\beta\varepsilon_1) & \exp(-\beta\varepsilon_1) & \exp(-\beta\varepsilon_1) & 1 \end{pmatrix}. \quad (6.19)$$

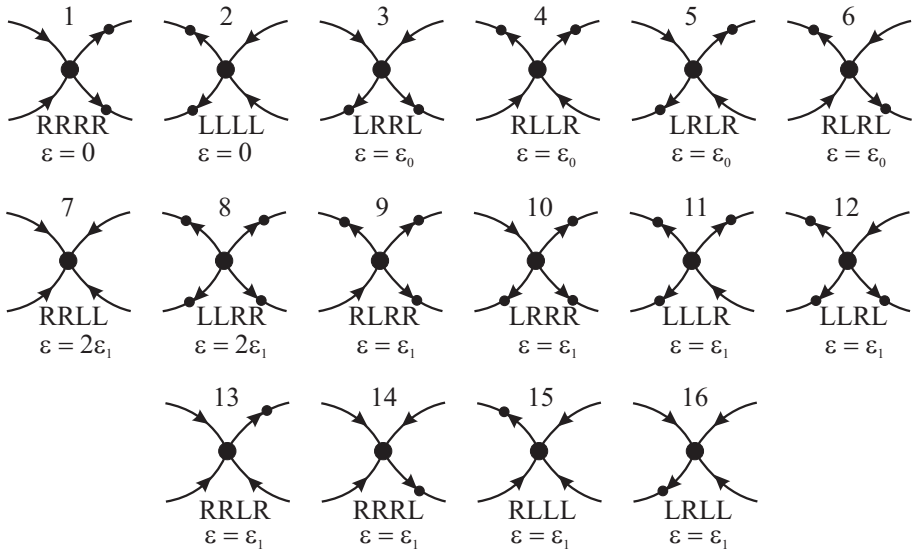

Figure 30: The hydrogen and arrow representations of sixteen microstates, whose Boltzmann's weights act as the entries of the transfer matrix (6.19) in Takagi's 1D KDP model.

The eigenvalues of the transfer matrix (6.19) are then given by the condition

$$\begin{vmatrix} 1-\lambda & \exp(-\beta\varepsilon_1) & \exp(-\beta\varepsilon_1) & \exp(-2\beta\varepsilon_1) \\ \exp(-\beta\varepsilon_1) & \exp(-\beta\varepsilon_0)-\lambda & \exp(-\beta\varepsilon_0) & \exp(-\beta\varepsilon_1) \\ \exp(-\beta\varepsilon_1) & \exp(-\beta\varepsilon_0) & \exp(-\beta\varepsilon_0)-\lambda & \exp(-\beta\varepsilon_1) \\ \exp(-2\beta\varepsilon_1) & \exp(-\beta\varepsilon_1) & \exp(-\beta\varepsilon_1) & 1-\lambda \end{vmatrix} = 0, \tag{6.20}$$

which yields after a little bit more involved calculation a complete set of the eigenvalues

$$\begin{aligned} \lambda_{1,2} &= \frac{1}{2}\left[1+2\exp(-\beta\varepsilon_0)+\exp(-2\beta\varepsilon_1)\right] \\ &\quad \pm\frac{1}{2}\sqrt{\left[1-2\exp(-\beta\varepsilon_0)+\exp(-2\beta\varepsilon_1)\right]^2+16\exp(-2\beta\varepsilon_1)}, \\ \lambda_3 &= 1-\exp(-2\beta\varepsilon_1), \qquad \lambda_4 = 0. \end{aligned} \tag{6.21}$$

It can be easily verified that the largest eigenvalue is the quadratic root with the plus sign irrespective of the temperature and thus, the Helmholtz free energy of the Takagi's 1D KDP model reduced per one KDP molecule becomes in the thermodynamic limit

$$\mathcal{F} = -k_{\mathrm{B}}T\lim_{N\to\infty}\frac{1}{N}\ln\mathcal{Z} = -k_{\mathrm{B}}T\ln\lambda_{\max}. \tag{6.22}$$

This result means that the Helmholtz free energy is an analytic function of the temperature and thence, it follows that there does not occur any phase transition in the modified

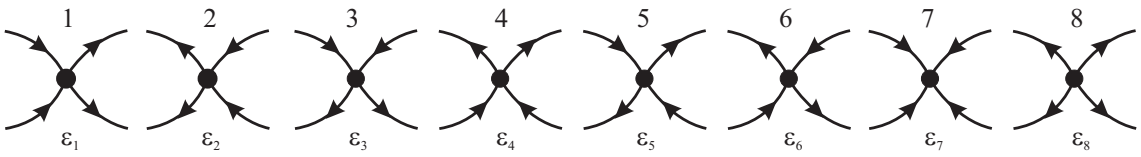

Figure 31: Eight possible arrow configurations of the eight-vertex model.

Takagi's 1D KDP model. This result is in accordance with our expectations, since 1D models with short-range forces cannot exhibit a phase transition towards spontaneously ordered phase once the conditional assumption of the non-singular potential is fulfilled.

6.3 Symmetric eight-vertex model

In this part, we shall consider the so-called zero-field (symmetric) eight-vertex model that has symmetrically equal energies

$$\varepsilon_1 = \varepsilon_2, \qquad \varepsilon_3 = \varepsilon_4, \qquad \varepsilon_5 = \varepsilon_6, \qquad \varepsilon_7 = \varepsilon_8, \tag{6.23}$$

for four pairs of vertex configurations displayed in Fig. 31. The condition (6.23) ensures that the energy of the considered model remains unchanged by reversing all arrows (dipole moments), what fully corresponds to the situation of ferroelectric (ferromagnetic) materials in an absence of the external electric (magnetic) field. Hence, the model with the energy assignment (6.23) is also referred to as the zero-field eight-vertex model.

First, let us make few remarks why to study the zero-field eight-vertex model, which seems at first sight very similarly as the six-vertex models. The reason is as follows: the six-vertex models evidently exhibit a pathological critical behaviour because all their low-temperature ordered states are 'frozen' in that their perfect ordering cannot be disturbed by the temperature unless the critical point is reached. From this point of view, the ordered states exhibit physical properties that do not diverge or vanish near the critical temperature as simple powers of the difference $T - T_c$ and thus, they cannot be characterized by the set of critical exponents (1.17). It is quite apparent that this pathological critical behaviour originates from the fact that individual vertex configurations cannot be changed within the completely ordered state, which is energetically favored below the critical temperature, since this would cost an infinite amount of the energy.

Owing to these facts, B. Sutherland (1970) [35], C. Fan and F. Y. Wu (1970) [36] suggested the generalized ice-type model by the rule: *the only allowed arrow configurations of a vertex are those with an even number of arrows pointing inwards or outwards a vertex*. The model satisfying this rule is called the eight-vertex model and this model permits another two arrow configurations besides the usual ones allowed by the ice rule. One of the most fundamental properties of the eight-vertex model is that two new vertex configurations with all arrows pointing inwards or outwards a vertex enable arrow reversals, which cost a finite amount of energy even within the low-temperature ordered states. Accordingly, the rising temperature might in principle gradually destroy the perfect ordering of the ordered state and one may hope that the eight-vertex model will be in this respect less pathological than the six-vertex one.

6.3.1 Linear eight-vertex model

The linear eight-vertex model defined through the energy assignment (6.23) can be exactly treated with the help of the same transfer-matrix approach as used for its six-vertex analogue. With regard to this, we shall leave out all the particular details and we shall present merely the most fundamental steps of this calculation. By assuming the periodic boundary condition, the partition function of 1D eight-vertex model can be defined as

$$\mathcal{Z} = \sum_{\text{config.}} \exp\left(-\beta \sum_{i=1}^{N} \mathcal{E}_i\right), \tag{6.24}$$

where the first summation is carried out over all possible arrow configurations of the eight-vertex model and the second summation enumerates all individual vertex energies within each macrostate. There also exists an alternative definition of the partition function

$$\mathcal{Z} = \sum_{\text{config.}} \exp\left(-\beta \sum_{j=1}^{8} n_j^{\text{c}} \varepsilon_j\right), \tag{6.25}$$

where the latter summation runs over eight possible vertex configurations and the number n_j^{c} enumerates a total number of vertices that have the same arrow configuration within each vertex configuration. In the spirit of the former definition, the partition function of the linear eight-vertex model can be calculated as a trace of the transfer matrix raised to

the Nth power and this trace is directly equal to a sum over all its eigenvalues

$$\mathcal{Z} = \mathrm{Tr}\left[T^N(\varepsilon_1, \varepsilon_3, \varepsilon_5, \varepsilon_7)\right] = \sum_{i=1}^{4} \lambda_i^N, \tag{6.26}$$

whereas the relevant transfer matrix can be defined as

$$\begin{aligned} T \equiv & \begin{pmatrix} T(LL_{i-1}, LL_i) & T(LL_{i-1}, LR_i) & T(LL_{i-1}, RL_i) & T(LL_{i-1}, RR_i) \\ T(LR_{i-1}, LL_i) & T(LR_{i-1}, LR_i) & T(LR_{i-1}, RL_i) & T(LR_{i-1}, RR_i) \\ T(RL_{i-1}, LL_i) & T(RL_{i-1}, LR_i) & T(RL_{i-1}, RL_i) & T(RL_{i-1}, RR_i) \\ T(RR_{i-1}, LL_i) & T(RR_{i-1}, LR_i) & T(RR_{i-1}, RL_i) & T(RR_{i-1}, RR_i) \end{pmatrix} \\ = & \begin{pmatrix} \exp(-\beta\varepsilon_1) & 0 & 0 & \exp(-\beta\varepsilon_7) \\ 0 & \exp(-\beta\varepsilon_3) & \exp(-\beta\varepsilon_5) & 0 \\ 0 & \exp(-\beta\varepsilon_5) & \exp(-\beta\varepsilon_3) & 0 \\ \exp(-\beta\varepsilon_7) & 0 & 0 & \exp(-\beta\varepsilon_1) \end{pmatrix}. \end{aligned} \tag{6.27}$$

The straightforward calculation relying on the secular equation consecutively yields a complete spectrum of eigenvalues of the transfer matrix (6.27)

$$\lambda_{1,2} = \exp(-\beta\varepsilon_1) \pm \exp(-\beta\varepsilon_7), \qquad \lambda_{3,4} = \exp(-\beta\varepsilon_3) \pm \exp(-\beta\varepsilon_5). \tag{6.28}$$

It is quite evident from Eq. (6.28) that the largest eigenvalue is one of two eigenvalues with the plus sign and hence, it follows that the largest eigenvalue might possibly change with temperature. In this respect, the suitable choice of the vertex energies ε_1, ε_3, ε_5 and ε_7 could entail an occurrence of the discontinuous (first-order) transition even in the linear eight-vertex model.

Let us analyze several particular cases of the linear eight-vertex model by restricting the vertex energies ε_1, ε_3, ε_5 and ε_7 up to three different values. It is noteworthy that two pairs of vertex energies (ε_1, ε_7) and (ε_3, ε_5) enter symmetrically into two eigenvalues

$$\lambda_1 = \exp(-\beta\varepsilon_1) + \exp(-\beta\varepsilon_7), \qquad \lambda_3 = \exp(-\beta\varepsilon_3) + \exp(-\beta\varepsilon_5). \tag{6.29}$$

which determine the largest eigenvalue of the transfer matrix and consequently, the one of vertex energies (say ε_1) can be considered without loss of the generality as the smallest one $\varepsilon_1 = \min\{\varepsilon_1, \varepsilon_3, \varepsilon_5, \varepsilon_7\}$. Under these circumstances, the phase transition might possibly occur just when $\varepsilon_3 = \varepsilon_5$ and $\varepsilon_1 \neq \varepsilon_7$, whilst there does not occur any phase transition as

long as one vertex energy from the first pair (ε_1, ε_7) is equal at least to one vertex energy from the second pair (ε_3, ε_5) or vice versa.

Bearing this in mind, the particular case with the vertex energies $\varepsilon_1 < \varepsilon_7 \neq \varepsilon_3 = \varepsilon_5$ might possibly exhibit a phase transition and it is therefore the most valuable for further investigation. Under these conditions, the eigenvalue λ_1 represents the largest eigenvalue if and only if

$$\lambda_1 > \lambda_3 \quad \Longleftrightarrow \quad x + x^n > 2x^m, \tag{6.30}$$

where the function $x \equiv \exp(-\beta\varepsilon_1)$ can be regarded as a new rescaled temperature variable bounded to the interval $x \in [0;1]$, $n = \varepsilon_7/\varepsilon_1$ and $m = \varepsilon_3/\varepsilon_1$ are positive real numbers greater than one that determine the relation between the lowest vertex energy ε_1 and the higher vertex energies ε_3, ε_5 and ε_7. The necessary and sufficient condition for an appearance of phase transition can be found with the aid of inequality between the arithmetic and geometric means, which is further abbreviated as AG inequality[16]. By applying AG inequality one readily proves that

$$\frac{x + x^n}{2} \geq \sqrt{x x^n}, \tag{6.31}$$

$$x + x^n \geq 2x^{\frac{n+1}{2}}. \tag{6.32}$$

If

$$m > \frac{n+1}{2} \tag{6.33}$$

then

$$x^m < x^{\frac{n+1}{2}}, \tag{6.34}$$

since the new temperature variable x is bounded to the interval $x \in [0;1]$. By combining the inequalities (6.32) and (6.34) one gets

$$x + x^n > 2x^m, \tag{6.35}$$

[16] AG inequality states that the arithmetic mean of a set of non-negative real numbers is greater than or equal to the geometric mean of the same set of non-negative real numbers $\frac{x_1+x_2+\ldots+x_n}{n} \geq \sqrt[n]{x_1 x_2 \ldots x_n}$. The equality holds if and only if all numbers from this set are equal one to each other $x_1 = x_2 = \ldots = x_n$.

which is valid whenever the condition (6.33) is met. In this respect, the condition (6.33) represents the necessary and sufficient condition that ensures an absence of the phase transition due to the validity of inequality $\lambda_1 > \lambda_3$ between the two largest eigenvalues in the whole temperature range. On the other hand, the inverted condition

$$m < \frac{n+1}{2} \quad \Longleftrightarrow \quad n > 2m-1 \quad \Longleftrightarrow \quad \varepsilon_7 > 2\varepsilon_3 - \varepsilon_1 \tag{6.36}$$

must represents the necessary and sufficient condition ensuring an appearance of the first-order phase transition in the linear zero-field eight-vertex model. Accordingly, the energy ε_7 of two new vertex configurations with all arrows pointing inwards or outwards a vertex must be much larger than the second largest vertex energy ε_3 (remember that ε_1 is the smallest vertex energy).

At this stage, let us confirm an occurrence of phase transition by exploring some particular case that matches the requirement (6.36). For this purpose, we shall investigate in detail the special case with the vertex energies ε_1, $\varepsilon_3 = \varepsilon_5 = 3\varepsilon_1$ and $\varepsilon_7 = 7\varepsilon_1$ ($m = 3$ and $n = 7$). The critical condition that determines the critical temperature T_c (x_c) is given by the equality between the two largest eigenvalues

$$\lambda_{1\mathrm{c}} = \lambda_{3\mathrm{c}} \qquad \Longleftrightarrow \qquad x_\mathrm{c} + x_\mathrm{c}^7 = 2x_\mathrm{c}^3. \tag{6.37}$$

It is quite obvious that the above equation is a single-variable polynomial of degree seven, which should have according to the fundamental theorem of algebra as many complex roots as its degree[17]. After the elementary calculation, one indeed finds seven different complex roots

$$x_1 = 0, \quad x_{2,3} = \pm 1 \quad \text{and} \quad x_{4,5,6,7} = \pm\sqrt{-\frac{1}{2} \pm \frac{\sqrt{5}}{2}}. \tag{6.38}$$

The only physical root, which is from inside the interval $x \in [0;1]$, then determines a critical point of the discontinuous phase transition to emerge at finite temperature

$$x_\mathrm{c} = \sqrt{\frac{\sqrt{5}-1}{2}}. \tag{6.39}$$

[17]The fundamental theorem of algebra states that each single-variable polynomial equation has exactly as many complex roots as its degree if its repeated roots are counted according to their multiplicity.

The aforelisted equation is consistent with this exact value of the critical temperature

$$\frac{k_{\mathrm{B}}T_{\mathrm{c}}}{\varepsilon_1} = \frac{2}{\ln\left(\frac{\sqrt{5}-1}{2}\right)}. \tag{6.40}$$

Note that the largest eigenvalue is equal to λ_1 below this critical temperature ($T < T_{\mathrm{c}} \Leftrightarrow x < x_{\mathrm{c}}$), while above it λ_3 becomes the largest eigenvalue. It is easy to check from Eq. (6.36) that the internal energy of the low-temperature ordered (ferroelectric) and the high-temperature disordered (paraelectric) phases must follow the relations

$$\text{if } \; T < T_{\mathrm{c}} \quad \text{then} \quad \frac{\mathcal{U}_1}{N\varepsilon_1} = \frac{x + nx^n}{x + x^n}, \tag{6.41}$$

$$\text{if } \; T > T_{\mathrm{c}} \quad \text{then} \quad \frac{\mathcal{U}_2}{N\varepsilon_1} = 2m, \tag{6.42}$$

while the entropy of both these phases obeys the relations

$$\text{if } \; T < T_{\mathrm{c}} \quad \text{then} \quad \mathcal{S}_1 = \frac{N\varepsilon_1}{T}\frac{x + nx^n}{x + x^n} + Nk_{\mathrm{B}}\ln(x + x^n), \tag{6.43}$$

$$\text{if } \; T > T_{\mathrm{c}} \quad \text{then} \quad \mathcal{S}_2 = Nk_{\mathrm{B}}\ln 2. \tag{6.44}$$

In the consequence of that, the latent heat

$$\mathcal{L} = T_{\mathrm{c}}\Delta\mathcal{S} = N\frac{(n-1)x_{\mathrm{c}}^n - (m-1)x_{\mathrm{c}}^m}{x_{\mathrm{c}} + x_{\mathrm{c}}^n} \tag{6.45}$$

as a generic feature of the discontinuous phase transition must be either absorbed or released at a critical point.

6.3.2 Square lattice eight-vertex model

As it has been shown in the preceding part, the linear zero-field eight-vertex model may exhibit a similar discontinuous phase transition as 1D KDP model does on behalf of a singular potential assigned to vertex configurations with an odd number of arrows pointing inwards or outwards a vertex. However, the most important progress achieved by solving the linear zero-field eight-vertex model consists in the fact that this model sheds light on how the rising temperature gradually destroys the spontaneous ordering to emerge at sufficiently low temperatures. In addition, 2D zero-field eight-vertex models exhibit much more complex critical behaviour compared to their six-vertex analogues, which show the

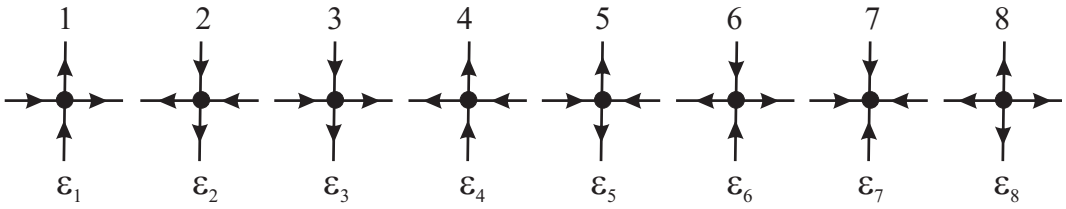

Figure 32: Eight possible arrow configurations of the eight-vertex model on a square lattice.

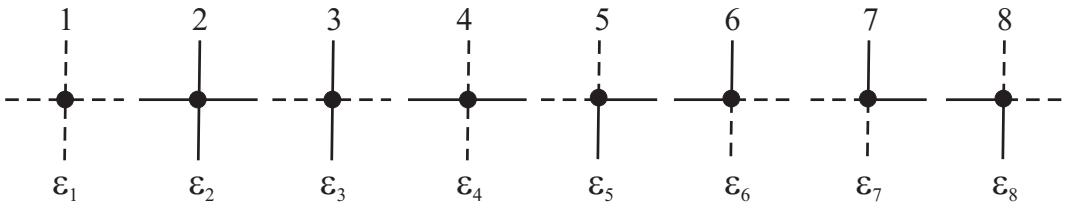

Figure 33: The bond representation of the eight possible arrow configurations shown in Fig. 32.

discontinuous phase transition at the same critical temperature independently of their spatial dimensionality (J. F. Nagle [37]).

In order to provide a deeper insight into an intricate critical phenomena of the eight-vertex model on the higher-dimensional lattices, let us look a little bit more closely at the zero-field eight-vertex model on the square lattice. The eight arrow arrangements allowed for a vertex are schematically illustrated in Fig. 32 and the vertex energies are pairwise equal to each other as required by the zero-field condition (6.23). It should be remarked that the latter two equalities $\varepsilon_5 = \varepsilon_6$ and $\varepsilon_7 = \varepsilon_8$ do not actually represent any restriction. As a matter of fact, the vertices with configurational energies ε_7 and ε_8 represent sinks and sources of arrows, respectively, and if the toroidal boundary condition is imposed their total number must necessarily be the same within each allowable macrostate. Similarly, the vertex with configurational energy ε_5 is a sink of horizontal arrows and a source of vertical arrows, while the opposite is true for the vertex with configurational energy ε_6. In this respect, the total number of vertices with the configurational energy ε_5 must be necessarily equal to the total number of vertices with the configurational energy ε_6. As a result, the vertex energies ε_5, ε_6, ε_7 and ε_8 occur in the partition function just in the combinations $\varepsilon_5 + \varepsilon_6$ and $\varepsilon_7 + \varepsilon_8$, so one may choose without loss of the generality $\varepsilon_5 = \varepsilon_6$ and $\varepsilon_7 = \varepsilon_8$. The particularly interesting situation emerges if also another two symmetric conditions $\varepsilon_1 = \varepsilon_2$ and $\varepsilon_3 = \varepsilon_4$ are imposed, since the vertex energies then become invariant under the reversal of all arrows and thus, the eight-vertex model possesses a

remarkably high symmetry.

The eight-vertex model has been previously introduced in terms of the arrow representation as a generalization of the six-vertex model, however, it should be remarked that there are several alternative ways how to formulate it. Figs. 32 and 33 show the connection between the arrow and bond representations. The bond configuration can be obtained from the corresponding arrow configuration by following this rule: *if an arrow points up or to right, then draw a broken line instead of an arrow, otherwise draw a solid line*. In this way, the arrow representation of the eight-vertex model can be transformed into the line graph of closed polygons, because only even number of lines can meet at a vertex. From this point of view, the bond representation of the eight-vertex model strongly resembles the configuration line graphs of the Ising model to be obtained by means of the dual transformation. Note that this conformity is not accidental, since the zero-field eight-vertex model is nothing else as the generalization of the Ising model as firstly remarked in 1971 by F. Y. Wu [38], L. P. Kadanoff and R. J. Wegner [39].

Let us prove the above statement. First, consider the square lattice $\mathcal{S}$ and its dual lattice $\mathcal{D}$ (Fig. 4a). Remember that vertices of the dual lattice $\mathcal{D}$ are obtained by situating a vertex at centers of each face of the original square lattice $\mathcal{S}$. If the Ising spins are located at vertices of the dual lattice $\mathcal{D}$, then, there exist two-to-one correspondence between the spin configurations on the dual lattice $\mathcal{D}$ and, respectively, the polygon configurations on the original square lattice $\mathcal{S}$. As a matter of fact, one and just one (unique) polygon configuration on the original square lattice $\mathcal{L}$ can be constructed from any spin configuration on the dual lattice $\mathcal{D}$ as follows: *draw solid lines on edges of the square lattice $\mathcal{L}$ if they separate unlike spins placed on the dual lattice $\mathcal{D}$, otherwise draw broken lines*. Conversely, there correspond two different spin configurations on the dual lattice $\mathcal{D}$ (one is being obtained from the other by reversing all spins) to each polygon line graph on the square lattice $\mathcal{L}$. The correspondence between the spin and line configurations available for each vertex is diagrammatically displayed in Fig. 34. Accordingly, the partition function of the eight-vertex model $\mathcal{Z}_{8-\mathrm{v}}$ on the square lattice $\mathcal{L}$ can be related to the partition function of some spin-1/2 Ising model $\mathcal{Z}_{\mathrm{Ising}}$ on its dual lattice $\mathcal{D}$

$$\mathcal{Z}_{8-\mathrm{v}} = \frac{1}{2}\mathcal{Z}_{\mathrm{Ising}}. \tag{6.46}$$

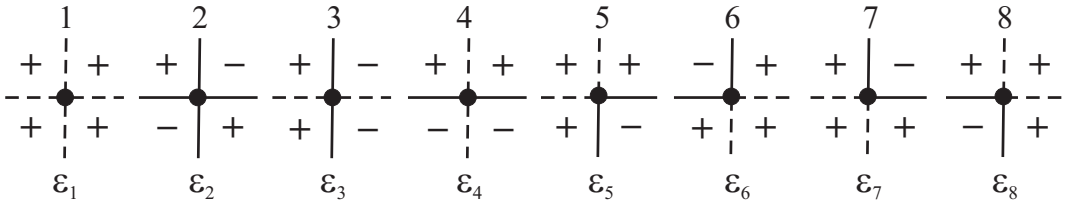

Figure 34: Eight possible line configurations for a vertex of the eight-vertex model on a square lattice and their corresponding spin configurations at vertices of its dual lattice.

The factor $\frac{1}{2}$ comes from the two-to-one mapping between spin and vertex configurations.

Let us validate the mapping relation (6.46) between both the partition functions by supplying a missing connection between interaction parameters of both these models. The most general Hamiltonian of the spin-1/2 Ising model on the square lattice of M rows and N columns (the periodic boundary conditions are imposed and $M = N$), which is invariant with respect to the reversal of all spins, reads

$$\mathcal{H} = -\sum_{i=1}^{M}\sum_{j=1}^{N}\Big(J_0 + J_h\sigma_{i,j}\sigma_{i,j+1} + J_v\sigma_{i,j}\sigma_{i+1,j} + J\sigma_{i,j+1}\sigma_{i+1,j} + J'\sigma_{i,j}\sigma_{i+1,j+1} + J''\sigma_{i,j}\sigma_{i,j+1}\sigma_{i+1,j}\sigma_{i+1,j+1}\Big), \quad (6.47)$$

where J_0 is an additive constant, J_h and J_v denote the nearest-neighbour spin-spin interactions in the horizontal and vertical directions, respectively, J and J' represent the second-neighbour spin-spin interactions along two different diagonal directions and J'' labels the interaction between four corner spins forming an elementary face (square plaquette) of the dual lattice $\mathcal{D}$. The total Hamiltonian (6.47) can also be written as a sum of face Hamiltonians $\mathcal{H} = \sum_{k\in\square}\mathcal{H}_k$, where the indicated summation runs over all square faces of the dual lattice $\mathcal{D}$. In this respect, each face Hamiltonian $\mathcal{H}_k$ involves all the interaction terms surrounding one vertex of the original square lattice $\mathcal{L}$

$$\mathcal{H}_k = -J_0 - \frac{J_h}{2}\left(\sigma_{i,j}\sigma_{i,j+1} + \sigma_{i+1,j}\sigma_{i+1,j+1}\right) - \frac{J_v}{2}\left(\sigma_{i,j}\sigma_{i+1,j} + \sigma_{i,j+1}\sigma_{i+1,j+1}\right) - J\sigma_{i,j+1}\sigma_{i+1,j} - J'\sigma_{i,j}\sigma_{i+1,j+1} - J''\sigma_{i,j}\sigma_{i,j+1}\sigma_{i+1,j}\sigma_{i+1,j+1}. \quad (6.48)$$

The interaction terms entering into the face Hamiltonian are schematically shown in Fig. 35 and each face Hamiltonian (6.48) contains only half of the horizontal and vertical interactions in order to avoid a double counting of those interactions. The vertex energies can be now straightforwardly obtained by taking into account the mapping relation

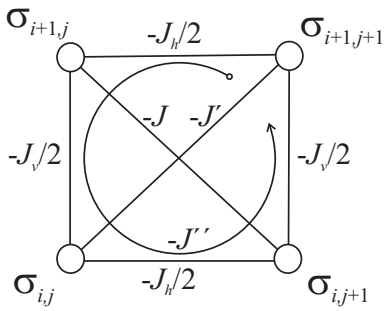

Figure 35: The interaction terms of the most general spin-1/2 Ising model on a square lattice, which preserves a complete spin reversal symmetry.

between the spin and line configurations displayed in Fig. 34. For instance, the spin configuration with four identical spins (all four spins are either 'up' or 'down') corresponds according to this mapping to the vertex without any solid line and other vertex energies can be obtained in a similar manner. In this way, it is easy to write down the vertex energies with the help of Ising interactions

$$\varepsilon_1 = -J_0 - J_h - J_v - J - J' - J'', \tag{6.49}$$

$$\varepsilon_2 = -J_0 + J_h + J_v - J - J' - J'', \tag{6.50}$$

$$\varepsilon_3 = -J_0 + J_h - J_v + J + J' - J'', \tag{6.51}$$

$$\varepsilon_4 = -J_0 - J_h + J_v + J + J' - J'', \tag{6.52}$$

$$\varepsilon_5 = \varepsilon_6 = -J_0 - J + J' + J'', \tag{6.53}$$

$$\varepsilon_7 = \varepsilon_8 = -J_0 + J - J' + J''. \tag{6.54}$$

In agreement with the aforementioned arguments, the vertex energies $\varepsilon_5 = \varepsilon_6$ and $\varepsilon_7 = \varepsilon_8$ are equal one to each other without loss of the generality. However, the zero-field eight-vertex model necessitates the validity of another two equalities $\varepsilon_1 = \varepsilon_2$ and $\varepsilon_3 = \varepsilon_4$, which can be simply achieved by setting $J_h = J_v = 0$. In this case, the vertex energies (6.49)–(6.54) simplify to

$$\varepsilon_1 = \varepsilon_2 = -J_0 - J - J' - J'', \tag{6.55}$$

$$\varepsilon_3 = \varepsilon_4 = -J_0 + J + J' - J'', \tag{6.56}$$

$$\varepsilon_5 = \varepsilon_6 = -J_0 - J + J' + J'', \tag{6.57}$$

$$\varepsilon_7 = \varepsilon_8 = -J_0 + J - J' + J''. \tag{6.58}$$

Among other matters, the mapping relations (6.55)–(6.58) mean that the zero-field eight-vertex model on the square lattice is equivalent to the spin-1/2 Ising model on two square lattices, which are coupled together through the four-spin interaction [38, 39]. Of course, the mapping relations (6.55)–(6.58) can also be inverted and the spin-1/2 Ising model with two- and four-spin interactions can be expressed in terms of the equivalent zero-field eight-vertex model

$$J_0 = -\frac{1}{4}(\varepsilon_1 + \varepsilon_3 + \varepsilon_5 + \varepsilon_7), \tag{6.59}$$

$$J = -\frac{1}{4}(\varepsilon_1 - \varepsilon_3 + \varepsilon_5 - \varepsilon_7), \tag{6.60}$$

$$J' = -\frac{1}{4}(\varepsilon_1 - \varepsilon_3 - \varepsilon_5 + \varepsilon_7), \tag{6.61}$$

$$J'' = -\frac{1}{4}(\varepsilon_1 + \varepsilon_3 - \varepsilon_5 - \varepsilon_7). \tag{6.62}$$

Notice that the set of Eqs. (6.55)–(6.58) and (6.59)–(6.62) formally complete the proof of an equivalence between the zero-field eight-vertex model and the general Ising model with two- and four-spin interactions on a square lattice. From this point of view, the zero-field eight-vertex model should exhibit a continuous (second-order) phase transition from the universality class of the nearest-neighbour Ising model once the four-spin interaction J'' vanishes due to a particular equality between the vertex energies $\varepsilon_1 + \varepsilon_3 = \varepsilon_5 + \varepsilon_7$. Nevertheless, the non-zero four-spin interaction of the general zero-field eight-vertex model implies that this model might exhibit much more complex critical behaviour than the nearest-neighbour Ising model without the four-spin interaction.

The zero-field eight-vertex model on the square lattice has been exactly solved by R. J. Baxter (1972) [40] and this outstanding exact solution has opened up another interesting issue in the field of phase transitions and critical phenomena. Namely, Baxter's exact solution predicts for the zero-field eight-vertex model a striking phase transition whenever its Boltzmann's weights $\omega_i = \exp[-\beta\varepsilon_i]$ $(i = 1 - 8)$ satisfy the condition

$$\omega_1 + \omega_3 + \omega_5 + \omega_7 = 2\mathrm{max}\{\omega_1, \omega_3, \omega_5, \omega_7\}. \tag{6.63}$$

The most striking feature of these phase transitions is that their critical exponents (1.17)

$$\alpha = \alpha' = 2 - \frac{\pi}{\mu}, \quad \beta = \frac{\pi}{16\mu}, \quad \nu = \nu' = \frac{\pi}{2\mu}, \quad \gamma = \frac{7\pi}{8\mu}, \quad \delta = 15, \quad \eta = \frac{1}{4} \tag{6.64}$$

vary as inverse linear functions of the expression $\mu = 2\arctan\left(\sqrt{\omega_5\omega_7/\omega_1\omega_3}\right)$ depending on the Boltzmann's weights (interaction parameters) unlike the critical exponents of other exactly solved models investigated previously. This means that the critical exponents of the zero-field eight-vertex model might depend continuously on the energy parameters of the model in contradiction with the ordinary universality hypothesis. It should be stressed, however, that the critical exponents (6.64) obey the equalities (1.18)–(1.22) derived with the help of the scaling hypothesis, what means that the universality and scaling hypotheses are independent assumptions even although they are frequently coupled together. As a matter of fact, the scaling hypothesis turns out to hold even within the zero-field eight-vertex model, while the ordinary universality hypothesis fails. Baxter's exact results reported on the continuously varying critical exponents of the zero-field eight-vertex model consecutively inspired M. Suzuki (1974) [41] to propose the weak universality hypothesis, which allows changes of the critical exponents do not violating the concept based on the scaling laws.

Exercises

1. Reformulate 1D ice model in terms of the transfer-matrix method and find a complete spectrum of eigenvalues of the relevant transfer matrix. Show that the Helmholtz free energy, internal energy and entropy reduce in the thermodynamic limit to the results presented in Eq. (6.2).

2. Find an exact solution for 1D analogue of antiferrolectric F model by employing the transfer-matrix approach. The antiferroelectric F model suggested by F. Rys (1963) [42] can be regarded as the six-vertex model defined through the six allowed arrow configurations shown in Fig. 23 with the following vertex energies $\varepsilon_1 = \varepsilon_2 = \varepsilon_3 = \varepsilon_4 = \varepsilon_0 > 0$ and $\varepsilon_5 = \varepsilon_6 = 0$. Does the antiferroelectric F model exhibit a phase transition?

3. Calculate the spontaneous polarization of the low-temperature (ferroelectric) phase within the linear zero-field eight-vertex model and discuss its dependence on the temperature. Evaluate the spontaneous polarization at a critical point of the first-order phase transition for the particular case with ε_1, $\varepsilon_3 = \varepsilon_5 = 3\varepsilon_1$ and $\varepsilon_7 = 7\varepsilon_1$ ($m = 3$ and $n = 7$).

4. Find out how the critical exponents of zero-field eight-vertex model on the square lattice depend on the two- and four-spin interactions of its equivalent square lattice Ising model. Verify whether the values of critical exponents are in the limit of vanishing four-spin interaction from the standard Ising's universality class.

7 Conclusion

The present textbook was conceived as a slim knowledge source of the simplest exactly solved models, which is suitable for undergraduate students who have an academic focus in mathematical physics, statistical physics or condensed matter physics. In the present state of science, it seems almost impossible to even enumerate the most notable exactly solved lattice-statistical models. Essentially, this textbook deals with the low-dimensional lattice-statistical models such as the Ising, Heisenberg and vertex models. Although the original idea was to provide a more comprehensive textbook including many other rigorously solved models like the spherical model [43], the dimer model [44], the mean-field model [45], the Baxter-Wu model [46], the quantum XY model [47], the quantum Ising model [48] and the quantum Heisenberg model [23], however, this would be unreasonable due to a considerable extent of the textbook that would significantly surpass any standard course for undergraduate students. Contrary to this, it was rather tempting to use just an unique powerful mathematical device, the transfer-matrix method, for obtaining most of the exact solutions and in such a way to avoid detailed description of other sophisticated methods (Pffafian method [44], Bethe-ansatz method [23], Jordan-Wigner fermionization [49], etc.) needed for accurate treatment of other exactly solvable lattice-statistical models. With respect to this, the transfer-matrix technique represents the main subject of the present course from the methodological point of view.

Before concluding, it should be noted that there are still many unresolved problems to be tackled in the area of exactly solvable models, which are usually recognized as the highest intellectual challenge for theoretical physicists [50]. The ambitious students who wish to continue in studying this exciting research field are therefore referred to several comprehensive monographs listed in the bibliography list at the end of this textbook. Among these, I recommend R. J. Baxter's book *Exactly Solved Models in Statistical Mechanics* as a starting follow-up literature, since this book represents advanced but simultaneously sufficiently detailed tutorial review. It is also the author's hope that this textbook will be extended in the next edition by topics, which are specifically taught at P. J. Šafárik University within the postgraduate course *Exactly Solvable Models in Statistical Physics*.

References

[1] L. Onsager, *Crystal Statistics. I. A Two-Dimensional Model with an Order-Disorder Transition*, Phys. Rev. 65 (1944) 117. https://doi.org/10.1103/PhysRev.65.117

[2] H. A. Kramers and G. H. Wannier, *Statistics of the Two-Dimensional Ferromagnet. Part I*, Phys. Rev. 60 (1941) 252. https://doi.org/10.1103/PhysRev.60.252

[3] M. Blume, V. J. Emery, and R. B. Griffiths, *Ising Model for the λ Transition and Phase Separation in ^{3}He-^{4}He Mixtures*, Phys. Rev. A 4 (1971) 1071. https://doi.org/10.1103/PhysRevA.4.1071

[4] M. Mijatovič, S. Miloševič, and V. Urumov, *Absence of the second-order phase transitions in the dimerized Ising chains with spin larger than 1/2*, J. Magn. Magn. Mater. 23 (1981) 79. https://doi.org/10.1016/0304-8853(81)90071-8

[5] J. F. Dobson, *Many-Neighbored Ising Chain*, J. Math. Phys. 10 (1969) 40. https://doi.org/10.1063/1.1664757

[6] E. Ising, *Beitrag zur Theorie des Ferromagnetismus*, Z. Phys. 31 (1925) 253. https://doi.org/10.1007/BF02980577

[7] R. Peierls, *On Ising's model of ferromagnetism*, Proc. Cambridge Phil. Soc. 32 (1936) 477. https://doi.org/10.1017/S0305004100019174

[8] R. B. Griffiths, *Peierls Proof of Spontaneous Magnetization in a Two-Dimensional Ising Ferromagnet*, Phys. Rev. 136 (1964) 437. https://doi.org/10.1103/PhysRev.136.A437

[9] B. L. van der Waerden, *Die lange Reichweite der regelmäßigen Atomanordnung in Mischkristallen*, Z. Physik 118 (1941) 473. https://doi.org/10.1007/BF01342928

[10] I. Syozi, *Statistics of Kagomé Lattice*, Prog. Theor. Phys. 6 (1951) 306. https://doi.org/10.1143/ptp/6.3.306

[11] C. N. Yang, *The Spontaneous Magnetization of a Two-Dimensional Ising Model*, Phys. Rev. 85 (1952) 809. https://doi.org/10.1103/PhysRev.85.808

[12] W. Lenz, *Beitrag zum Verständnis der magnetischen Erscheinungen in festen Körpern*, Z. Phys. 21 (1920) 613.

[13] W. P. Wolf, *The Ising model and real magnetic materials*, Braz. J. Phys. 30 (2000) 794. https://doi.org/10.1590/S0103-97332000000400030

[14] L. J. De Jongh and A. R. Miedema, *Experiments on simple magnetic model systems*, Adv. Phys. 23 (1974) 1. https://doi.org/10.1080/00018739700101558

[15] D. Bloch, *The 103 law for the volume dependence of superexchange*, J. Phys. Chem. Solids 27 (1966) 881. https://doi.org/10.1016/0022-3697(66)90262-9

[16] L. K. Runnels, *Phase Transition of a Bethe Lattice Gas of Hard Molecules*, J. Math. Phys. 8 (1967) 2081. https://doi.org/10.1063/1.1705123

[17] T. P. Eggarter, *Cayley trees, the Ising problem, and the thermodynamic limit*, Phys. Rev. B 9 (1974) 2989. https://doi.org/10.1103/PhysRevB.9.2989

[18] E. Müller-Hartmann and J. Zittarz, *New Type of Phase Transition*, Phys. Rev. Lett. 33 (1974) 893. https://doi.org/10.1103/PhysRevLett.33.893

[19] R. J. Baxter, *Exactly Solved Models in Statistical Mechanics*, Academic Press, New York, 1982, pp. 47-59. https://physics.anu.edu.au/research/ftp/mpg/baxterbook.php

[20] W. Heisenberg, *Zur Theorie des Ferromagnetismus*, Z. Physik 49 (1928) 619. https://doi.org/10.1007/BF01328601

[21] M. E. Fisher, *Magnetism in One-Dimensional Systems—The Heisenberg Model for Infinite Spin*, Am. J. Phys. 32 (1964) 343. https://doi.org/10.1119/1.1970340

[22] C. K. Majumdar and D. K. Ghosh, *On Next-Nearest-Neighbor Interaction in Linear Chain. I and II*, J. Math. Phys. 10 (1969) 1388 & 1399. https://doi.org/10.1063/1.1664978 & https://doi.org/10.1063/1.1664979

[23] H. A. Bethe, *Zur Theorie der Metalle I. Eigenwerte und Eigenfunktionen der linearen Atomkette*, Z. Phys. 71 (1931) 205. https://doi.org/10.1007/BF01341708

[24] B. S. Shastry and B. Sutherland, *Exact ground state of a quantum mechanical antiferromagnet*, Physica B+C 108 (1981) 1069. https://doi.org/10.1016/0378-4363(81)90838-X

[25] I. Bose, *Antiferromagnetic spin models in two dimensions with known ground states*, Phys. Rev. B 45 (1992) 13072. https://doi.org/10.1103/PhysRevB.45.13072

[26] M. W. Long and R. Fehrenbacher, *An exactly soluble one-dimensional quantum mechanical Heisenberg and Nagaoka t-J model*, J. Phys.: Condens. Matter 2 (1990) 2787. https://doi.org/10.1088/0953-8984/2/12/003

[27] M. P. Gelfand, *Linked-tetrahedra spin chain: Exact ground state and excitations*, Phys. Rev. B 43 (1991) 8644. https://doi.org/10.1103/PhysRevB.43.8644

[28] L. Pauling, *The Structure and Entropy of Ice and of Other Crystals with Some Randomness of Atomic Arrangement*, J. Am. Chem. Soc. 57 (1935) 2680. https://doi.org/10.1021/ja01315a102

[29] J. C. Slater, *Theory of the Transition in* KH_2PO_4, J. Chem. Phys. 9 (1941) 16. https://doi.org/10.1063/1.1750821

[30] E. H. Lieb, *Exact Solution of the Problem of the Entropy of Two-Dimensional Ice*, Phys. Rev. Lett. 18 (1967) 692. https://doi.org/10.1103/PhysRevLett.18.692; & *Residual Entropy of Square Ice*, Phys. Rev. 162 (1967) 162. https://doi.org/10.1103/PhysRev.162.162

[31] J. F. Nagle, *The One-Dimensional KDP Model in Statistical Mechanics*, Am. J. Phys. 36 (1968) 1114. https://doi.org/10.1119/1.1974374

[32] B. Sutherland, *Exact Solution of a Two-Dimensional Model for Hydrogen-Bonded Crystals*, Phys. Rev. Lett. 19 (1967) 103. https://doi.org/10.1103/PhysRevLett.19.103

[33] E. H. Lieb, *Exact Solution of the Two-Dimensional Slater KDP Model of a Ferroelectric*, Phys. Rev. Lett. 19 (1967) 108. https://doi.org/10.1103/PhysRevLett.19.108

[34] Y. Takagi, *Theory of the Transition in* KH_2PO_4, J. Phys. Soc. Jpn. 3 (1948) 273. https://doi.org/10.1143/JPSJ.3.273

[35] B. Sutherland, *Two-Dimensional Hydrogen Bonded Crystals without the Ice Rule*, J. Math. Phys. 11 (1970) 3183. https://doi.org/10.1063/1.1665111

[36] C. Fan and F. Y. Wu, *General Lattice Model of Phase Transitions*, Phys. Rev. B 2 (1970) 723. https://doi.org/10.1103/PhysRevB.2.723

[37] J. F. Nagle, *Proof of the first order phase transition in the Slater KDP model*, Commun. Math. Phys. 13 (1969) 62. https://doi.org/10.1007/BF01645270

[38] F. Y. Wu, *Ising Model with Four-Spin Interactions*, Phys. Rev. B 4 (1971) 2312. https://doi.org/10.1103/PhysRevB.4.2312

[39] L. P. Kadanoff and R. J. Wegner, *Some Critical Properties of the Eight-Vertex Model*, Phys. Rev. B 4 (1971) 3989. https://doi.org/10.1103/PhysRevB.4.3989

[40] R. J. Baxter, *Partition function of the Eight-Vertex lattice model*, Ann. Phys. 70 (1972) 193. https://doi.org/10.1016/0003-4916(72)90335-1

[41] M. Suzuki, *New Universality of Critical Exponents*, Prog. Theor. Phys. 51 (1974) 1992. https://doi.org/10.1143/PTP.51.1992

[42] F. Rys, *Über ein zweidimensionales klassisches Konfigurationsmodell*, Helv. Phys. Acta 36 (1963) 537. https://www.e-periodica.ch/digbib/volumes?UID=hpa-001

[43] T. H. Berlin and M. Kac, *The Spherical Model of a Ferromagnet*, Phys. Rev. 86 (1952) 821. https://doi.org/10.1103/PhysRev.86.821

[44] P. W. Kasteleyn, *The statistics of dimers on a lattice: I. The number of dimer arrangements on a quadratic lattice*, Physica 27 (1961) 1209. https://doi.org/10.1016/0031-8914(61)90063-5

[45] M. Kac, G. H. Uhlenbeck, and P. L. Hemmer, *On the van der Waals Theory of the Vapor-Liquid Equilibrium. I. Discussion of a One-Dimensional Model*, J. Math. Phys. 4 (1963) 216. https://doi.org/10.1063/1.1703946

[46] R. J. Baxter and F. Y. Wu, *Exact Solution of an Ising Model with Three-Spin Interactions on a Triangular Lattice*, Phys. Rev. Lett. 31 (1973) 1294. https://doi.org/10.1103/PhysRevLett.31.1294

[47] E. H. Lieb, T. D. Schultz, and D. C. Mattis, *Two soluble models of an antiferromagnetic chain*, Ann. Phys. 16 (1961) 407. https://doi.org/10.1016/0003-4916(61)90115-4

[48] S. Katsura, *Statistical Mechanics of the Anisotropic Linear Heisenberg Model*, Phys. Rev. 127 (1962) 1508. https://doi.org/10.1103/PhysRev.127.1508

[49] P. Jordan and E. Wigner, *Über das Paulische Äquivalenzverbot*, Z. Physik 47 (1928) 631. https://doi.org/10.1007/BF01331938

[50] E. H. Lieb, *Some problems in statistical mechanics that I would like to see solve*d, Physica A 263 (1999) 491. https://doi.org/10.1016/S0378-4371(98)00517-2

Bibliography

- C. Domb and M. S. Green, *Phase Transitions and Critical Phenomena, Vol. 1*, Academic Press, New York, 1972.
- C. J. Thompson, *Mathematical Statistical Mechanics*, Princeton University Press, New Jersey, 1979.
- R. J. Baxter, *Exactly Solved Models in Statistical Mechanics*, Academic Press, New York, 1982.
- C. J. Thompson, *Classical Equilibrium Statistical Mechanics*, Oxford University Press, New York, 1988.
- H. E. Stanley, *Introduction to Phase Transitions and Critical Phenomena*, Oxford University Press, Oxford, 1993.
- C. King and F. Y. Wu, *Exactly Soluble Models in Statistical Mechanics*, World Scientific, Singapore, 1996.
- D. A. Lavis and G. M. Bell, *Statistical Mechanics of Lattice Systems, Vol. 1*, Springer, Berlin-Heidelberg, 1999.
- D. A. Lavis and G. M. Bell, *Statistical Mechanics of Lattice Systems, Vol. 2*, Springer, Berlin-Heidelberg, 1999.
- J. M. Yeomans, *Statistical Mechanics of Phase Transitions*, Oxford University Press, Oxford, 2002.
- T. Tanaka, *Methods of Statistical Physics*, Cambridge University Press, Cambridge, 2002.
- E. H. Lieb, *Condensed Matter Physics and Exactly Soluble Models*, Springer, Berlin-Heidelberg, 2004.
- B. Sutherland, *Beautiful Models: 70 Years of Exactly Solved Quantum Many-Body Problems*, World Scientific, Singapore, 2004.

Exactly Solvable Models in Statistical Physics
Academic textbook

Author: doc. RNDr. Jozef Strečka, PhD.

Publisher: Pavol Jozef Šafárik University i n Košice
Publishing ŠafárikPress

Year: 2022
Pages: 136
Author's sheets: 6,5
Edition: second

ISBN 978-80-574-0124-7 (e-publication)